THREE DIMENSIONAL SEEPAGE ANALYSIS BELOW A BARRAGE (BY FEM)
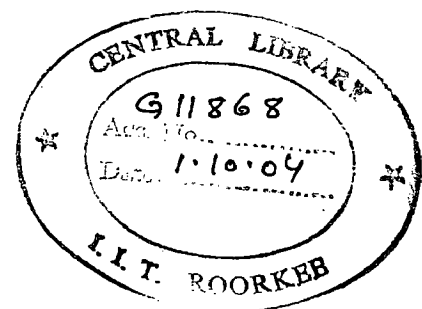
A DISSERTATION

*Submitted in partial fulfillment of the
requirements for the award of the degree*
of
MASTER OF TECHNOLOGY
in
**WATER RESOURCES DEVELOPMENT
(CIVIL)**

By

P.N. ZAMINDAR

**WATER RESOURCES DEVELOPMENT TRAINING CENTRE
INDIAN INSTITUTE OF TECHNOLOGY ROORKEE
ROORKEE - 247 667 (INDIA)
JUNE, 2004**

CANDIDATE'S DECLARATION

I hereby certify that the dissertation entitled **"THREE DIMENSIONAL SEEPAGE ANALYSIS BELOW A BARRAGE" (By FEM)** is being submitted by me in partial fulfillment of requirement for the award of degree of "Master of Technology in Water Resources Development" at the Water Resources Development Training Centre, Indian Institute of Technology, Roorkee is an authentic record of my own work carried out during the period from July, 2003 to June 2004 under the supervision of Dr. B.N.Asthana, Visiting Professor and Dr. Ram Pal Singh Professor, WRDTC, IITR.

The matter embodied in the dissertation has not been submitted by me for the award of any other degree or diploma.
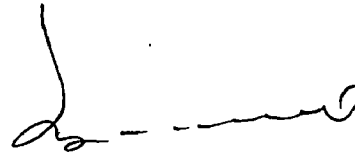
Dated: June 30, 2004

Place : Roorkee

(P.N.Zamindar)

This is to certify that above statement made by the candidate is correct to the best of our knowledge.

(Dr. Ram Pal Singh)
Professor, WRDTC
Indian Institute of Technology,
Roorkee

(Dr. B.N.Asthana)
Visiting Professor, WRDTC.
Indian Institute of Technology
Roorkee

ACKNOWLEDGMENTS

CONTENTS

LIST OF TABLES

LIST OF FIGURES

Hydraulic structures such as weirs and barrages on pervious foundation are generally designed on the basis of Khosla's theory considering 2-D sub surface flow below the structures. The correct approach in the estimation of uplift pressure below hydraulic structures (barrages) built on previous foundation would be the one that takes into account the 3-dimensional flow conditions due to high water table behind the abutments. The subsoil water table conditions have a marked influence on the uplift pressures in the barrage floor adjacent to the abutments. It is also important to study the variation of uplift pressures due to variation of water table.

The practice is to take adhoc measures to control and reduce the pressures on the floors due to variation in water table elevation behind the abutments such as provision of intermediate filters, pressure relief wells etc. Their efficiency is not quantifiable. The floor of the bay adjoining the abutment are designed for about 15 to 20% extra uplift pressure. In important major structures, this aspect is sometimes examined on electrical analogy model. It has several limitations and is time consuming and costly.

An attempt is made in this study to work out analytical solution to the problem. The study is carried out using 3D-FEM technique through ANSYS package program. In this study as an illustration Kanpur barrage is taken as an example.

It has been observed that uplift pressure on the downstream floor of barrage increases with the extent of water table elevation behind the abutment and the safety factor for exit gradient decreases with increase in water table elevation. The increase in uplift pressure and exit gradient is significant near the abutments. The 3D effect of uplift pressure are obtained at 0.37L, 0.28L, 0.26L from the abutments, where L is the width of the structure (abutment to abutment) for the potentials behind abutments at 100%, 90% and (90% to 50%) respectively.

INTRODUCTION

1.1 BACK GROUND OF STUDY

Study of seepage is important not only from the point of view of ground water development but also from the point of view of design of hydraulic structures. In the later case, water seeping below the floors causes not only loss of water but uplift pressure on the impervious floor of structures. It may also cause piping against which precautions are necessary.

Practically in every hydraulic structure which is founded on previous strata, seepage endangers the stability in two ways.

(i)   Piping or undermining, if exit gradient is not with in permissible limit.

(ii)   Up lift pressure if in excess of the weight on the floor.

It is well known that all fluids flow from a point of higher potential to the point of lower potential in all the directions. Depending upon the gradient available in any particular direction the fluid flow will, therefore, be generally three dimensional.

The correct approach in the estimation of uplift pressure below hydraulic structures (barrages) built on pervious foundation would be the one that takes into account the 3-dimensional flow conditions. Generally 2-D analysis as per Khosla theory is carried out and the uplift pressures are increased in an adhoc manner in the bays adjacent to the abutment. In important major structures 3-D electrical analogy experimental model studies are carried out.

1.2   NECESSITY OF THE STUDY

The general practice of the design is to treat the sub soil flow problem under hydraulic structures as only two dimensional.

The investigation conducted in the Irrigation Research Institute U.P. [10] on the model of Jagpura siphon constructed on Sarda main canal provided reliable evidence of the 3-dimensional nature of seepage flow.

In case of hydraulic structures (barrages) constructed across wide streams where the width of the floor is considerably greater then its length, the seepage path of the flow lines in the middle portion of the structure will be more or less in vertical planes and can therefore be treated as 2 dimensional. However, even in such structures (barrages) the flow pattern under the bays near the abutments will be 3 dimensional, because the seepage flow from the pond raises water level behind the abutments. In cases where the width/length ratio of the structures (barrages) is small, the seepage flow will be markedly 3 dimensional. The seepage flow in such cases will be through the porous media below the structure as well as adjacent to it and behind the abutments. Apart from this, the effect of the ground water mound which starts building up between bottom of the structures and the existing water table due to infiltration from the stream has also to be taken into cognizance in the 3 dimensional approach of the problem. The existing water table which eventually fluctuates with the ground water mound has its effect on the flow lines and the seepage path and hence the seepage pressures under the floors get modified. The correct approach in the estimation of uplift pressure below hydraulic structures built on porous media appears to be a 3-D seepage flow.

1-2

The solution to the problem of particular geometry can be developed through systematic study by either of the following techniques:

(i)   Hydraulic model investigation.

(ii)   Electric analogy test.

(iii)   Analytical method (finite element method)

1.3   SCOPE OF THE STUDY

The objective of this study is to assess uplift pressure distribution on the base of barrage floor, in addition to find exit gradients near the toe of structure, analytically using Finite Element Method (FEM). In this study Kanpur barrage is taken as an example for study under different water levels behind abutments and solution is obtained analytically by FEM. The results have also been compared with Electro Hydro Dynamic Analysis (EHDA) experimental method used by Irrigation Research Institute, Roorkee.

1.4   ORGANIZATION OF STUDY

The study is presented in 6 chapters. The contents of each chapter are briefly given below:

Chapter 1: Gives an introduction to the subject, necessity, objectives, scope of study and organization of dissertation report.

Chapter 2: Deals with literature review, including brief historical development of ground water flow, theories & principles of ground water flow, procedures for solving seepage problems.

Chapter 3: Review of FEM, and its theory and application in seepage problem.

Chapter 4: Deals with preparation of models in Ansys software, model boundaries for seepage flow. The models prepared are as below:

(i)   Standard form (equal sheet piles at u/s and d/s end for horizontal floor) analysed in CBI No. 12 [7].

(ii)   2-D model of Kanpur barrage

(iii)   3-D model of Kanpur barrage

Chapter 5: Deals with result and analysis. This includes (i) validity of ANSYS with Khosla experimental and theoretical results (ii) comparison of 2-D results of EHDA and ANSYS (iii) comparison of 3-D EHDA and ANSYS results under different test conditions (iv) determination of flow length affected by 3-D floor under different GWL conditions behind abutment.

Chapter 6: Contains conclusion, recommendations and suggestion for future studies.

LITERATURE REVIEW AND THEORY OF GROUNDWATER FLOW

2.1 HISTORICAL DEVELOPMENT OF THE STUDY OF SEEPAGE PROBLEM

A rational basis to the study of subsoil flow was for the first time given by French hydraulician Darcy in 1856. While flowing, ground water experiences a loss in energy due to friction against the surface of the particles of granular medium along its seepage path. This loss per unit length traveled, or the hydraulic gradient is proportional to the velocity of flow. The proportionality is expressed mathematically by a linear equation known as Darcy's law

$$V = K.\frac{H}{L}$$

where

V = velocity of flow

L = length of the path of flow

K = A constant called the transmission constant or "Hydraulic Conductivity"

The validity of this law in relation to weir design was tested by Col. Clibborn in 1896 in connection with proposals for repairs to the damages to Khanki weir on Chenab river. Damages of khanki weir soon after construction gave food for thought to the engineers responsible for construction & maintenance.

As a result of experiments by Clibborn the hydraulic gradient theory of design of weirs was developed by Ottley and Higham.

On the basis of Darcy's work, significant contribution to the subsoil hydraulics were made by Boussinesq, Dupit, Forchheimer and Theim in the later half of nineteenth century and more recently by Dechler, Kozency Hazen King and Slitcher.

The hydraulic gradient theory became generally accepted by 1898 in India.

In 1910 Bligh put forth his theory based on Col. Clibborn work. Bligh stated that the length of the path of flow had the same effectiveness, length for length in reducing the uplift pressure whether it was along the horizontal or the vertical.

Forchheimer developed a geometrical method of plotting stream lines and equipotantial lines in1911. This method is known as the flow net method for determining the potentials at various points in the flow field with a free surface.

In 1915 Colman carried out tests with models of weir rested on sand to find the distribution of pressure on the base of the floor and the effect of upstream and downstream cutoffs.

In 1929, Karl Terzaghi made a notable contribution to the design criteria. He stated and proved by laboratory experiments that failures of structure occur by undermining when the exit gradient is in excess of the flotation gradient.

The first full size experiments were conducted by A.N. Khosla around 1930, on the upper Chenab siphons and the main conclusions derived from these researches gave the idea that "Failure of structure would occur if the exit gradient exceeds the critical gradient. It was also found that the outer faces of the vertical cut offs has greater efficiency than the inner faces.

About the same time Prof. Warren Weaver developed his mathematical treatment of the 2-dimensional flow of water through permeable sub soil.

In 1934, Lane proposed his weighted creep theory as modification of Bligh's theory and suggested a weight of 3 for vertical and 1 for horizontal creep. In this theory the flow was assumed to follow the line of contact between the structure of the dam and its foundation. While this theory was an improvement on the original Bligh's theory it was empirical and lacked the background of rational or analytical basis.

In 1934, Haigh and Harza carried out investigation on the lines suggested by Weaver and results were verified with electric model. Based on this investigation Harza suggested that a cut of at the toe is necessary to have a safe exit gradient.

The problem of determination of uplift pressure on structure with sheet pile was studied by Pavlovsky and Muskat independently and results were found to agree with those obtained by experiments based on electrical analogy. The effect of sheet pile on the seepage below floors in two dimensional flows was analyzed mathematically by Poluborinova Kochina, Pavlovsky, Harr [4].

The method of analysis employing electrical resistance network is simple and permits easy representation of even complex boundary conditions and layered strata of different permeability.

The analytical solution of Laplacian equation for 3 dimensional seepage flows with appropriate boundary condition is very complicated.

The study "Analysis of seepage in pervious abutments of dams" was carried out by Twelker around 1957 [9] using flow nets based upon Dupuit-Forchheimer Theory for flow with free surface. At U.P. Irrigation Research Institute studies, 1957 [10] were

conducted on electric model of Jagpura syphon across Sarda Main canal to analyse 3-D effect on structure.

2.2 THEORIES & PRINCIPLES OF GROUND WATER FLOW

Recent development in soil mechanics, better knowledge of the behavior of such soil strata and modern techniques of exhaustive sub-surface exploration compiled with the development of complex variables provided stimulus to the development of the science of ground water seepage, so much so that today, most of intricate problem connected with seepage and seepage pressure on hydraulic structures can be solved analytically or experimentally with appreciable degree of precision.

In such problems, it is very well known that the medium of seepage, (viz) the soil mass is continuous consisting of many inter connected openings. This medium may some time consists of cavernous cells inter connected by narrow channels. A precise description of the pore channels in soil mass is impossible. Ground water problems were not amenable to rational solutions until the knowledge of Darcy's Law.

In ground water problems we consider only the macroscopic flow across a section consisting of many pore channels is taken as uniform.

Movement of water through soil does not only obey Darcy's law but has been found almost all the fundamental laws of fluid mechanics as discussed below.

2.2.1 Energy Equation
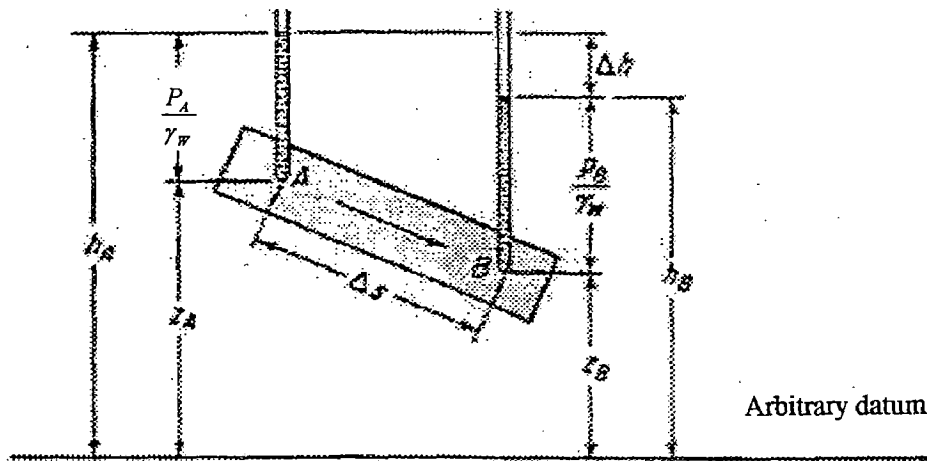
Fig. : 2.1

The Bernoulli's equation for non viscous incompressible fluids is given by

$$\frac{p}{\gamma_w} + Z + \frac{\bar{V}^2}{2g} = \text{constant} = h \qquad \ldots\ldots \quad (1)$$

Where

p = pressure

γ_w= unit weight of fluid

$\bar{V}$ = seepage velocity

g = Gravitational constant

h = Total head

Also,

$\frac{p}{\gamma_w}$ = Pressure head

z = Elevation head

$\frac{\bar{V}^2}{2g}$ = Velocity head

The sum of which (1) at any point in the flow region is constant.

In ground water flow, the loss of head due to the viscous resistance within individual pores is accounted for by representing the total head loss as Δh and the equation becomes

$$\frac{P_A}{\gamma_w} + Z_A + \frac{\overline{V}_A^2}{2g} = \frac{P_B}{\gamma_w} + Z_B + \frac{\overline{V}_B^2}{2g} + \Delta h$$

In most of the ground water problems the kinetic energy (velocity head) as velocity .015ft/sec. ($\frac{v^2}{2g}$ is very small) being rather small, can be neglected and the equation can be taken as.

$$\frac{P_A}{\gamma_w} + Z_A = \frac{P_B}{\gamma_w} + Z_B + \Delta h$$

At any print in the flow domain the total head is given by

$$h = \frac{p}{\gamma_w} + z$$

2.2.2 Continuity Equations
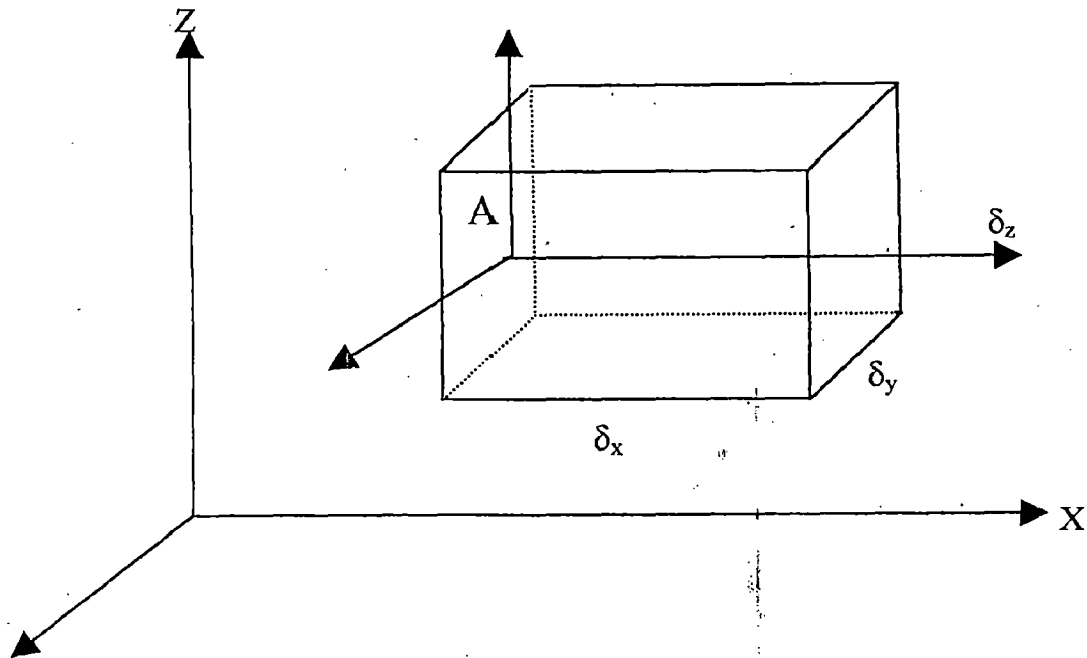
Consider an elementary parallelepiped figure of soil of dimension δ_x, δ_y, δ_z, let A (x,y,z) be the center of this rectangular block and let v_x, v_y and v_z represent the components of seepage velocity at the time t in x, y and z direction respectively let p represent the mass density of fluid.

The mass of fluid passing through the area dy-dz through the print A is (ρ, v_x, δ_y, δ_x) since ρv_x is general varies in x direction for a given value of y and z, the mass flowing through face δ_y, δ_z per unit time will be

$$= \rho v_x . \delta_y . \delta_z - \frac{\delta}{\delta_x}\left(\rho . v_x . \delta_y . \delta_z\right)\frac{\delta_x}{z}$$

$$= \delta_y . \delta_z\left[\rho v_x - \frac{\partial}{\partial x}(\rho v_x)\frac{\delta_x}{z}\right] \tag{1}$$

The mass of fluid flowing out per unit time

$$= \left(\rho v_x \delta_y . \delta_z\right) + \frac{\partial}{\partial x}\left(\rho v_x . \delta_y . \delta_z\right)\frac{\delta_x}{2}$$

$$= \delta_y . \delta_z\left[\rho v_x + \frac{\partial}{\partial_x}(\rho v_x)\frac{\delta x}{2}\right] \tag{2}$$

The net rate of inflow of mass (subtract (2) from (1)

$$= \delta_y . \delta_z\left[\rho v_x - \frac{\partial}{\partial_x}(\rho v_x)\frac{\delta_x}{2} - \rho v_x - \frac{\partial}{\partial_x}(\rho v_x)\frac{\delta_x}{2}\right]$$

$$= -\frac{\partial}{\partial x}\left(\rho v_x\right)\delta_x . \delta_y . \delta_z$$

Similarly the net rate of mass inflow through face δ_x. δ_y.

$$= -\frac{\partial}{\partial z}\left(\rho v_z\right)\delta_x . \delta_y . \delta_z$$

And the net rate of mass inflow through face $\delta_x.\delta_z$

$$= -\frac{\partial}{\partial y}\left(\rho v_y\right)\delta_x.\delta_y.\delta_z$$

The mass of fluid is represented by $\rho.\delta_x.\delta_y.\delta_z$

The rate of change of mass $= \frac{\partial}{\partial t}\rho.\delta_x.\delta_y.\delta_z$

The total rate of mass inflow into the parallelepiped through all the faces must be equal to the rate of change of mass of the parallelepiped.

$$\delta_x\delta_y.\delta_z.\frac{\partial \rho}{\partial t} = -\frac{\partial(\rho v_x)}{\partial x}\delta_x\delta_y\delta_z - \frac{\partial}{\partial y}\left(\rho v_y\right)\delta_x\delta_y\delta_z$$

$$-\frac{\partial}{\partial z}\left(\rho v_z\right)\delta_x\delta_y\delta_z$$

Dividing both the sides try $\delta_x,\delta_y,\delta_z$ and transposing

$$\frac{\partial \rho}{\partial t} + \frac{\partial(\rho v_x)}{\partial x} + \frac{\partial(\rho v_y)}{\partial y} + \frac{\partial(\rho v_z)}{\partial z} = 0$$

Which is continuity equation in Cartesian co-ordinary system? For incompressible fluids

$$\frac{\partial \rho}{\partial t} = 0$$

And the equation becomes

$$\frac{\partial v_x}{\partial x} + \frac{\partial v_y}{\partial y} + \frac{\partial v_z}{\partial z} = 0 \qquad\qquad (3)$$

2.2.3   Darcy's Law and the Sub-Soil Flow

The French hydraulician Henary Darcy in 1856 enunciated simple relation,

$$V = k \cdot i = -k \frac{\partial H}{\partial L}$$

i = Average hydraulic gradient $-\dfrac{dH}{dL}$

K = the coefficient of proportionality (otherwise called coefficient of permeability) having dimension of velocity

L = Elementary length along the path of flow.

It was established by Reynold's by series of experiments that within the range of laminar flow there exists a linear proportionality between hydraulic gradient and velocity of flow.

Ground water flow being mostly in laminar range, Darcy's law given an accurate representation of the flow within porous medium.

Darcy's low can be taken as valid when Reynold number is equal to or less then unity.

As already mentioned the movement of water in many cases of seepage flow may extend in three dimensions. In studying such problems we have to imagine the velocity of flow as having been resolved into three components along the three Cartesian co-ordinates for isotropic homogeneous media the vector law of Darcy represented by the equation can be written as

$$V_x = -k\frac{\partial H}{\partial x}$$

$$V_y = -k\frac{\partial H}{\partial y} \tag{4}$$

$$V_z = -k\frac{\partial H}{\partial z}$$

The equation of continuity is $\dfrac{\partial p}{\partial t} + \dfrac{\partial v_x}{\partial x} + \dfrac{\partial v_y}{\partial y} + \dfrac{\partial v_z}{\partial z} = 0$

Where ρ = mass density fluid for incompressible fluid as in the present case

$$\frac{\partial \rho}{\partial z} = 0$$

Since the flow of water in porous medium is similar to the flow in incompressible fluid which is assumed to replace both the water in the soil and soil itself. The equation of continuity reduces to

$$\frac{\partial v_x}{\partial x} + \frac{\partial v_y}{\partial y} + \frac{\partial v_z}{\partial z} = 0 \qquad\qquad (5)$$

This means that the volume of water flowing in an elementary volume of soil during a certain interval of time is equal to the volume of flowing out of it during the same interval of time.

By substitution of value of (1) in (2) we obtain the relation.

$$\frac{\partial^2 H}{\partial x^2} + \frac{\partial^2 H}{\partial y^2} + \frac{\partial^2 H}{\partial z^2} = 0$$

Which is well known Laplacian equation governing the subsoil flow?

The pressure head function 'H' satisfying this Laplacian equation is called potential function.

Analytical solution of seepage problems involves solution of the Laplacian equation with appropriate boundary conditions in each particular problem.

The function is continuous, finite and single valued at all points of the medium and the usual method of solution in potential theory can be employed.

The equation for the 2 dimensional flows will be

$$\frac{\partial^2 H}{\partial x^2} + \frac{\partial^2 H}{\partial y^2} = 0$$

2.2.4 Dupuit's Theory of Unconfined Flow

The Dupuit's theory of unconfined flow stems form two main assumptions.

(i)   For small inclination of the line of seepage the stream lines of seepage the stream lines can be taken as horizontal (hence, the equipotential lines approach the vertical).

(ii)   The hydraulic gradient is equal to the slope of the free surface and is invariant with depth.

Though the nature of these assumptions appears paradoxical, the solutions based on them have been found to compare favorably with experimental values.

Unconfined flow through soils was analyzed by Forchhemer and later by kochina. The other assumptions involved are;

(i)   Flow is with in the validity range of Darcy's law

(ii)   Soil is homogenous

(iii)   Fluid is incompressible

(iv)   The angular slope of free surface is small such that $\sin\theta = \tan\theta$

(v)   The flow region considered is such that the point to point variation is small

(vi)   The velocity of flow is almost horizontal i.e. the vertical component of the velocity is negligible.

2.3   DIFFERENT PROCEDURES FOR SOLVING SEEPAGE PROBLEM

(i)   Graphical method

(ii)   Hydraulic method

2-11

(iii)   Electrical analogy method

(iv)   Analytical method

2.3.1   Graphical Method (Flow Net Method)

The method of graphical field plotting is a widely used method more popularly known as "Forchhemer solution". The process is begun on a scale drawing of boundaries with assigned potentials by plotting any suitable number of intermediate equipotential lines. Flow lines or stream lines are then drawn to cut the equipotential lines orthogonally and to form curvilinear squares. The errors are corrected by systematic improvements as suggested by Taylor.

Advantages

1)   It requires little equipment and yields quick results.

2)   It gives result with considerable accuracy

3)   It gives clear idea about the subsoil flow of water.

Limitation & Disadvantages

1)   Graphical method is confined to two dimensional cases.

2)   Much experience and foresight are needed for correct representation of flow net by the trial and error method.

2.3.2   Hydraulic Models

Hydraulic models may be

(a)   Viscous fluid models

(b)   Scale models

Viscous fluid models are based on the principals that flow through two parallel plates placed at very small distance apart follow the Laplacian equation. The model is

fitted in and the fluid usually water or glycerin is made to flow under the model from the upstream to down stream side. When the flow become steady the stream lines can be traced by adding a colored solution of the same fluid at points and marking or photographing the path of such lines. Then equipotential lines are drawn orthogonal to the stream lines.

In hydraulic scale model sand is filled between two parallel plates. The pressures are observed by means of piezometric pipes introduced at proper points. The flow lines were made visible through sand by projecting potassium chromate and silver nitrate separately. As a result of chemical reaction red precipitate of silver chromate was produced along the stream lines which become clearly visible.

Advantages of Viscous Fluid Models

(1)   It is useful in giving a quick picture of stream lines under any work.

Disadvantages

The application of viscous fluid method is very limited.

Advantages of Hydraulic Scale Model

1)   The scope of hydraulic model is wide.

2)   It can reproduce effect of stratification and temperature variation.

3)   Hydraulic model can reproduce tail erosion and can effectively show the behavior of the standing wave and damage likely to occur from various conditions of surface flow.

4)   The accuracy of hydraulic model is within permissible limits i.e. reasonable.

Disadvantages or limitation of hydraulic scale model

2-13

1) In hydraulic models the scale and shape of model and the relative size of pressure points are the major source of error.

2) In much smaller scale hydraulic model capillary force will vitiate the results.

2.3.3 Electrical Analogy Method

Electrical analogy method is most common method. The analogy developed between the flow of fluid through pressure media which follows Darcy's law and flow of electricity through on electrolyte which follows Ohm's law is used. Two dimensional as well as three dimensional problems can be solved by this technique. This technique can be employed with reasonable accuracy to determine pressure under weirs, flow towards. Tube-wells, flow net in earth dams flow nets in galleries and coffer dams.

The electrical analogy technique was first tried for the study of 2-dimensional problems of seepage through porous media by Pavlovsky. The first successful attempt for the use of this technique in the study of 3 dimensional seepage problems was made by Reltov in 1933. The technique was letter employed by the Poona research station, U.S. Army water ways experiments station Vicksburgh, Irrigation Research Institute Roorkee.

It can be shown that there is an interesting analogy between the flow of electric current through a homogeneous conducting medium and the flow of water through a porous medium.

The Laplacian equation for the seepage flow of water through a porous medium and for the flow of electricity in homogeneous conductors are identical, the analogy will be more clear by comparison of the two laws viz. Darcy's law and ohms law as under

Darcy's law	Ohm's law

$$Q = \frac{K.A.H}{L}$$

$$I = \frac{K'.A'.V}{L'}$$

Q= Rate of flow of fluid

I = Rate of flow of electricity

K= Permeability coefficient of porous media

K' = conductivity coefficient of electrolyte

A = Area of cross section for the flow of water

A'= Area of cross section for the flow of Current

H = Head causing flow

V = voltage causing current.

L = Length of path of percolation

L' = length of path of current.

It is quite evident form the above comparison that there exists a striking similarity between the two laws and hence the seepage flow can be represented by an electric model.

Advantages of Electrical Analogy Method

1) Electric analogy method is much quicker then hydraulic model method.

2) The equipment is brief simple to setup. Reading can be taken very quickly.

3) Since probe is fine point which can locate the position of any pressure point with great precision. Electrical analogy method is more accurate then hydraulic model analogy.

4) Many complex problems which might have been difficult to solve can be solved by electrical analogy method.

Limitations of electrical analogy method.

(i) Electrical analogy methods yield good results only for flows within the range of Darcy's law.

(ii)   In problems of irrotational flow e.g. flow around submerged bodies of revolution, if separation occurs, the results in electrical analogy are no longer applicable as such flows can not be represented in analogue.

(iii)   There is no analogous force to the force of gravity to produce or represent pharatic surface

(iv)   The geologic feature like faults, fissures, dips, bedding planes etc. cannot be accounted for in the technique.

(v)   Anisotropy of the soil is not truly accounted for.

(vi)   The top flow lines must be located mathematically or by sand models.

(vii)   The permeability coefficient of the soil and the electrical resistance can not be related to each other and such direct assessment of the quantity, seepage below the structure is not possible.

(viii)   The working limitation such as fluctuations in impressed voltage, thickness of investigating probe, varying temperature and pH value of electrolyte solution, dissolved air and polarization on electrodes, unevenness of surface of copper plate and non uniformity of Resistance of potentiometers wire, are always present in model experiments.

(ix)   The reproduction of prototype conditions by reduction in scale of models, shape and size of model tray, limited depth of electrolyte for infinite depth of aquifer. Width of copper plates representing pervious reaches is not complete in model representation.

2.3.4 Analytical Method

Analytical method aims at the solution of Laplace equation mathematically which can be done with the help of conformal transformations and conjugate functions. In this method boundary conditions of the problem are expressed by equation and solution obtained mathematically. The method gives exact solution of the problem, although the method becomes involved for complicated boundary conditions.

Advantages of Analytical Method

(i)   Analytical method is accurate method

Limitation:

For complex boundary condition, it is very cumbersome to solve the problem.

Now with the help of powerful digital computer these complex problems can be solved by finite element method up to desirable accuracy.

Finite Element Method

High speed electronic digital computers have enabled engineers to employ various numerical discretisation techniques for approximate solution of complex problems. The finite element method (FEM) is one such technique. It was originally developed as a tool for structural analysis but the theory and formulation have been progressively so refined and generalized that the method has been applied successfully to such other fields as heat flow, seepage, hydrodynamics and rock mechanics. As a result of broad applicability and the systematic generality of the associated computer codes, the method has gained wide acceptance by designers and research engineers.

Finite element method or finite element analysis some times abbreviated as FEM or FEA was first introduced by R. Courant in 1943. He proposed breaking a continuum

problem into approximation within the triangular regions and replacing the fields with piecewise approximations within the triangles, and it was probably established by several pioneers almost independently. But substantial development took place after 1966 when Clough and Wood Ward introduced finite element method to the geotechnical engineering.

Many of the equations governing the flow problems are non linear and most of the natural conditions are extremely complex. Analytical (closed form) methods are usually not suitable for such problems, and recourse to the recently developed numerical methods becomes necessary. Finite element method is technique where by difficulty of mathematically solving large complex geometric problems are transferred from a differential equation approach to a linear algebraic problem.

2.4   CONCLUSION

From the above literature review, it may be concluded that finite element method is a suitable technique for 3-dimensional seepage analysis. The details are given in chapter 3.

THE FINITE ELEMENT METHOD

3.1 GENERAL

The finite element method is a numerical analysis technique for obtaining approximate solutions to a wide variety of engineering problems like analyzing structures for stresses and deformation, surface and subsurface floors for hydraulic structures. The most distinctive feature of finite element method that separates it from others is the division of a given domain into a set of sub-domains, called elements. The finite element procedure produces many simultaneous algebraic equations, which are generated and solved on a digital computer. Results are rarely exact. However, processing more equations minimizes errors, and results become accurate enough for engineering purposes at reasonable cost.

Using such elements, the structural idealization is obtained merely by dividing the original continuum into segments, all the material properties of the original system being retained in the individual elements. This is known as discretisation. Instead of solving the problem for entire body in one operation, the solutions are formulated at each constituent unit and combined to obtain the solution for the original structure.

3.2 DESCRIPTION OF THE METHOD

3.2.1 Discretization of the Continuum

Discretization is the process in which the given body is subdivided into an equivalent system of finite elements. Hence the body of the structure is essentially a piece of the whole. These elements provide natural representation of the properties of the original continuum. It may be noted that the continuum is simply zoned into small

regions by imaginary planes in 3-D bodies and by imaginary lines in 2-D bodies. The first decision is to make the choice of the elements type. The boundaries of finite element may be straight or curvilinear.

The size of the element and the number in which the continuum is to be discretized depends upon the choice of the designer. As a general guideline it can be said that where the stress or strain gradients are expected to be comparatively flat i.e. variation is not rapid, the mesh can be coarse to reduce computations. Whereas in the zones in which stress or strain gradients are expected to be steep i.e. pronounce variation occurs a finer mesh indicated to get more accurate results. Theoretically speaking to get an exact solution the number of nodal points is finite. So a compromised has to be made between computation effort and corresponding accuracy.

3.2.2 Selection of Proper Interpolation or Displacement Model

In finite element method we approximate a solution to a complicated problem by subdividing the region of interest into finite number of elements and representing the solution within each element by a relatively simple function of polynomials for ease of computation. The degree of the polynomial chosen depends on the number of nodes assigned to the element.

For the triangular element the linear polynomial

$$\phi = \alpha_1 + \alpha_2 x + \alpha_3 y \qquad\qquad (3.1)$$

is appropriate,

where α_1, α_2, and α_3 are constants which can be expressed in terms of ϕ_1, ϕ_2 and ϕ_3 which are the values of ϕ at these nodes.

For 10 node tetrahedral element, a quadratic variation is given by

3-2

$$\phi = \alpha_1 + \alpha_2 x + \alpha_3 y + \alpha_4 z + \alpha_5 x^2 + \alpha_6 y^2 + \alpha_7 z^2 + \alpha_8 xy + \alpha_9 xz + \alpha_{10} yz \quad (3.2)$$

To have a complete polynomial of nth order, the tetrahedral must have $\frac{1}{6}(n+1)*(n+2)*(n+3)$ nodes when ϕ is the only nodal variable.

For the four nodded quadrilateral the bilinear function

$$\phi = \alpha_1 + \alpha_2 x + \alpha_3 y + \alpha_4 xy \quad (3.3)$$

is appropriate.

Eight node quadrilateral has eight α_i in its polynomial expansion and can represent a parabolic function.

Equation (3.1) and (3.3) are interpolations of function ϕ in terms of the position (x, y) within an element.

3.2.3 Convergence Requirements

In any acceptable numerical formulation the numerical solution must converge or tend to the exact solution of the problem. For this the criteria are:

a) **Displacement models must be continuous within the element and the displacements must be compatible within the adjacent elements.**

The first part is automatically satisfied if displacement functions are polynomials. The second part implies that the adjacent elements must deform without causing openings, overlaps or discontinuities between them. This can be satisfied if displacements along the side of an element depend only upon displacements of the nodes occurring on that side. Since the displacements of nodes on common boundary will be same, displacement for boundary line for both elements will be identical.

b) The displacement model must include rigid body displacement of the element.

Basically, this condition states that there should exist such combinations of value of coefficients in displacement function that cause all points in the elements to experience the same displacement.

c) The displacement model must include the constant strain stress of elements.

This means that there should exist such combinations of values of the coefficients in the displacement function that cause all points on the element to experience the same strain. The necessity of this requirement can be understood, if we imagine that the continuum is divided into infinitesimally small elements. In such a case the strains in each element approach constant values all over the element. The elements, which meet first criterion, are called compatible or conforming. The elements which meet second and third criteria are called complete. For plain strain and plain stress and 3-D elasticity the three conditions mentioned above are easily satisfied by linear polynomials.

3.2.4 Nodal Degree Of Freedom

The nodal displacements, rotations and/or strains necessary to specify completely the deformation of finite elements or the parameter assigned to an element are called degree of freedom (DOF) of elements.

3.2.5 Element Stiffness Matrix

The equilibrium equation derived from principle of minimum potential energy between nodal loads and nodal displacements is expressed as

$$\{F\}e = [K]e \{\delta\}e$$

Where, $\{F\}e$ = nodal force vector

$[K]e$ = element stiffness matrix, and

$\{\delta\}e$ = nodal displacement vector.

The stiffness matrix consists of the coefficients of equilibrium equations derived from material and geometric properties of the element. Stiffness of a structure is an influence coefficient that gives the force at one point on a structure associated with a unit displacement at the same or a different point.

Local material properties as stated above are one of the factors, which determine stiffness matrix. For an elastic isotropic body, Modulus of elasticity (E) and Poison's Ratio (ν) define the local material properties. The stiffness matrix is essentially a symmetric matrix, which follows from the principle of stationary potential energy, that "In an elastic structure work done by internal forces is equal in magnitude to the change in strain energy". And also from Maxwell Betti reciprocal theorem which states that: " If two sets of loads $\{F\}_1$ and $\{F\}_2$ act on a structure, work done by the first set in acting through displacements caused by the second set is equal to the work done by second set in acting through displacements caused by first set".

3.2.6 Nodal Forces and Loads

Generally when subdividing a structure we select nodal locations that coincide with the locations of the concentrated external forces. In case of distributed loading over the body such as water pressure on dam or the gravity forces the loads acting over an element are distributed to the nodes of that element by principle of minimum potential energy. If the body forces are due to gravity only then they are equally distributed among the three nodes of a triangular element.

3-5

3.2.7 Assembly of Algebraic Equations for the Overall Discretized Continuum

This procedure includes the assembly of overall or global stiffness matrix for the entire body from individual stiffness matrices of the elements and the overall or global force or load vectors. In general the basis for an assembly method is that the nodal interconnections require the displacement at a node to be the same for all elements adjacent to that node. The overall equilibrium relations between global stiffness matrix [K], the total load vector {F} and the nodal displacement vector for entire body {δ} is expressed by a set of simultaneous equations.

$$[K]\{\delta\} = \{F\}$$

The global stiffness matrix K will be banded and also symmetric of size of n x n where, n = total number of nodal points in the entire body. The steps involved in generation of global stiffness matrix are:

i) **All elements of global stiffness matrix [K] are assumed to be equal to zero.**

ii) **Individual element stiffness matrix [K] is determined successively.**

iii) **The element k_{ij} of element stiffness matrix are directed to the address of element K_{ij} of global stiffness matrix which means**

$$K_{ij} = \Sigma\ k_{ij}$$

Similarly nodal load $\{F_i\}^e$ at a node 'i' of an element 'e' is directed to the address of $\{F_i\}$ of total load vector i.e.

$$\{F_i\} = \Sigma\ \{F_i\}^e$$

3.2.8 Boundary Conditions

A problem in solid mechanics is not completely specified unless boundary conditions are prescribed. Boundary conditions arise from the fact that at certain points or near the edges the displacements are prescribed. The physical significance of this is that a loaded body or a structure is free to experience unlimited rigid body motion unless some supports or kinematic constraints are imposed that will ensure the equilibrium of the loads. These conditions are called the boundary conditions. There are two basic types of boundary conditions, geometric and natural. One of the principal advantages Finite Element Method is, we need to specify only geometric boundary conditions, and the natural boundary conditions are implicitly satisfied in the solution procedure as long as we employ a suitable valid variational principle. In other numerical methods, solutions are to be obtained by trial and error method to satisfy boundary conditions whereas in Finite Element Method boundary conditions are inserted prior to solving algebraic equations and the solution is obtained directly without requiring any trial.

3.2.9 Solution for the Unknown Displacements

The algebraic equations $[K]\{\delta\} = \{F\}$ formed are solved for unknown displacements $\{\delta\}$ wherein, $[K]$ and $\{F\}$ are already determined. The equations can be solved either by iterative or elimination procedure. Once the nodal displacements are found, then elements strains or stress can be easily found from generalized Hooke's law for a linear isotropic material.

The assumption in displacement function is, the stresses or strains are constant at all points over the element, may cause discontinuities at the boundaries of adjacent elements. To avoid this, sometimes it is assumed the values of stresses and strains

3-7

obtained are for the centers of gravity of the elements and linear variation is assumed to calculate them at other points in the body.

3.3   SUMMARY OF PROCEDURE

The principal computational steps of linear static stress analysis by Finite Element Method are now listed.

i)   **Input and Initialization**: Input the number of nodes and elements, nodal co-ordinates, structure node numbers of each element, material properties, temperature changes, mechanical loads and boundary conditions. Reserve storage space for structure arrays [K] and {F}. Initialize [K] and {F} to null arrays. If array ID is used to manage boundary conditions, initialize ID and then convert it to a table of equation numbers.

ii)   **Compute Element Properties**: For each element, compute element property matrix [k] and element load vector {f}.

iii)   **Assemble The Structure**: Add [k] into [K] and {f} into {F}. Go back to step (ii), repeat steps (ii) and (iii) until all elements are assembled. Add external loads {P} to {F}. Impose displacement boundary conditions (if not imposed implicitly during assembly by use of array ID).

iv)   **Solve The Equations**: $[K]\{\delta\} = \{F\}$ for $\{\delta\}$

v)   **Stress Calculation**: For each element extract nodal D.O.F. of element $\{\delta\}e$ from nodal D.O.F. of structure$\{\delta\}$. Compute mechanical strains, if any and convert resultant strains to stresses.

3-8

3.4   MATHEMATICAL MODEL

3.4.1   General

Most Engineers and Scientists studying physical phenomena are involved with two major tasks:

1. Mathematical formulation of the physical process.

2. Numerical analysis of the mathematical model.

Development of the mathematical model of a process is achieved through assumptions concerning how the process works. In a numerical simulation, we use a numerical method and a computer to evaluate the mathematical model. While the derivation of the governing equations for most problems is not unduly difficult, their solution by exact methods of analysis is a formidable task. In such cases, approximate methods of analysis provide alternative means of finding solution. Amongst this Finite Element Method is most frequently used.

Finite Element Method is endowed with three basic features.

i.   A geometrically complex domain of the problem is represented as a collection of geometrically simple sub domains called finite elements.

ii. Over each element, the approximation functions are derived using the basic idea that any continuous function can be represented by a linear combination of algebraic polynomials.

iii. Algebraic relations among the undetermined coefficients (i.e. nodal values) are obtained by satisfying the governing equations over each element.

The approximation functions are derived using concepts from interpolation theory and are called interpolation functions. The degree of interpolation functions depends on the number of nodes in the element and the order of differential equation being solved.

3.4.2 Interpolation Function

The finite element approximation $U^e(x,y)$ of $u(x,y)$ over an element Ω^e must satisfy the following conditions in order for the approximate solution to be convergent to the true one.

1. U^e must be differentiable.

2. The polynomials used to represent U^e must be complete (i.e. all terms beginning with a constant term up to the highest order used in the polynomial should be included in U^e).

3. All terms in the polynomial should be linearly independent.

The number of linearly independent terms in the representation of U^e dictates the shape and number of DOF of the element.

3.4.3 Displacement Function
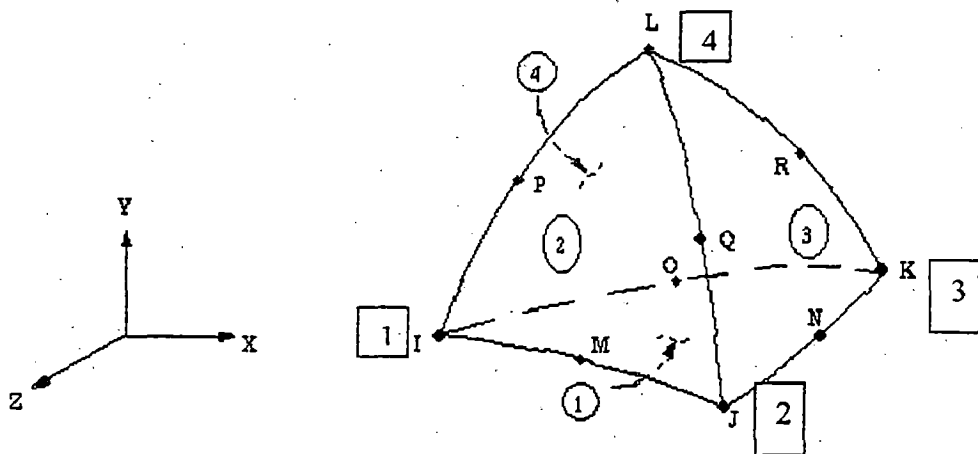
SOLID87 3-D 10-Node Tetrahedral Thermal Solid

Figure 3.1

3-10

A 10 nodded isoparametric finite element is shown in fig. 3.1. For a typical finite element 'e' defined by nodes i, j, k etc. the displacements {f} within the element are expressed as:

$$\{f\} = [N] \{\delta\}^e$$

where $[N] = [N_i \quad N_j \quad N_m \quad ....]$ (3.4)

and $\{\delta\}^e = \{\delta_i \quad \delta_j \quad \delta_m \quad ....\}$ (3.5)

The components of [N] are in general functions of position and $\{\delta\}^e$ represents a listing of nodal displacements for a particular element.

For the three dimensional element

$$\{f\} = \begin{Bmatrix} u \\ v \\ w \end{Bmatrix}$$ (3.6)

represents the displacements in x, y and z directions at a point within the element and

$$\{\delta_i\} = \begin{Bmatrix} u_i \\ v_i \\ w_i \end{Bmatrix}$$ (3.7)

are the corresponding displacements of node i.

$[N_i]$ is equal to $[IN]$ where N_i is the shape function of node I and I is an identity matrix.

3.4.4 Shape Functions

The shape functions of a 10-node isoparametric tetrahedral element used in this study (shown in fig.3.1) are given by the following.

At corner nodes (node numbers I, J, K, L)

$$N_i = L_i(2L_i-1) \tag{3.8a}$$

For mid side nodes:

i) $N_M = 4L_1L_2$ (3.8b)

ii) $N_O = 4L_1L_3$ (3.8c)

iii) $N_P = 4L_1L_4$ (3.8d)

iv) $N_N = 4L_2L_3$ (3.8e)

v) $N_R = 4L_3L_4$ (3.8f)

vi) $N_Q = 4L_2L_4$ (3.8g)

Where, $L_1+L_2+L_3+L_4 = 1$ (3.9)

L_1, L_2, L_3 and L_4 are the local (volume) coordinates of the point concerned.

The other elements used in 2-D and 3-D analysis are given in figure 3.2 to figure 3.5.
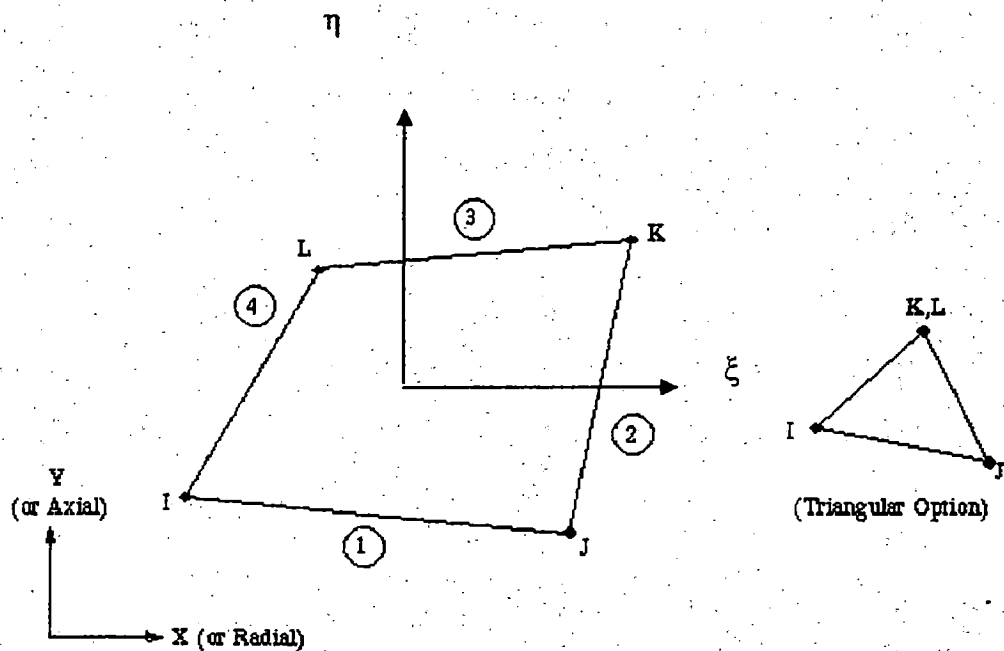
PLANE55   2-D Thermal Solid

Figure 3.2 (2-D four nodded rectangular element)

The shape function for four nodded rectangular element used in analysis

(Plane 55 2-D thermal solid) are given by the following:

$N_i = 1/4(1+\xi_0)(1+\eta_0)$, where $\xi_0 = \xi^* \xi_i$, $\eta_0 = \eta^* \eta_i$,
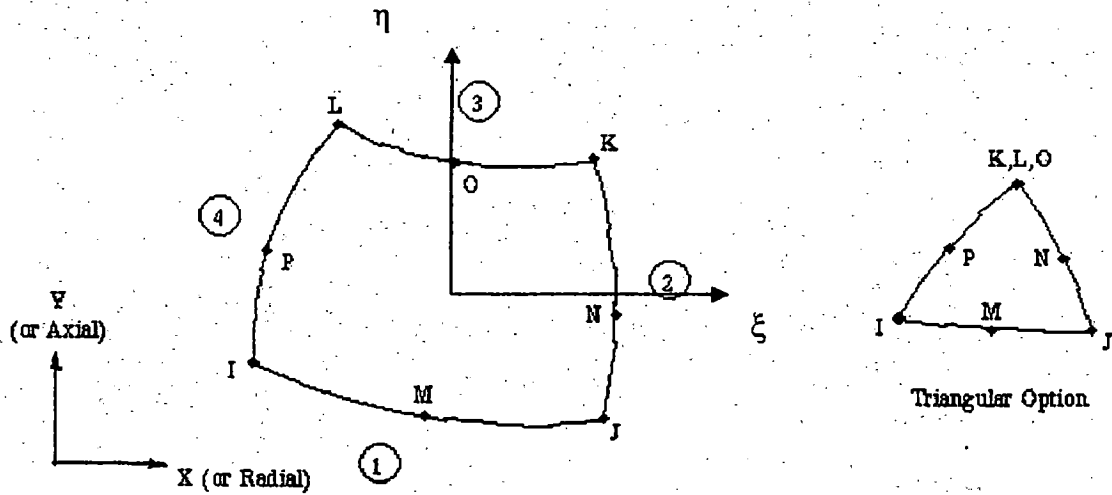
PLANE77 2-D 8-Node Thermal Solid

Figure   3.3,   8 Nodded Quadratic (parabolic element) element.

The shape function for 8 nodded quadratic element used in analysis (Plane

77 2-D thermal solid) are given by the following:

At corner nodes (node numbers I, J, K, L)

$N_i = 1/4(1+\xi_0)(1+\eta_0)(-1+ \xi_0 +\eta_0)$, where $\xi_0 = \xi^* \xi_i$, $\eta_0 = \eta^* \eta_i$,

For mid side nodes (Node O&M)

$N_i = 1/2(1- \xi^2)(1+\eta_0)$, where $\xi = 0$, $\eta_0 = \pm 1$,

For mid side nodes (Node P & N)

$N_i = 1/2(1- \eta^2)(1+\xi_0)$, where $\xi = \pm 1$, $\eta = 0$,
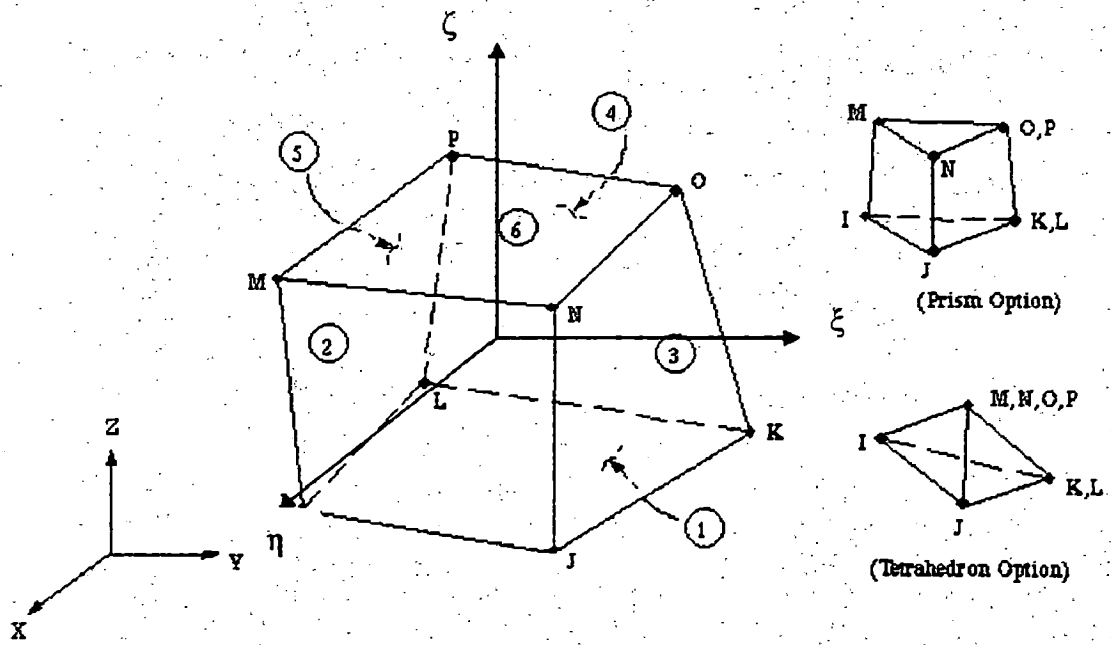
Figure   SOLID70   3-D Thermal Solid

Figure 3.4, 8 Nodded cuboid element.

The shape function for eight nodded cuboid element used in analysis (Solid 70, 3-D thermal solid) are given by following:

Shape function for nodes (I,J,K,L,M,N,O,P)

$$N_i = 1/8(1+\xi_0)(1+\eta_0)(1+\zeta_0),$$
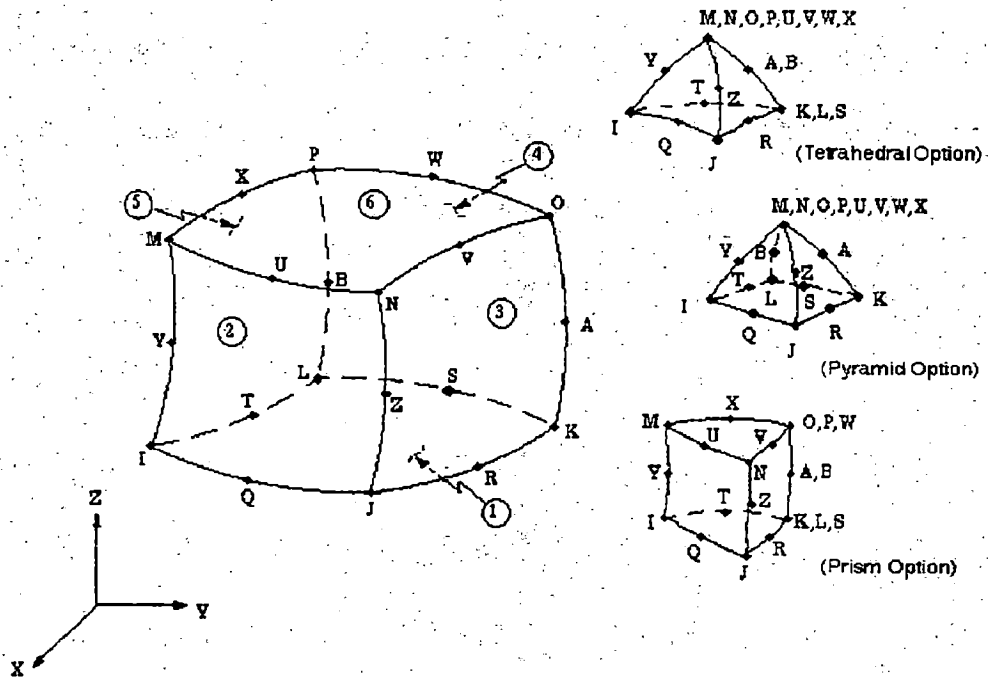
SOLID90 3-D 20-Node Thermal Solid

Figure 3.5, 20 Nodded brick element.

The shape functions for twenty nodded brick element used in analysis (Solid 90, 3-D thermal solid) are given by following:

At corner nodes (I, J, K, L, M, N, O, P)

$N_I = 1/8(1+\xi_0)(1+\eta_0)(1+\zeta_0)(-2+\xi+\eta+\zeta)$, Where, $\xi_0 = \xi * \xi_i$

$\eta_0 = \eta * \eta_i$, $\zeta_0 = \zeta * \zeta_i$.

At mid nodes (R, T, V, X)

$N_i = 1/4(1-\eta^2)(1+\xi_0)(1+\zeta_0)$, Where, $\xi_0 = \xi * \xi_i$, $\zeta_0 = \zeta * \zeta_i$.

At mid nodes (Q, S, W, U)

$N_i = 1/4(1-\xi^2)(1+\eta_0)(1+\zeta_0)$

At mid nodes (A, B, Y, Z)

$N_i = 1/4(1-\zeta^2)(1+\xi_0)(1+\eta_0)$

3-15

3.4.5 Strains

With displacements known at all points within the element the strains at any point can be determined. Six strain components are relevant in three-dimensional analysis and the strain vector can be expressed as:

$$
\{\in\} = \begin{Bmatrix} \in_x \\ \in_y \\ \in_z \\ \in_{xy} \\ \in_{yz} \\ \in_{zx} \end{Bmatrix} = \begin{Bmatrix} \dfrac{\partial u}{\partial x} \\[6pt] \dfrac{\partial v}{\partial y} \\[6pt] \dfrac{\partial w}{\partial z} \\[6pt] \dfrac{\partial u}{\partial y}+\dfrac{\partial v}{\partial x} \\[6pt] \dfrac{\partial v}{\partial z}+\dfrac{\partial w}{\partial y} \\[6pt] \dfrac{\partial w}{\partial x}+\dfrac{\partial u}{\partial z} \end{Bmatrix}
\tag{3.10}
$$

This can be further written as:

$$
\{\in\}=[B]\{\delta\}^e= [B_i\ \ B_j\ \ B_k\ \ ...]\ \{\delta\}^e
\tag{3.11}
$$

in which $[B_i]$ is the strain displacement matrix.

$[B_i]$ is given by

$$[B_i] = \begin{bmatrix} \dfrac{\partial N_i}{\partial x} & 0 & 0 \\[2ex] 0 & \dfrac{\partial N_i}{\partial y} & 0 \\[2ex] 0 & 0 & \dfrac{\partial N_i}{\partial z} \\[2ex] \dfrac{\partial N_i}{\partial y} & \dfrac{\partial N_i}{\partial x} & 0 \\[2ex] 0 & \dfrac{\partial N_i}{\partial z} & \dfrac{\partial N_i}{\partial y} \\[2ex] \dfrac{\partial N_i}{\partial z} & 0 & \dfrac{\partial N_i}{\partial x} \end{bmatrix} \qquad (3.12)$$

with other sub matrices obtained in a similar manner simply by interchange of subscripts.

For isoparametric elements

$$x = \sum_{i=1}^{n} N_i x_i \quad ; \; y = \sum_{i=1}^{n} N_i y_i \quad ; \; z = \sum_{i=1}^{n} N_i z_i \quad ;$$

$$u = \sum_{i=1}^{n} N_i u_i \quad ; \; v = \sum_{i=1}^{n} N_i v_i \quad ; \; w = \sum_{i=1}^{n} N_i w_i \qquad (3.13)$$

The summation being over total number of nodes in an element.

Because the displacement model is formulated in terms of the natural coordinates L_1, L_2 and L_3, and it is necessary to relate Eq. (3.12) to the derivatives with respect to these local coordinates.

The natural coordinates L1, L2 and L3 are functions of global coordinates x, y, and z. Using the chain rule of partial differentiation we can write:

$$\frac{\partial N_i}{\partial L_1} = \frac{\partial N_i}{\partial x} \cdot \frac{\partial x}{\partial L_1} + \frac{\partial N_i}{\partial y} \cdot \frac{\partial y}{\partial L_1} + \frac{\partial N_i}{\partial z} \cdot \frac{\partial z}{\partial L_1} \qquad (3.14)$$

Performing the same differentiation with respect to the other two co-ordinates and writing in matrix form

$$\begin{Bmatrix} \dfrac{\partial N_i}{\partial L_1} \\[2mm] \dfrac{\partial N_i}{\partial L_2} \\[2mm] \dfrac{\partial N_i}{\partial L_3} \end{Bmatrix} = \begin{bmatrix} \dfrac{\partial x}{\partial L_1} & \dfrac{\partial y}{\partial L_1} & \dfrac{\partial z}{\partial L_1} \\[2mm] \dfrac{\partial x}{\partial L_2} & \dfrac{\partial y}{\partial L_2} & \dfrac{\partial z}{\partial L_2} \\[2mm] \dfrac{\partial x}{\partial L_3} & \dfrac{\partial y}{\partial L_3} & \dfrac{\partial z}{\partial L_3} \end{bmatrix} * \begin{Bmatrix} \dfrac{\partial N_i}{\partial x} \\[2mm] \dfrac{\partial N_i}{\partial y} \\[2mm] \dfrac{\partial N_i}{\partial z} \end{Bmatrix} = [J] \begin{Bmatrix} \dfrac{\partial N_i}{\partial x} \\[2mm] \dfrac{\partial N_i}{\partial y} \\[2mm] \dfrac{\partial N_i}{\partial z} \end{Bmatrix} \qquad (3.15)$$

Where [J] is given by:

$$[J] = \begin{bmatrix} \dfrac{\partial x}{\partial L_1} & \dfrac{\partial y}{\partial L_1} & \dfrac{\partial z}{\partial L_1} \\[2mm] \dfrac{\partial x}{\partial L_2} & \dfrac{\partial y}{\partial L_2} & \dfrac{\partial z}{\partial L_2} \\[2mm] \dfrac{\partial x}{\partial L_3} & \dfrac{\partial y}{\partial L_3} & \dfrac{\partial z}{\partial L_3} \end{bmatrix} \qquad (3.16)$$

The matrix [J] is called the Jacobian matrix. The global derivatives can be found by inverting [J] as follows:

$$\begin{Bmatrix} \dfrac{\partial N_i}{\partial x} \\[2mm] \dfrac{\partial N_i}{\partial y} \\[2mm] \dfrac{\partial N_i}{\partial z} \end{Bmatrix} = [J]^{-1} \begin{Bmatrix} \dfrac{\partial N_i}{\partial L_1} \\[2mm] \dfrac{\partial N_i}{\partial L_2} \\[2mm] \dfrac{\partial N_i}{\partial L_3} \end{Bmatrix} \qquad (3.17)$$

Substituting Eq. (3.13) into Eq. (3.16) the Jacobian matrix is given by

$$[J] = \begin{bmatrix} \sum \dfrac{\partial N_i}{\partial L_1} x_i & \sum \dfrac{\partial N_i}{\partial L_1} y_i & \sum \dfrac{\partial N_i}{\partial L_1} z_i \\[3mm] \sum \dfrac{\partial N_i}{\partial L_2} x_i & \sum \dfrac{\partial N_i}{\partial L_2} y_i & \sum \dfrac{\partial N_i}{\partial L_2} z_i \\[3mm] \sum \dfrac{\partial N_i}{\partial L_3} x_i & \sum \dfrac{\partial N_i}{\partial L_3} y_i & \sum \dfrac{\partial N_i}{\partial L_3} z_i \end{bmatrix} \qquad (3.18a)$$

3-18

$$[J] = \begin{bmatrix} \dfrac{\partial N_1}{\partial L_1} & \dfrac{\partial N_2}{\partial L_1} & \cdots\cdots \\[2mm] \dfrac{\partial N_1}{\partial L_2} & \dfrac{\partial N_2}{\partial L_2} & \cdots\cdots \\[2mm] \dfrac{\partial N_1}{\partial L_3} & \dfrac{\partial N_2}{\partial L_3} & \cdots\cdots \end{bmatrix} \begin{bmatrix} x_1 & y_1 & z_1 \\ x_1 & y_1 & z_1 \\ x_1 & y_1 & z_1 \\ \cdot & \cdot & \cdot \\ \cdot & \cdot & \cdot \\ \cdot & \cdot & \cdot \end{bmatrix} \qquad (3.18b)$$

Stresses

The stresses are related to the strains as:

$$\{\sigma\} = [D](\{\in\} - \{\in_0\})\{\sigma_0\} \qquad (3.19)$$

Where [D] is an elasticity matrix containing the appropriate material properties.

$\{\in_0\}$ is the initial strain vector.

$\{\sigma\}$ is the stress vector given by,

$$\{\sigma\} = \{\sigma_x, \quad ,\sigma_y, \quad \sigma_z, \quad \sigma_{xy}, \quad \sigma_{yz}, \quad \sigma_{zx}, \quad \}^T \text{ and }$$

$\{\sigma_0\}$ is the initial stress vector.

For elastic, isotropic material the elasticity matrix is given by

$$[D] = \dfrac{E}{(1+\nu)(1-2\nu)} \begin{bmatrix} 1-\nu & \nu & \nu & 0 & 0 & 0 \\ \nu & 1-\nu & \nu & 0 & 0 & 0 \\ \nu & \nu & 1-\nu & 0 & 0 & 0 \\ 0 & 0 & 0 & \dfrac{1-2\nu}{2} & 0 & 0 \\ 0 & 0 & 0 & 0 & \dfrac{1-2\nu}{2} & 0 \\ 0 & 0 & 0 & 0 & 0 & \dfrac{1-2\nu}{2} \end{bmatrix} \qquad (3.20)$$

Where E is the Young's modulus of elasticity and ν is the Poisson's ratio of the material of the element.

Stiffness Matrix

The stiffness matrix of the element is given by the following relation

$$\{F\}^e = [K]^e \{\delta\}^e \qquad (3.21)$$

Where $\{F\}^e$ is the element nodal load vector, $\{\delta\}^e$ is nodal displacement vector and $[K]^e$ is the element stiffness matrix given by:

$$[K]^e = \int_v [B]^T [D][B] \, dV = [B]^T[D][B] \int_v dV = [B]^T[D][B]\, V \qquad (3.22)$$

Where V refers to the volume of the element.

The equivalent nodal forces are obtained as

i)   Forces due to body forces $\{\Phi_x, \Phi_y, \Phi_z\}^T$ per unit volume are given by

$$\{F\}_b = \int_v [N]^T \{\Phi\} dV \qquad (3.23a)$$

ii)   Forces due to pressure distribution $\{p_x, p_y, p_z\}^T$ per unit area are given by:

$$\{F^e\}_p = \int [N]^T \{p\} dA \qquad (3.23b)$$

For the complete structure relation of the form

$$[K] \{\delta\} = \{F\}$$

is obtained.

Where $\{\delta\}$ is the vector of global displacements, $\{F\}$ the nodal vector and [K] the stiffness matrix.

The global stiffness matrix [K] is obtained by directly adding the individual stiffness coefficients in the global stiffness matrix. Similarly the global load vector for the

system is also obtained by adding individual element loads at the appropriate locations in the global vector.

The mathematical statement of the assembly procedure is:

$$[K] = \sum_{e=1}^{E} [K]^e$$

$$\{F\} = \sum_{e=1}^{E} \{F\}^e \tag{3.25}$$

Where E is the total number of elements.

To transform the variable and the region with respect to which the integration is made the relationship

$$dV = dx\ dy\ dz = \det[J]\ dL_1\ dL_2\ dL_3 \tag{3.26}$$

is used.

Writing explicitly

$$\int_v L_1^\alpha L_2^\beta L_3^\gamma L_4^\delta = \frac{\alpha!\,\beta!\,\gamma!\,\delta!}{(\alpha+\beta+\gamma+\delta)!}\ 6V \tag{3.27}$$

and the characteristic element stiffness matrix can be expressed as

$$[K]^e = [B]^T\,[D]\,[B]\int_v L_1^\alpha L_2^\beta L_3^\gamma L_4^\delta \tag{3.28}$$

A 2 x 2 x 2 integration has been used for the three dimensional analysis.

3.5 SIGN CONVENTION
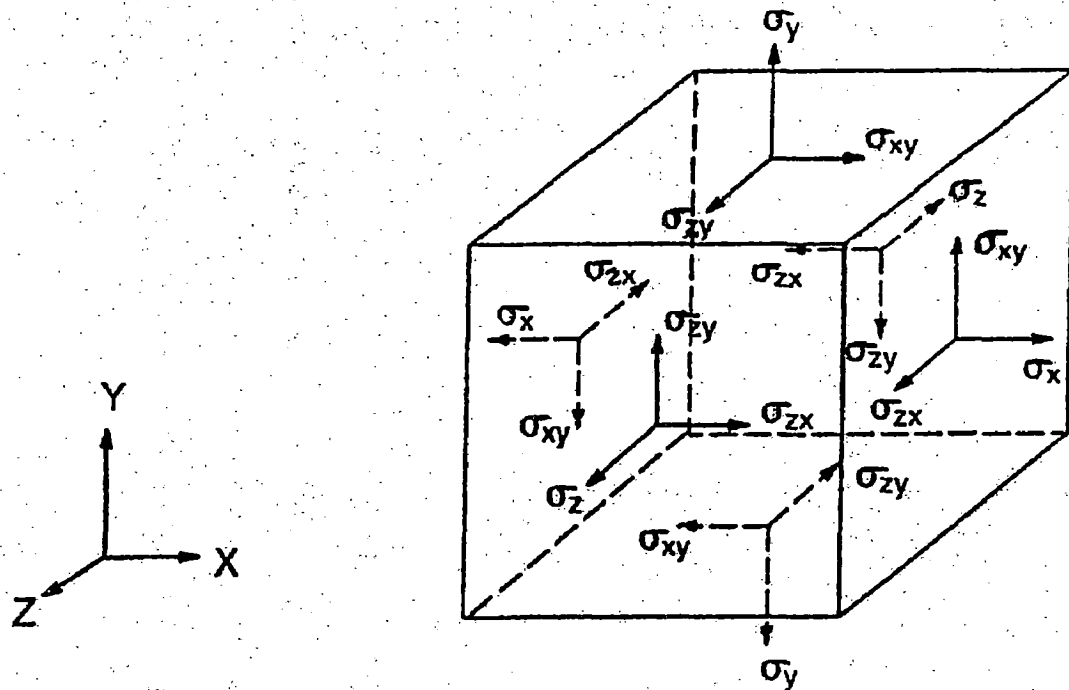
FIG.3.6: STRESS VECTOR DEFINITION

The stress vectors are shown in fig.3.6. The sign convention for ANSYS programme is that tension is positive and compression is negative. Shear is positive when it rotates in anti-clockwise direction about positive axes.

3.6 FINITE ELEMENT METHOD FOR FIELD PROBLEMS(10, 26)

The basic differential equation governing, torsion, heat conduction, and seepage may be expressed in general form as

$$\frac{\partial}{\partial x}\left(k_x \frac{\partial \phi}{\partial x}\right) + \frac{\partial}{\partial y}\left(k_y \frac{\partial \phi}{\partial y}\right) + \frac{\partial}{\partial z}\left(k_z \frac{\partial \phi}{\partial z}\right) + Q = C\frac{\partial \phi}{\partial t}$$

where ϕ is unknown temperature, or potential, k_x, k_y, and k_z are thermal conductivities or permeability coefficient, in x, y and z directions Q is externally applied heat flux, Q is positive for pumping in and negative for pumping out, C is specific heat, if time dependent term on right hand side vanishes then the problem becomes steady state.

3.6.1 Steps in Finite Elements Method for Field Problem

i)   Discretization of the continuum. In this process the continuum is divided into an equivalent system of finite elements. Our concept of the continuum assemblage is broadened. In the seepage problem, for example, our elements are fixed in space and do not change in size or shape while the fluid seeps through them.

ii) Selection of the field variable models. Assumed patterns of the filed variables within each element are selected, usually in polynomial form. The unknowns of the system thereby become the amplitude of the variables at the nodes, for seepage the field variables is usually the hydraulic head. This is scalar quantity while displacements are the vectors. Hence only one unknown amplitude occurs at each node (if gradients are not used as basic unknowns).

(iii) Derivation of finite element equations. The derivation of the finite element equations may be achieved by direct methods, variational methods or residual method. The associated functional for the seepage problem is

$$A = \iiint_v \frac{1}{2}\left[k_x\left(\frac{\partial\phi}{\partial x}\right)^2 + k_y\left(\frac{\partial\phi}{\partial y}\right)^2 + k_z\left(\frac{\partial\phi}{\partial z}\right)^2 \right] dv.$$

Here ϕ is the hydraulic head and k's are the permeabilities of the medium. The resulting property matrix is the permeability matrix.

3-23

4. Assembly of the algebric equations for the overall discretized continuum. The assembly process is exactly analogous to that for the displacement method, that is, the direct stiffness method is used to obtain an overall permeability matrix.

5. Solution for the nodal field variable vector. The solution of the overall equation is achieved by the matrix method. If the problem is nonlinear, incremental procedures, iterative procedures, mixed procedures and others can also be applied provided the nature of the material or geometric non linearity is understood.

6. Computation of the element resultants from the nodal field variables amplitudes, computation of the element resultants, or secondary field variables, will be governed by the type of problem being considered. However this process is generally analogous to the calculation of stress and for strains in the displacement method. In the seepage problem typical element resultants derived are the potential, gradient, fluid velocities and for flow rates. This analysis is concerned with potentials & gradients.

3.6.2 Seepage Equations

The steady state seepage through a porous medium is governed by the following differential equation:

$$\frac{\partial}{\partial x}\left[Kx.\frac{\partial \Phi}{dx}\right]+\frac{\partial}{\partial y}\left[Ky.\frac{\partial \Phi}{dy}\right]+\frac{\partial}{\partial z}\left[Kz.\frac{\partial \Phi}{dz}\right]+Q=0$$

with the boundary condition $\phi=\phi_B$ on S_1 where

ϕ : is the unknown (potential)

K_x, K_y and K_z : are the permeability coefficients in x,y and z directions respectively.

Q= internal recharge in the continuum (pumping is negative Q)

S_1 = that part of the boundary on which the potential ϕ is prescribed

3-24

S_2 = is the other part of the boundary which the external flux is prescribed

The energy term corresponding to the above equation will be

$$\Pi = \int \frac{1}{2}\left[K_x \left(\frac{\partial \phi}{\partial x}\right)^2 + K_y \left(\frac{\partial \phi}{\partial y}\right)^2 + K_z \left(\frac{\partial \phi}{\partial z}\right)^2 \right] dv - \int Q\phi\, dv$$

Now,

$$K_x [\frac{\partial \phi}{\partial x}]^2 K_y (\frac{\partial \phi}{\partial y})^2 + K_z (\frac{\partial \phi}{\partial z})^2 = \left\{\frac{\partial \phi}{\partial x}\ \frac{\partial \phi}{\partial y}\ \frac{\partial \phi}{\partial z}\right\} \begin{bmatrix} K_z & 0 & 0 \\ 0 & Ky & 0 \\ 0 & 0 & Kz \end{bmatrix} \begin{Bmatrix} \dfrac{\partial \phi}{\partial x} \\ \dfrac{\partial \phi}{\partial y} \\ \dfrac{\partial \phi}{\partial z} \end{Bmatrix}$$

$$\text{Let } \begin{Bmatrix} \dfrac{\partial \phi}{\partial x} \\ \dfrac{\partial \phi}{\partial y} \\ \dfrac{\partial \phi}{\partial z} \end{Bmatrix} = \{g\}\, and \begin{bmatrix} K_x & 0 & 0 \\ 0 & Ky & 0 \\ 0 & 0 & Kz \end{bmatrix} = [D]$$

$$\therefore = \frac{1}{2}\int \{g\}^T [D]\{g\}dv - \int Q\phi\, dv$$

$$\phi^e = \sum_{i=1}^{n} N_i\phi_i = N_1\phi_1 + N_2\phi_2 + \ldots\ldots + N_n\phi_n$$

Where   n = no. of nodes/ element

ϕ_i = potential at node i

N_i = shape function for node i

$$\frac{\partial \phi}{\partial x} = \sum \frac{\partial N_i}{\partial x}\phi_i ; \frac{\partial \phi}{\partial y} = \sum \frac{\partial N_i}{\partial y}\phi_i \text{ and } \frac{\partial \phi}{\partial z} = \sum \frac{\partial N_i}{\partial z}\phi_i$$

3-25

$$\therefore \{g\} = \begin{Bmatrix} \dfrac{\partial \phi}{\partial x} \\ \dfrac{\partial \phi}{\partial y} \\ \dfrac{\partial \phi}{\partial z} \end{Bmatrix} = \begin{bmatrix} \dfrac{\partial N_i}{\partial x} & \dfrac{\partial N_2}{\partial x} & \dfrac{\partial N_n}{\partial x} \\ \dfrac{\partial N_1}{\partial y} & \dfrac{\partial N_2}{\partial y} & \dfrac{\partial N_n}{\partial z} \\ \dfrac{\partial N_1}{\partial z} & \dfrac{\partial N_2}{\partial z} & \dfrac{\partial N_n}{\partial z} \end{bmatrix} \begin{Bmatrix} \phi_1 \\ \phi_2 \\ . \\ . \\ . \\ \phi_n \end{Bmatrix}$$

Or $\{g\} = [B]\ \{\phi^e\}$

Where $[B] = \begin{bmatrix} \dfrac{\partial N_1}{\partial x} & \dfrac{\partial N_2}{\partial x} \cdots \dfrac{\partial N_n}{\partial x} \\ \dfrac{\partial N_1}{\partial y} & \dfrac{\partial N_2}{\partial y} \cdots \dfrac{\partial N_n}{\partial z} \\ \dfrac{\partial N_1}{\partial z} & \dfrac{\partial N_2}{\partial z} \cdots \dfrac{\partial N_n}{\partial z} \end{bmatrix}$ and $\{\phi^e\}$: vector of nodal potentials $\begin{Bmatrix} \phi_1 \\ \phi_2 \\ . \\ . \\ . \\ \phi_n \end{Bmatrix}$

Therefore the energy term is

$$\prod = \frac{1}{2}\int \{\phi^e\}^T [B]^T [D][B]\{\phi^e\}dv - \int Q\phi\ dv$$

Now $\phi = [N]\ \{\phi^e\}$

Where $[N] = [N_1\ N_2 \ldots N_n]$

Therefore, the energy form becomes

$$\prod = \frac{1}{2}\int \{\phi^e\}^T [B]^T [D][B]\{\phi^e\}dv - \int Q[N]\{\phi^e\}dv$$

Since for equilibrium $\dfrac{\partial \prod}{\partial \phi} = 0$

Therefore $\int [B]^T [D][B]\{\phi^e\}dv - \int Q[N]^T dv = 0$

If there is no recharge or pumping $Q = 0$

Then $[K^e]\{\phi^e\} = 0$

Where $[K^e] = \int [B]^T [D][B]dv$.

3.7 PROCESSES IN ANSYS

ANSYS programme has many finite element analysis capabilities, ranging from a simple linear, static analysis to a complex, non-linear, transient dynamic analysis.

The distinct steps in ANSYS are as follows:

i)   Building the model.

ii)   Define an element type.

iii)   Define material properties.

iv)   Meshing the model into elements and nodes.

v)   Apply boundary conditions and loads.

vi)   Obtain the solution.

ANSYS process status consists of

•   Form element matrices.

•   Prepares elements for solver.

•   Solves equations.

•   Calculates element results.

vii)   Review of results in general post processor.

3.8 ANSYS INPUTS

i) KXX=Thermal conductivity in x direction.

3-27

SEEPAGE MODELS

4.1   GENERAL

A criteria to determine the seepage model boundary is given by Arvin (1965) [1] for electrical analogy models. The same has been adopted in this study also.

4.1.1 Assumptions in the Seepage Analysis

The various simplified assumptions made are given below:

i)   The medium of flow is porous, isotropic, homogeneous and pervious of infinite depth.

ii)   Seepage flow is confined, steady, laminar and irrotational.

iii)   Fluid is incompressible.

iv)   Flow is within the validity range of Darcy's law.

4.2   MODELLING

Three different seepage models are prepared and analysed to obtain the flow characteristic beneath the structure.

4.2.1 Model-1 Floor with Sheet Piles at Either End

Two dimensional model has been prepared taking the same dimensions as used by Khosla (1954) [7] as a standard form to determine uplift pressure and exit gradient for floor with sheet piles at either end. It is shown in Fig. 4.1.

Model is subjected to same upstream and downstream potentials. This study is carried out to validate the Ansys FEM programme by comparing uplift pressure and exit

gradient of FEM model with those obtained by Khosla's method of independent variables, experimental and analytical methods.
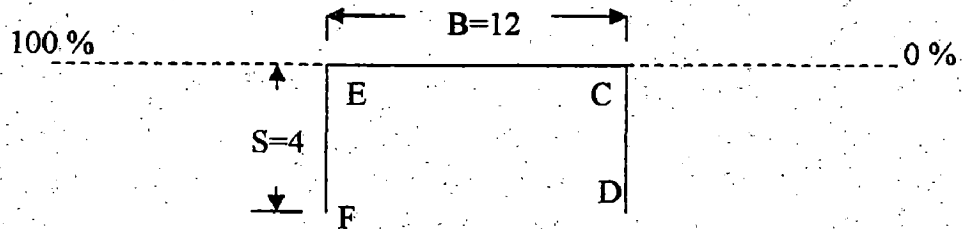
Fig. 4.1. Floor with sheet piles at either end (end piles equal)

The detailed steps in Ansys package for solving and viewing the results of the model are given in Annexure-I. The meshed model is given in figure 4.1a.

4.2.2 Modelling of Kanpur Barrage

Ganga Barrage is situated on river Ganga, 1.5 km U/S of Bhairoghat (Nawab Ganj) Kanpur. The Barrage is designed for a maximum flood discharge of 18,000 m^3/sec. The maximum pond level is 113.0 m. River bed level is 106.1m. Barrage consists of 4 bays each in right and left under sluice and 22 other bays each having width of 20m. The salient features and the dimension adopted in the models are:

Under Sluice

1.	Floor level in U/S of Under sluice	= 108.5 m
2.	Floor level in D/S of Under sluice	= 106.1m
3.	Floor length of Under sluice	= 48m
4.	Width of Right under sluice	= 80.0m
5.	Width of left under sluice	= 80.0m
6.	Bottom level of U/S sheet pile	= 101.0m
7.	Depth of U/S sheet pile	= 7.5m
8.	Bottom level of D/S sheet pile	= 96.7m
9.	depth of D/S sheet pile	= 9.4m

4-2

10.	No. of bays in left under sluice	= 4
11.	No. of bays in right under sluice	= 4
12.	Width of each bay	= 20m
13.	General Ground level	= 113.0m

Barrage Bays:

1	Pond level	= 113.0 m
2	Floor level in upstream of barrage axis	= 108.5m
3	Floor level in downstream of barrage axis	= 107.1m
4	Floor length of barrage	= 48.0m
5	Total width of barrage between abutments	= 615.0m
7	Bottom level of U/S sheet pile	= 102.0 m
8	Depth of U/S sheet pile	= 6.5m
9.	Bottom level of D/S sheet pile	= 98.0m
10.	Depth of D/S sheet pile	= 9.1m
11.	No. of other bays	= 22 No.
12.	Width of each bay	= 20m
14.	Width of barrage bays	= 445 m

The section of Kanpur barrage is given in (Fig. 4.2 and 4.3).

Two dimensional and three dimensional models of Kanpur barrage have been prepared as follows:

(i)   Model II 2-D seepage model

A two dimensional model of Kanpur barrage (under sluice bays) has been prepared taking same dimensions and boundary conditions as adopted in the barrage and analyzed by U.P. Irrigation and Research Institute as per Technical Memorandum No. 67, 1996, R.R. (GA-3) [11] by E.H.D.A. to determine uplift pressure and exit gradient. This is carried out to validate ANSYS FEM programme by comparing uplift pressure and exit

gradient of FEM model with the results obtained by EHDA and also with Khosla's method to establish in accuracy of FEM programme.

The detailed steps in ANSYS package for solving the problem to obtain the flow characteristics is given in Annexure – I. The meshed 2-D seepage model is given in (Fig. 4.3.1).

(ii)   Model III 3-D Seepage Model

A 3-D model of Kanpur barrage has been prepared having same dimensions as used in U.P. I.R.I. Technical Memorandum No. 67, 1996, R.R. (GA-4) [12] to determine uplift pressure and exit gradient. It is subjected to the same potentials over u/s, d/s and abutment portion. It is also done to validate the FEM programme by comparing the uplift pressure and exit gradient of FEM model with those obtained by EHDA method in 3-D analysis. Analysis is also carried out under different potentials, behind the abutments to get the effect of 3-D seepage behavior on floor of barrage (Fig. 4.3a).

The detailed steps in ANSYS package for solving the problem to obtain flow characteristics are given in Annexure – II. The different views of the model are given in (Fig. 4.3a to Fig. 4.8) The meshed model is given in (Fig. 4.8a).

The 3-D analysis on Kanpur Barrage model has been carried out for the following test conditions.

(i)   Test Condition – 1

100% potential on river bed upstream of barrage and 0% potential on river bed downstream of barrage has been applied on model. This is a test condition used in EHDA by U.P. I.R.I. 1996 [12]. A 3-D view of meshed model is given in (Fig. 4.9).

(ii) Test Condition – 2

100% potential on river bed upstream of barrage and 0% potential on river bed downstream of barrage and 100% potential near abutments has been applied on the meshed model. A 3-D view of meshed model is given in Fig. 4.10.

(iii) Test Condition - 3

100% potential on river bed upstream of barrage and 0% potential on river bed downstream of barrage and 90% potential near abutments has been applied on the meshed model. This is also a test condition used in EHDA by U.P. I.R.I. 1996 [12]. A 3-D view of meshed model is given in Fig. 4.10.

(iv) Test Condition - 4

100% potential on river bed upstream of barrage and 0% potential on river bed downstream of barrage and 90% - 50% potential near abutments has been applied on the meshed model. A 3-D view of meshed model is given in Fig. 4.11.

LOCATION AT WHICH RESULTS ARE OBTAINED

We define the lines A1,A2,A3,A4,A5 (parallel to the barrage axis), Fig. 4.3a corresponding to P1,P2,P3,P4 and P5 of undersluice bays (Fig. 4.2), respectively, and those to barrage bay portion as C1,C2,C3,C4 and C5. Similarly, we define the lines across the barrage axis as U1, U2, U3 and U4 for undersluice portion and B1, B2, B3, ...,B11 for barrage bay portion. The details of the configuration and the space coordinates of the points considered for analysis is shown in fig. 4.2, 4.3 and 4.3(a) and table 4.1 and 4.2.

The uplift pressures are obtained at the intersection points of line P and U for undersluice portion and at the intersection points of line C and B for barrage bay portion.

Similarly, the exit gradients are obtained at the intersection points of P5 and U for under

sluice portion and those for barrage bay portion at the intersection points of C5 and B.

Where P = P1, ...,P5, C = C1, ...,C5, U = U1, ...,U4 and B = B1,B2 .....,B11.

The results are obtained at locations shown in fig.4.2,4.3, on points P1 to P5,C1 to

C5, along section A1 to A5 as per table4.1, and U1 to U4,B1 to B11 as per table 4.2 and

figure 4.3a.

The results are presented in the form of pressure contours charts and figures at

respective sections.

Table 4.1 : Location of Sections in X-Direction

Section	X in meters	Particulars
A1.	50	Upstream edge of upstream floor and upstream sheet pile
A2.	62	End point of u/s floor
A3.	71	Upstream edge of downstream floor
A4.	84.5	Centre of downstream floor
A5.	98	End of downstream floor and downstream sheet pile.

Table 4.2: Location of Sections in Z-Direction

Section	Z in meters	Particulars
U1.	60	Centre point of under sluice bay no. 1
U2.	80	Centre point of under sluice bay no. 2
U3.	100	Centre point of under sluice bay no. 3
U4	120	Centre point of under sluice bay no. 4
B1	145	Centre point of barrage bay no. 1
B2	165	Centre point of barrage bay no. 2
B3	185	Centre point of barrage by no. 3
B4	205	Centre point of barrage bay no. 4
B5	225	Centre point of barrage bay no. 5
B6	245	Centre point of barrage bay no. 6
B7	265	Centre point of barrage bay no. 7
B8	285	Centre point of barrage bay no. 8
B9	305	Centre point of barrage bay no. 9
B10	325	Centre point of barrage bay no. 10
B11	345	Centre point of barrage bay no. 11
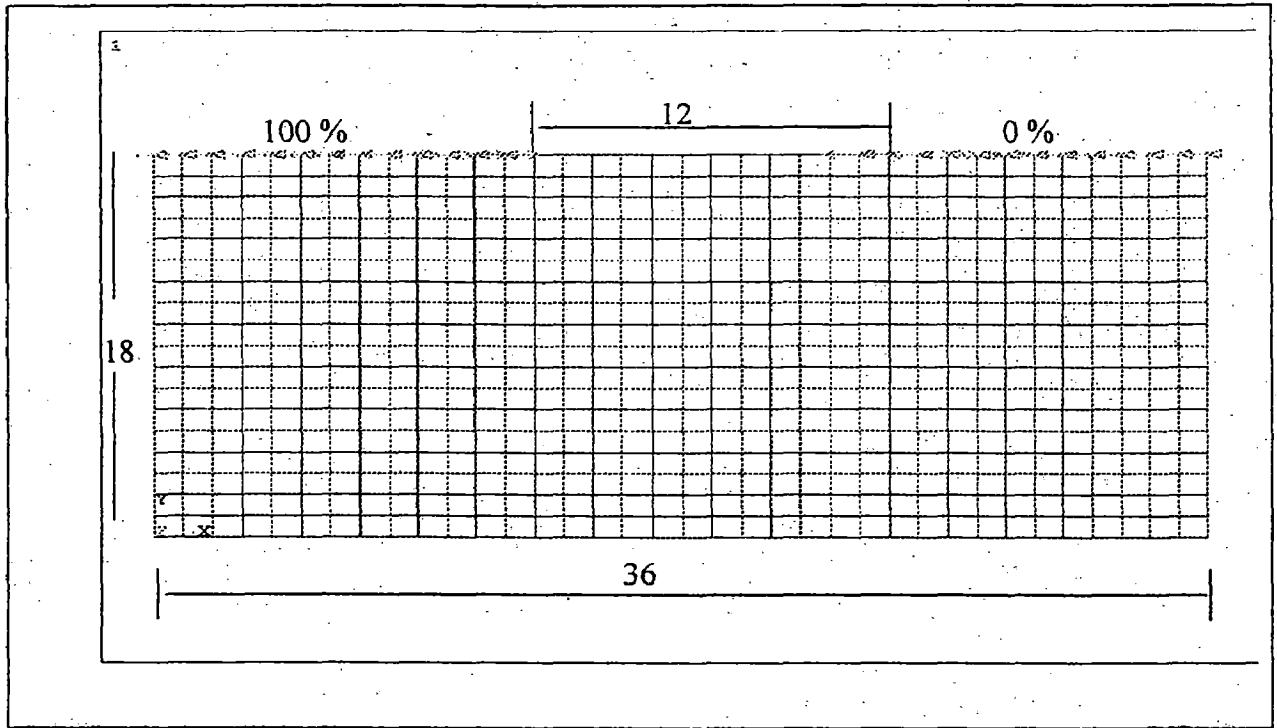
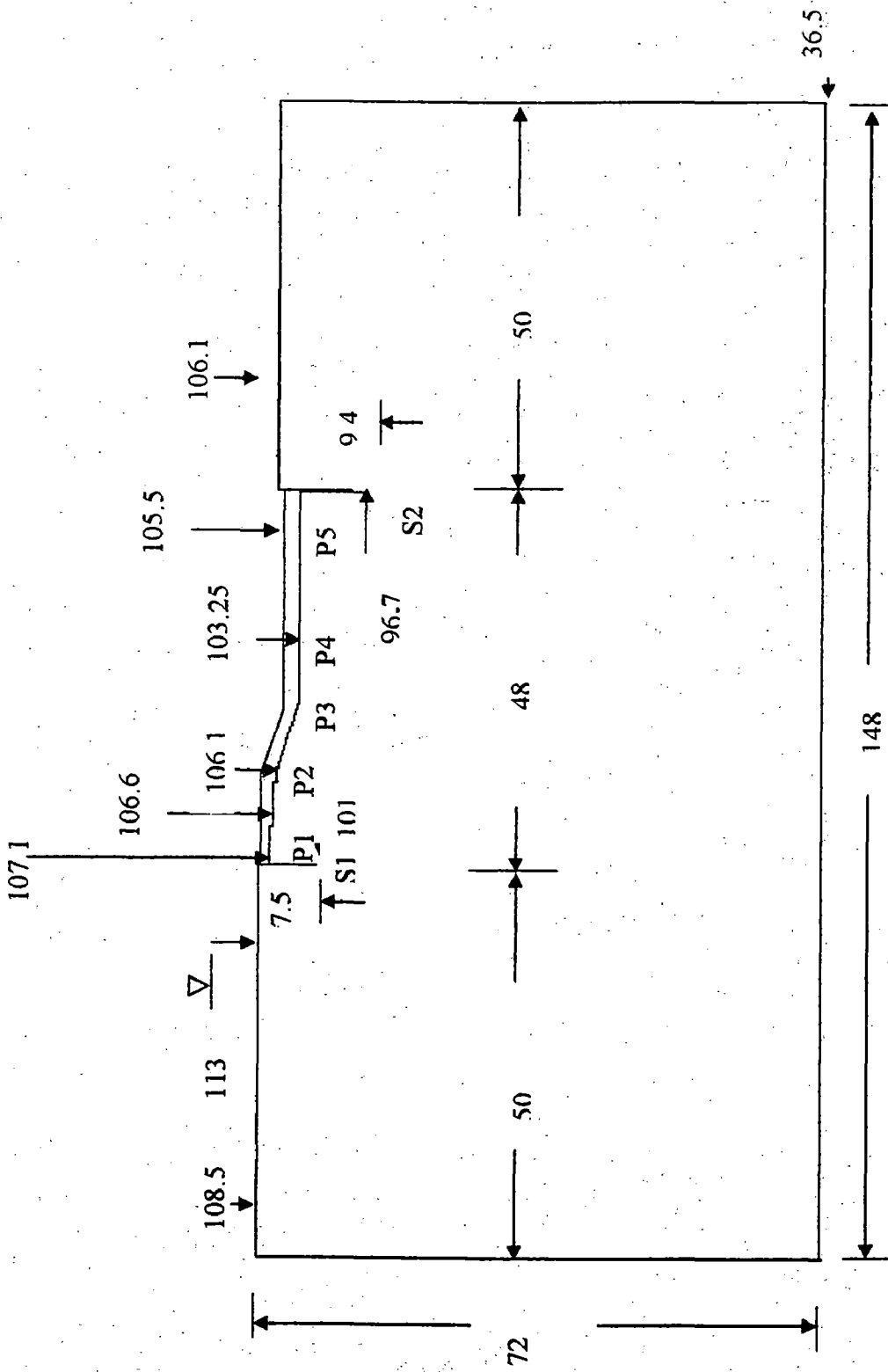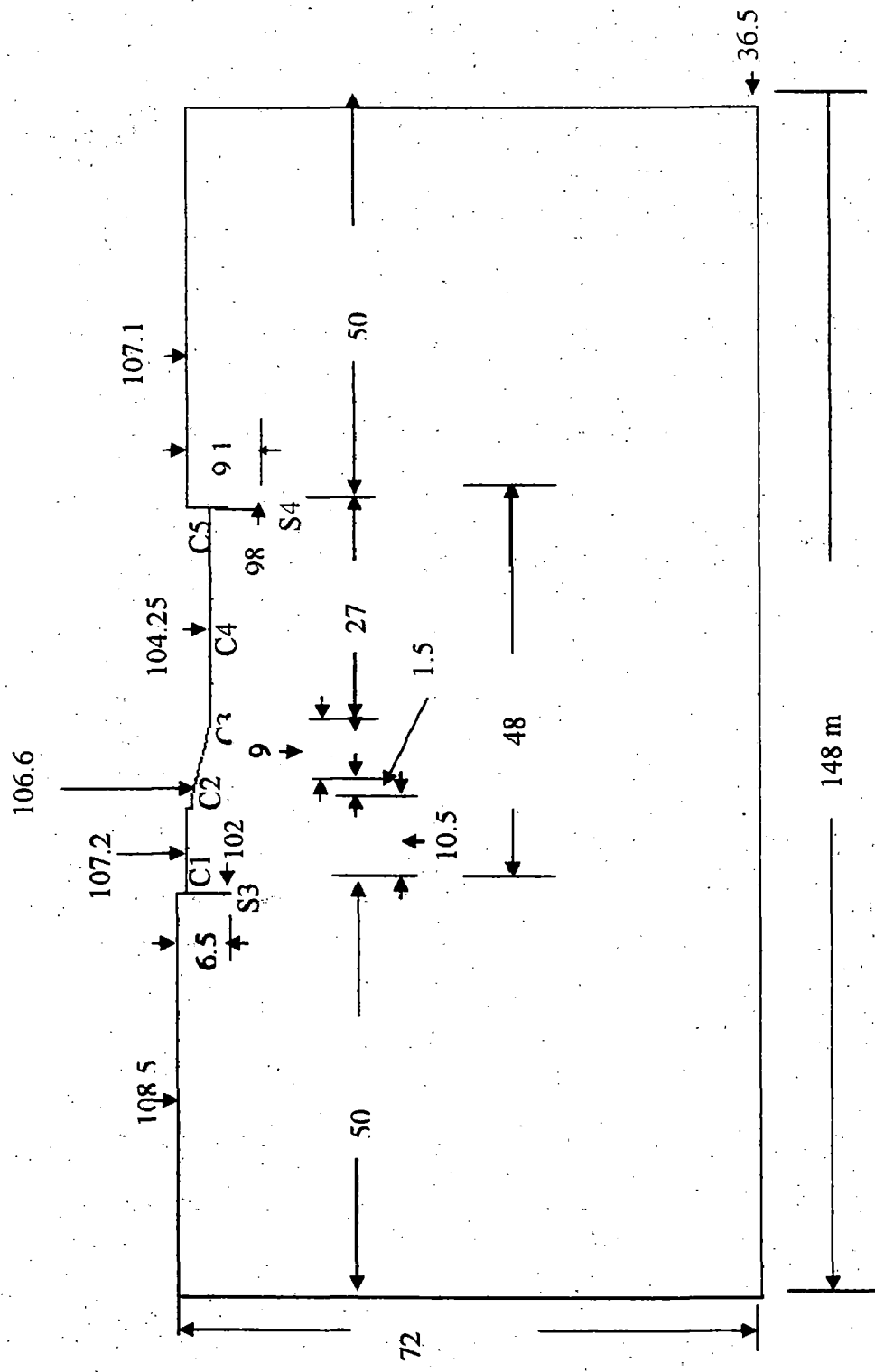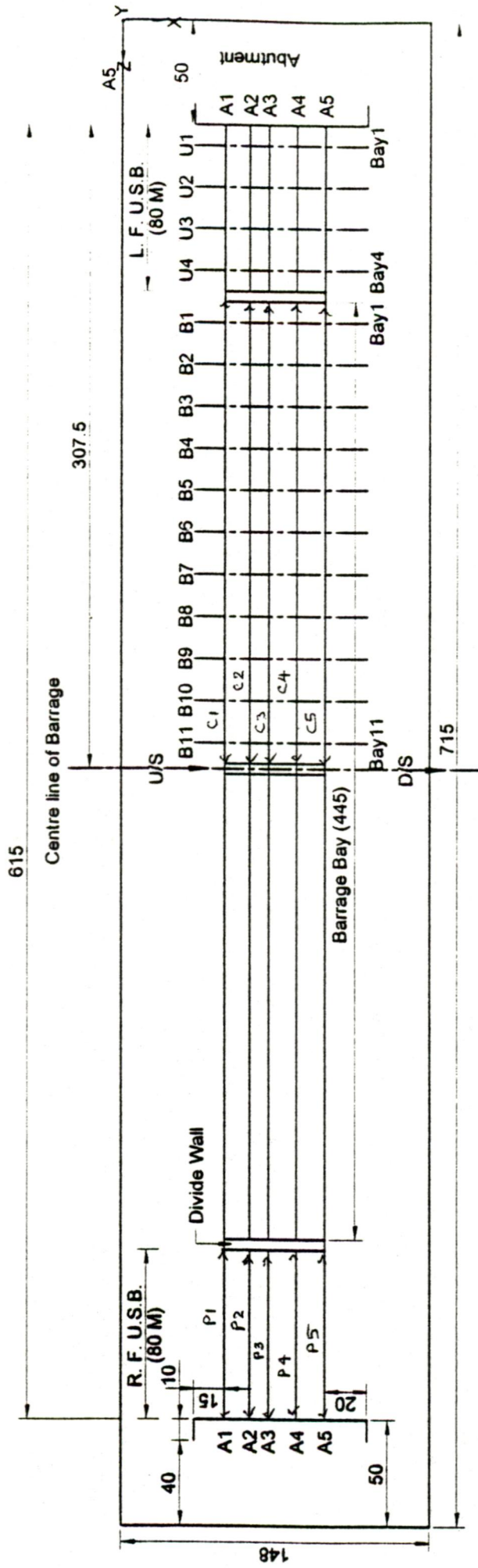**Figure 4.1a: Meshed model of sheet piles at either end.**

Figure 4.2 Kanpur Barrage under sluice bay section.

4-8

Figure 4.3, Kanpur barrage, Barrage bay section

Fig. No. 4.3a   PLAN OF SEEPAGE MODEL FOR BARRAGE FLOOR

Notes:

1. All Diamension in Meter
2. R. F. U. S. B. : Right Flank Under Sluic Bay
3. L. F. U. S. B. : Left Flank Under Sluic Bay
4. U/S : Up Stream
5. D/S : Down Stream
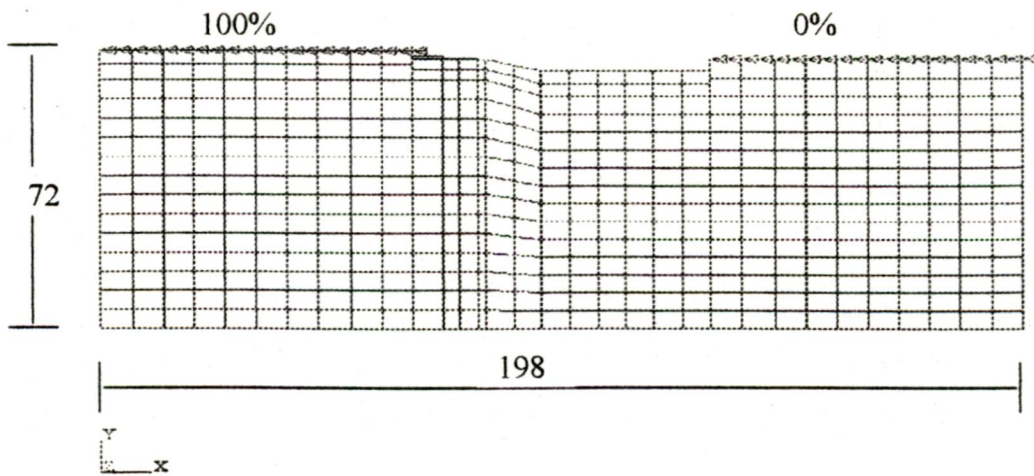
A1: X=50m(U/S edge of U/S Floor)
A2: X=62m(End of U/S Floor)
A3: X=71m(U/S edge of D/S Floor)
A4: X=84.5m(Center of D/S Floor)
A5: X=98m(End of D/S Floor)

U1: Z=60m(Under Sluice Bay No. 1)
U2: Z=80m(Under Sluice Bay No. 2)
U4: Z=120m(Under Sluice Bay No. 4)

B1: Z=145m(Barrage Bay No. 1)
B2: Z=165m(Barrage Bay No. 2)
B10: Z=325m(Barrage Bay No. 10)
B11: Z=345m(Barrage Bay No. 11)

4-10

Figure 4.3b: Meshed 2-D seepage model

72 M

715 M

148 M
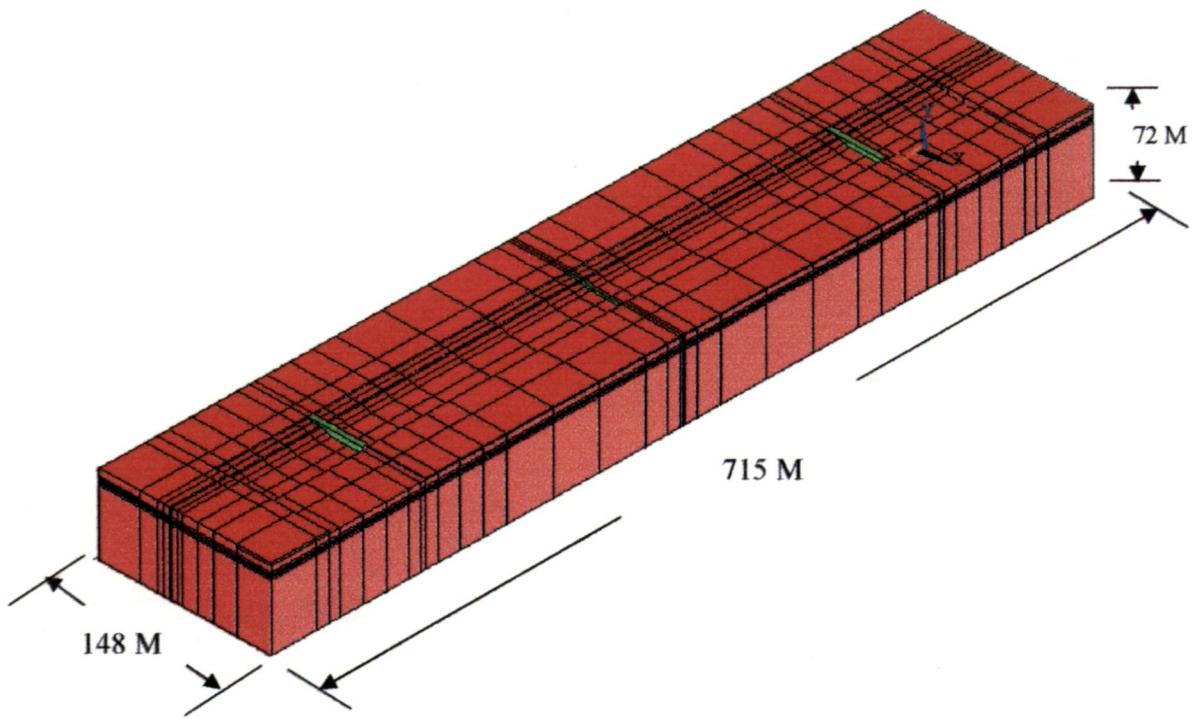
Figure 4.4, Kanpur barrage full model.
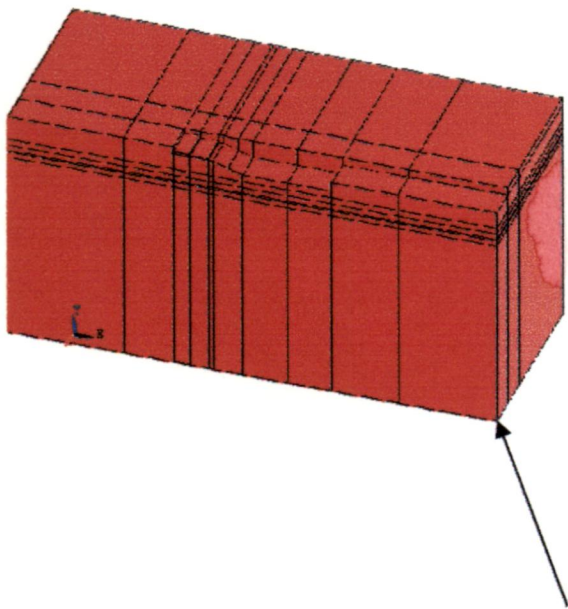
Figure 4.5, Kanpur barrage model (under sluice bay No.1 center 60m)

60

80

100

120
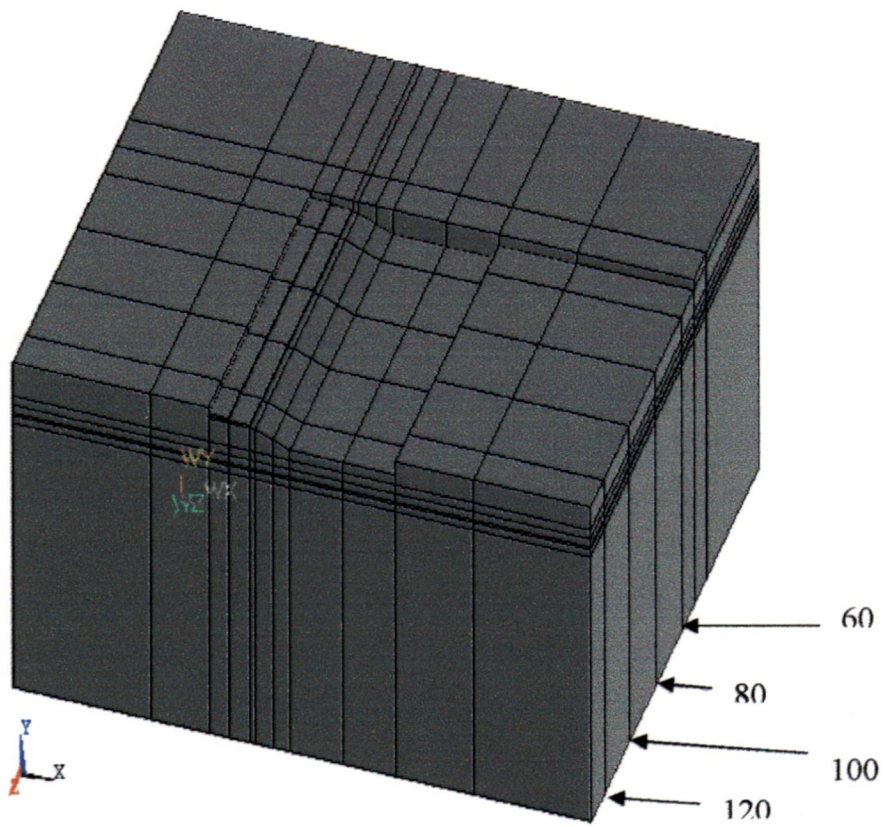
Figure 4.6: Kanpur barrage model showing center of under sluice bay N0. 1 to 4
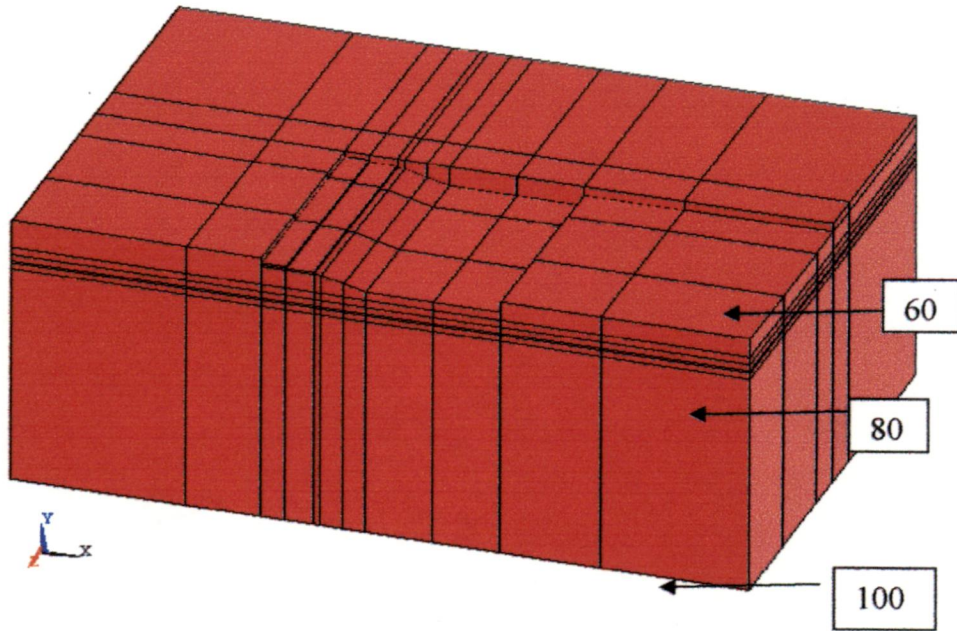
Figure 4.7: Kanpur barrage model Left side under sluice bay 1 to 3
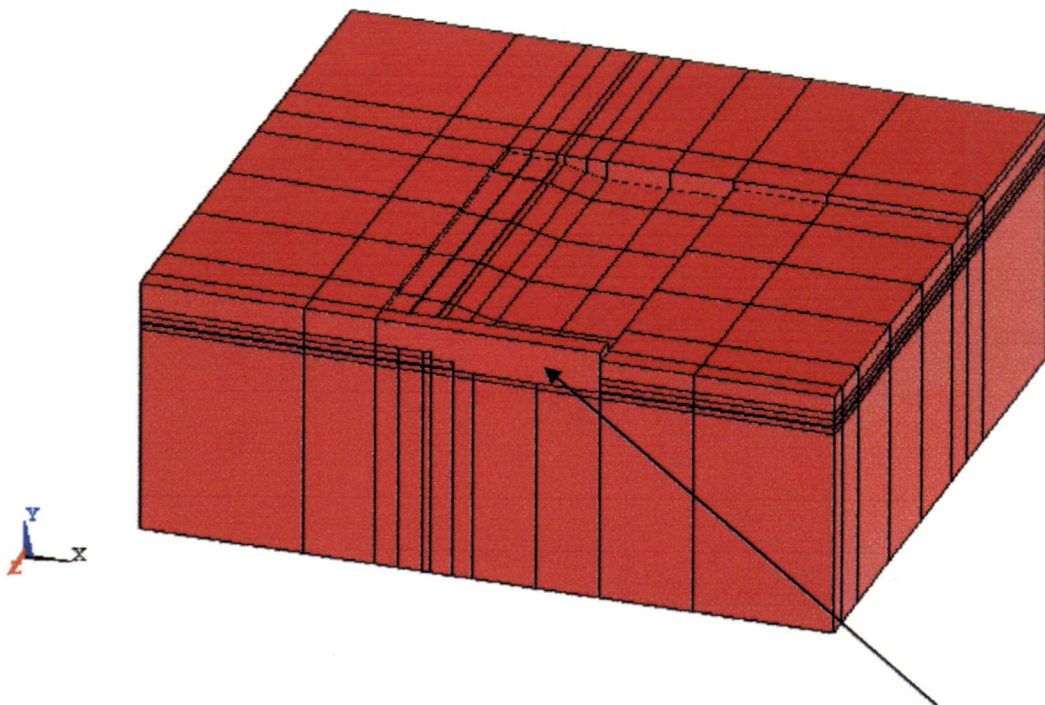
Figure 4.8: Kanpur Barrage model left side under sluice bay 1 to 4 & Divide wall.
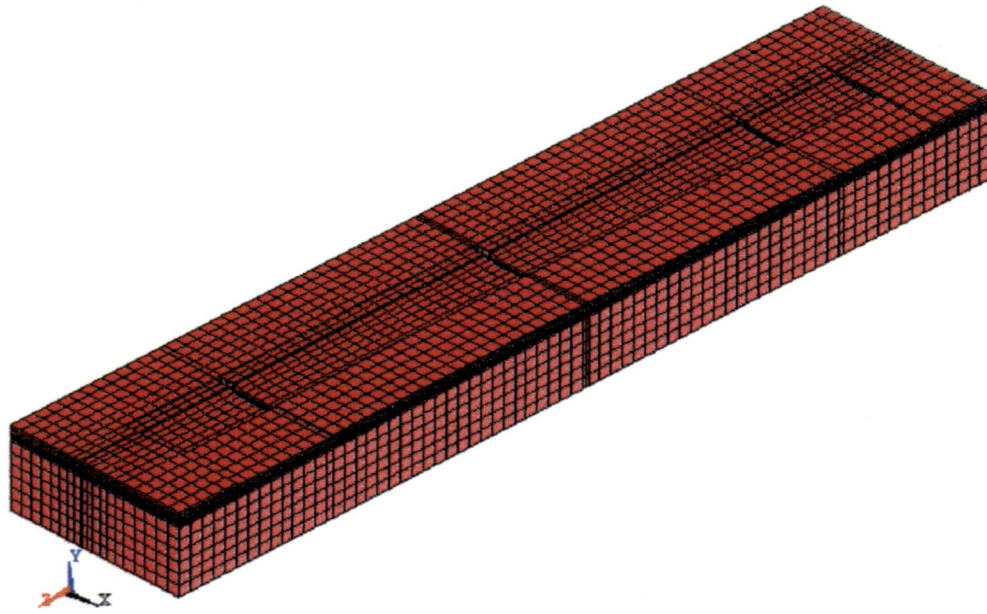
Figure 4.8a: Meshed 3-D seepage model
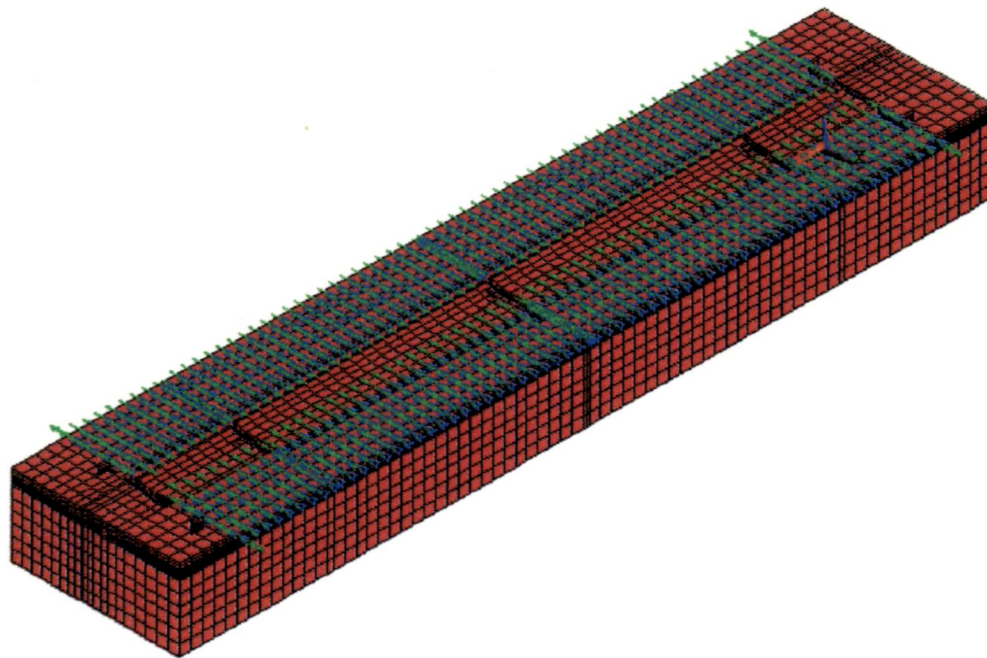
kanpur barrage Full model U/S100D/S0 potential (bu100d0)

Figure 4.9:-Meshed model with test condition 1

4-15
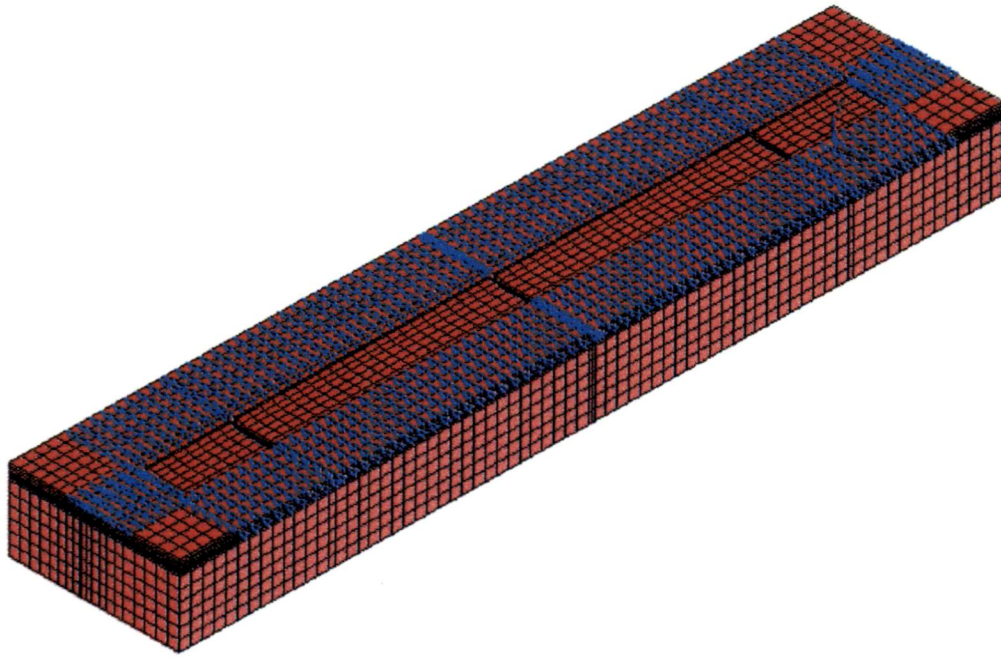
Figure 4.10:-Meshed model with test condition 2 & 3
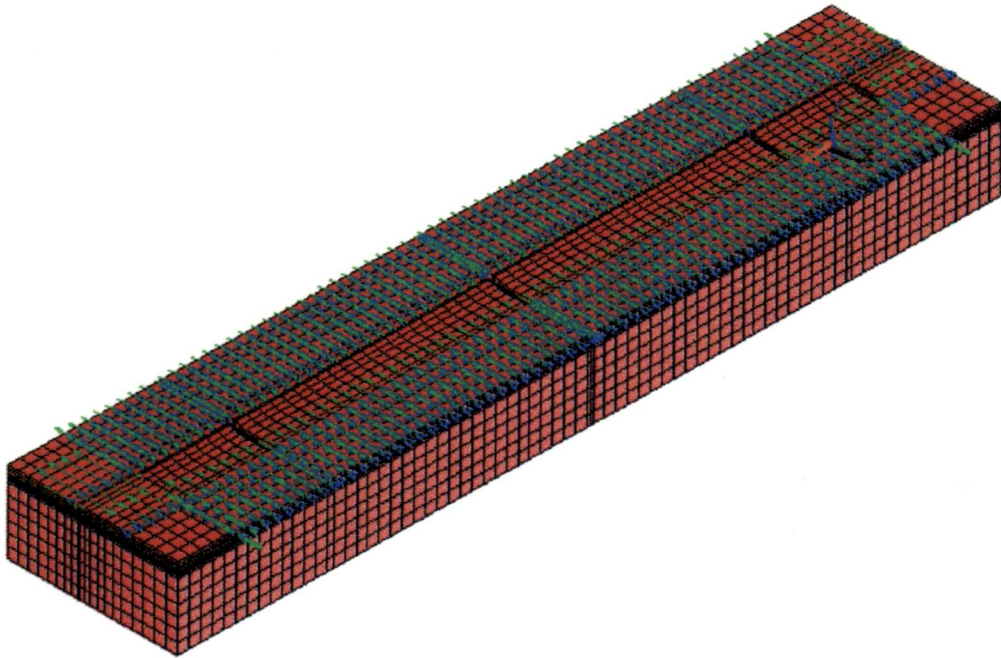
kanpur barrage u/s100d/susbb0abutment90_50 (u100d0a90_50)

Figure 4.11:-Meshed model with test condition 4

RESULTS OF ANALYSIS

5.0   GENERAL

The analyses have been carried out for three models as described in Chapter-4. Uplift pressures and exit gradient corresponding to each model have been obtained and the results are presented herewith.

5.1   MODEL – I FLOOR WITH SHEET PILES AT EITHER END

The uplift pressures corresponding to the points E,F,C and D using FEM Model are presented in Table 5.1 and Fig. 5.1.

The results obtained using FEM model are compared with the results obtained by Khosla's method using independent variables, experimental results (electrical analogy) and theoretical results [7].

The deviation of uplift pressure obtained using finite element method is 0.11 % to 1.2 % from those of theoretical values and 1.04 % to 1.46 % from those of Khosla's values. The deviations are shown in the Table 5.1.

- The variation of experimental results with theory is from 0.13% to 2.86%.

Table 5.1: Results of Analysis uplift pressure and Exit gradient,
(Floor with sheet piles at either end)

Uplift pressure	Theory	Experimental	Khosla	Ansys	Variation of Ansys Results in %		Variation of experimental results in %	
					Theo.	Khosla	Theo.	Khosla
ϕ_E	71.6	71.7		71.517	0.11	-	0.13	-
ϕ_F	58.6	58.2	58.5	59.109	0.86	1.04	0.68	0.52
ϕ_c	41.4	42.1	41.5	40.891	1.2	1.46	1.69	1.45
ϕ_D	28.4	29.2	-	28.483	0.29	-	2.86	-

5.1.1 Summary of Results

From the above results it can be summarized as:

- The results of Ansys FEM model are more accurate and close to the theoretical values as compared to the experimental values (e.g. Electrical Analogy Method).

- The deviation of uplift pressure with that of theoretical values are insignificant, thus, the analysis for 2D seepage flow can be carried out using 4 noded linear element in Ansys FEM Model with fair accuracy.

- The results can be further improved by selecting higher order element i.e. from 4 noded (plane 55) to 8 noded (parabolic, plane 77) element and/or by increasing the density of meshing. .

5.2 MODEL II 2-DIMENSIONAL MODEL OF KANPUR BARRAGE

The uplift pressures corresponding to point P1 and P5 using FEM model are shown in Fig. 5.2 and the exit gradient obtained by FEM model is shown in Fig 5.3.

The results obtained using FEM are compared with Khosla [7] and EHDA [11]. The uplift pressure at point P1 (upstream edge of upstream floor), P5 (end of downstream floor) by Ansys model are 72.709 % and 31.787% while at the same location by Khosla these are 70.351 % and 33.526% and by EHDA these are 67.8% and 32.6%.

The deviation of uplift pressure by FEM from Khosla theory is 3.33% to 5.1% and that from EHDA 6.75% to 2.4%.

The exit gradient obtained by Ansys model is 0.122, by Khosla 0.129 and by EHDA 0.133 respectively.

5.2.1. Summary of the Results

From the above result, it can be summarized that the results of FEM Ansys programme are closer to Khosla's values than with the EHDA results. The same was the conclusion of the results of Mode 1. Therefore, it can be said that the results obtained by Ansys FEM Model using 4 noded linear element can be used for all practical purposes with fair accuracy.

5.3 MODEL – III THREE-DIMENSIONAL SEEPAGE MODEL OF KANPUR BARRAGE

Three-dimensional analysis has been carried out for uplift pressures and exit gradient for the test conditions and the results obtained are as follows:

5.3.1 Test Condition – 1

100% potential on river bed upstream of barrage and 0% potential on river bed downstream of barrage was applied on the 3-D model (Fig. 4.3a, Fig. 4.9) ,and uplift pressures and exit gradients obtained from finite element method. The results are presented in the form of graphs (Fig. 5.5 to Fig. 5.20a).

(i)   Uplift Pressure

- It is observed that at the point P4U1 (X = 84.5 m) the pressure head is 42.406% of total head and at the point P4U4 it is 41.178 %. Here point P4U1 corresponds to bay no. 1, i.e. bay nearest to the abutment and P4U4 corresponds to bay No. 4 i.e. bay farthest from the abutment. The variation in pressure head is 1.228% of total head i.e. pressure head decreases as the distance from abutment increases, but the variation is insignificant.   The uplift pressure with respect to the distance measured from abutment is shown in fig.5.12.

- It is observed that at the point P3U1 (X = 71 m) the pressure head is 54.498% of total head and at the point P3U4 it is 55.977%. Here point P3U1 corresponds to bay no. 1 and P3U4 corresponds to bay No. 4. The variation in pressure head is 1.479% of total head, i.e. pressure head increases as the distance from abutment increases, but the variation is insignificant. The uplift pressure with respect to the distance measured from abutment is shown in fig.5.13.

- It is observed that at the point P5U1 (X = 98 m) the pressure head is 32.805% of total head and at the point P5U4 it is 30.008%. The variation in pressure head is 2.797% of total head, i.e. pressure head decreases as the distance from abutment increases, but the variation is insignificant. The uplift pressure with respect to the distance measured from abutment is shown in fig.5.14.

- At the tip of downstream sheet pile (S2) in under sluice the uplift pressures are 25.254 % and 22.29% of total head corresponding to bay no.1 and bay no.4, respectively. Here the uplift pressure decreases from bay No. 1 to bay No. 4 by 2.296% of total head. The result is shown in Fig. 5.15.

- The uplift pressure at the point P2U1 (X = 62 m) is 62.82% and P2U4 it is 66.035% . Here the variation is 3.215%. The uplift pressure increases as the distance from abutment increases. The result is shown in fig. 5.16.

- The uplift pressure in barrage bay corresponding to the points C3B1 (X = 71m), C3B2, C3B10 and C3B11 are 55.99%, 55.992%, 55.99% and 55.936%, respectively. Here the uplift pressure is almost the same for all barrage bays (Fig. 5.17).

- The uplift pressure in barrage bay corresponding to the points C4B1 (X = 84.5m), C4B2, C4B10 and C4B11 are 41.028%, 41.143%, 41.10% and 40.665%., respectively. Here the uplift pressure is almost the same for all barrage bays (Fig. 5.18). Similar trends are observed for all the barrage bays.

(ii)   Exit Gradient

- The exit gradient at down stream sheet pile of under sluice bay No. 1 and bay no. 4 are 0.164 (1/6.089) and 0.138 (1 in 7.265) i.e. exit gradient decreases as the distance from the abutment increases. A plot of the distance from abutment versus 1/ exit gradient is shown in Fig. 5.19.

- The exit gradient at down stream sheet pile of barrage bay portion is found to be 0.12 and is constant from bay no.2 to bay no.10. However, in bay no. 1 and 11 the exit gradient is less than the other bays, this may be due to the effect of the foundation level of the divide wall. (Fig. 5.20).

(iii)   Comparison with EHDA Results

The results of FEM analysis for this test condition 1 have been compared with the results of EHDA given in the test report of IRI U.P. The results are shown in table 5.2. The uplift pressure values are compared at the points P1U1, P2U1, P3U1, and P4U1 along the centre line of bay No. 1 of under sluice floor. The maximum variation is 3.97 %.

(iv)   Summary of the Results

From the above results it can be summarized as:

The variation of uplift pressure of FEM with EHDA is nominal and due to limitation of experimental method as described in chapter 2.

Seepage flow behaviour in this test condition is in general two-dimensional except near abutment where the uplift pressures are slightly higher than the pressures at a section away from the abutments. Similarly the exit gradient value at the downstream sheet pile is also higher than the value at a section away from the abutment.

5.3.2   Test Condition No. 2

The 100% potential on river bed upstream of barrage, 0% potential on riverbed downstream of barrage and 100% potential behind abutments was applied on the 3-D model and uplift pressures and gradients are obtained from Ansys FEM Model. The results are presented in the form of graphs and figures (Fig. 4.3a, 5.21 to 5.27).

(i)   Uplift Pressures

- Uplift pressure along section P1 (x = 50 m) of under sluice bay portion are found to be 83.74% and 76.50% corresponding to the point P1U1 and P1U4, respectively. Here, the variation is found to be 7.20% (Fig. 5.22).

- The uplift pressure along section P2 (x = 62 m) (end point of upstream floor). In under sluice portion it varies from 78.92% (bay no. 1) to 69.19% (Bay No. 4) the variation is 9.73 %. The pressures decrease from under sluice bay no. 1 (abutment side) to bay no. 4 (Fig. 5.23).

- At the section along P3 of under sluice floor (A3 (x = 71 m)) uplift pressures varies from 72.146% (Bay No.1) to 59.70% (Bay No. 4). The variation is 12.44%. The pressure decreases from Bay no. 1 to Bay no. 4 (Fig. 5.24).

- At the section along P4 of under sluice floor (A4 (x = 84.5 m)) uplift pressures varies from 59.885 % (Bay no. 1) to 44.951 % (Bay no. 4). The variation is 14.93 %. The pressure decreases from Bay No. 1 to Bay No. 4. (Fig. 5.25).

- Along the section P5 of under sluice floor (A5 (x = 98 m)) uplift pressures varies from 48.145 % (Bay No. 1) to 33.31% (Bay No. 4). The deviation is 14.89%. The uplift pressure decreases from Bay no. 1 to Bay no. 4 (Fig. 5.26).

- Along the section C1 of barrage bay floor (section A1 (x = 50, RL 107.2 m)), the uplift pressures varies from 76.50 % (Bay no. 1) to 75.1 % (Bay no. 11). The variation is 1.4 % and pressure is decreasing from Bay no. 1 to Bay no. 11 (Fig. 5.22).

- Along the section C2 (x = 62 m) of barrage bay, the uplift pressure varies from 67.98 % (Bay no. 1) to 66.23% (Bay no. 11) and The variation is 1.75%. The pressure decreases from Bay no. 1 to Bay no. 11. The variation is very small (Fig. 5.23).

- Along the section C3 (x = 71 m), C4(x = 84.5 m) and C5 (x = 98 m) of barrage bay, the uplift pressures vary from 58.06 % (Bay no. 1) to 56.0% (Bay no. 11), 43.03% (Bay no. 1) to 40.73% (Bay no. 11) and 31.08 % (Bay no. 1) to 30.71% (Bay no. 11), respectively. The corresponding variations are 2.06%, 2.3% and 3.7%. The uplift pressures decreases from Bay no. 1 to Bay no. 11. The variation is small and found to be maximum at the end of the downstream floor. (Fig. 5.24 to 5.26).

(ii)   **Exit Gradient**

- The exit gradient at down stream of sheet pile varies from 0.25 (1/4.01) to 0.15 (1 / 6.52) from Bay no. 1 to Bay no. 4 in under sluice bay portion and 0.125 (1 / 8) to 0.121 (1/8.23) from bay No. 2 to bay No. 10 of barrage bay. The exit gradient decreases from abutment towards centre of barrage (Fig. 5.27).

(iii) **Summary of the Results**

From the above results it can be summarized:

- The effect of head behind the abutment on uplift pressure in both under sluice bay and barrage bay on upstream floor is less than the downstream floor.

- The uplift pressure variation is significant in under sluice part of barrage and is maximum along the centre line of downstream floor and the maximum variation is 19.48%.

- The uplift pressure variation in barrage bay portion is less than the undersluice portion and the maximum variation is along the end line of the downstream floor.

- The uplift pressure are found affected by the head behind abutment upto a distance of 0.37L.

- The exit gradient decreases as the distance from the abutment increases. The variation is maximum in under sluice bay No. 1.

5.3.3 Test Conditions 3

100% potential on river bed upstream of barrage, 0% potential on riverbed downstream of barrage and 90% potential near abutments was applied on the 3-D model

and uplift pressures and exit gradients are obtained using Ansys FEM Model. The results are presented in the form of graphs and figures (Fig. 4.3a, 5.28 to 5.36).

(i)   Uplift Pressure

It is observed that along the section P3 of under sluice floor (section A3 (x = 71 m)) the uplift pressure varies from 68.801% (Bay no. 1) to 59.02% (Bay no. 4). The variation is 9.78% (Fig. 5.29).

Along the section P4 of under sluice bay (section A4 (x = 84.5 m)) the uplift pressure varies from 56.68% (Bay no. 1) to 44.28% (Bay no. 4). The variation is 12.40% (Fig. 5.30).

Along the section P5 of under sluice bay, the uplift pressures vary from 45.383% (Bay no. 1) to 32.265% (Bay no. 4). The variation is 13.118% (Fig. 5.31).

Along the section C3 of barrage bay floor section (A3 (x = 71 m)), the uplift pressure varies from 58.006% (Bay no. 1) to 56.005% (Bay no. 11). The variation is 2.00% (Fig. 5.32).

Along the section C4 of the barrage bay floor section (A4 (x = 84.5m)), the uplift pressure varies from 43.172 % (Bay no. 1) to 40.732% (Bay no. 11). The variation is 2.74% (Fig. 5.33).

Along the section C5 (A5 (x = 98 m)), the uplift pressure varies from 30.79% (Bay No. 1) to 30.70% Bay No. 11. There is almost no variation, (Fig. 5.34).

(ii)   Exit Gradient

The exit gradient down stream of sheet pile in under sluice portion varies from 0.23 (1 in 4.26) in bay no. 1 to 0.15 (1 in 6.64) in bay no. 4. The exit gradient decreases from bay no. 1 to bay no. 4   (Fig. 5.35).

The exit gradient at exit point in barrage bays is practically constant at a value of 0.124 in all the bays except the end bays i.e. 2 and 11 where the value is 0.11 (Fig. 5.36).

(iii)   Comparison with EHDA Results

The results of FEM analysis for this test condition 3 have been compared with the results of EHDA given in the test report of IRI U.P. The results are shown in table 5.3. The uplift pressure values are compared at the points P1U1, P2U1, P3U1, and P4U1 along the centre line of bay No. 1 of under sluice floor. The maximum variation is 10.80 %.

(iv)   Summary of Results

From the above results it can be inferred that the uplift pressure due to 90% head behind abutment are increased near the abutment and the effect reduces with distance from abutment. The effect does not exist beyond a distance (0.28 L).

The variation of uplift pressures values of FEM with EHDA is due limitations of experimental method as described in chapter 2

5.3.4. Test Condition No. 4

100% potential on river bed upstream of barrage, 0% potential on riverbed downstream of barrage and 90% to 50% potential behind abutments varying from u/s end to d/s end of floor was applied on the 3-D model and uplift pressures and gradients obtained out from Ansys FEM Model, and result are presented in the form of graphs and figures (Fig. 5.37 to 5.44).

(i)   Uplift Pressures

- It is observed that the uplift pressure along P4, (section A4 (X = 84.5 m, Y = 103.25 m)) of under sluice bay varies from 48.52% for bay no. 1 to 42.26% bay no. 2. The variation is 6.26% (Fig. 5. 38).

- Along P5, (section A5 (X = 98 m)) of under sluice bay, uplift pressures vary from 39.17% (bay no. 1) to 30.88% (bay no 4). The variation is 8.29% (Fig. 5.39)

- Along section P3 of under sluice bay (section A3 (X = 71 m, Y = 103.25 m)) the uplift pressures vary from 60.94% to 57.10%. The variation is 3.84% (Fig. 5.40).

- Along section C4 of barrage bay floor (section A4 (X = 84.5 m, Y = 104.25 m)), the uplift pressure variation is from 41.68% (bay no. 1) to 40.69% (bay no. 11). The variation is 0.99% (Fig. 5.41).

- Along the section C5 of barrage bay floor (section A5 (X = 98m, Y = 104.25 m)), the uplift variation is almost nil (Fig. 5.42).

(ii)   Exit Gradient

- The exit gradient at downstream sheet pile in under sluice bay varies from 0.19 (in 1 5.40) to 0.14 (1 in 7.02). The variation is 0.05, that corresponds to 26.31%. The exit gradient decreases from bay no. 1 to bay no. 4 (Fig. 5.43).

- The exit gradient at exit point in barrage bay varies from bay no. 1 and 2 from 0.11 to 0.12 i.e. about 7% and in the rest of the bays, it is almost constant and the value is 0.12 (Fig. 5.44).

(iii) Summary of Results

From the above results it can be summarized:

- The increase in uplift pressure in under sluice bays portion is significant in bay no. 1.

- The increase uplift pressure and its variation in barrage bays is very small.

- The exit gradient at exit point of under sluice is maximum in bay no. 1, near the abutment and is 26% higher than that of bay no. 4.

- The exit gradient at downstream of sheet pile in barrage bay is found unaffected by the head behind the abutment.

- The effect of head behind abutment is limited to under sluice bay (0.26L).

5.4. COMPARISON OF UPLIFT PRESSURE FOR DIFFERENT TEST CONDITIONS IN 3-D ANALYSIS

The comparison of uplift pressure distribution along the floor width have been made for the test conditions 1 to 4 to see the effect of consideration of water level behind the abutments. (Fig. 5.45 to 5.49 and Table 5.4 to 5.8).

The effect of varying head behind abutments can be visualized by comparing the results of test condition 2, 3 and 4 with the result of condition 1. It is seen that:

- The effect on uplift is maximum near the abutments.

- The effect on uplift is more if the head behind the abutment is more.

- The floor length which is affected is more when head behind the abutment is more. In this case under test condition 2, 3 and 4 the floor length affected is 0.37, 0.28 and 0.26L.

- The effect on uplift is more significant in the downstream floor.

Table 5.2
Comparison of uplift pressures results by FEM under test condition 1 with EHDA at Bay No. 1 of under sluice floor

S.No.	Location of result	Uplift pressure in %		Variation in %
		By ANSYS	By EHDA	
1	P1U1	70.17	66.20	3.97
2	P2U1	62.82	60.70	2.12
3	P3U1	54.49	55.30	0.81
4	P4U1	42.40	41.10	1.30

Table 5.3
Comparison of uplift pressures results by FEM under test condition 3 with EHDA at Bay No. 1 of under sluice floor

S.No.	Location of result	Uplift pressure in %		Variation in %
		By ANSYS	By EHDA	
1	P1U1	81.14	87.50	6.36
2	P2U1	75.83	83.20	7.37
3	P3U1	68.80	79.60	10.80
4	P4U1	56.67	66.40	9.73

			Distance along floor width in m.	Uplift pressure in %			
				Test condition 1	Test condition 2	Test condition 3	Test condition 4
S.No.	Location	Level Y in m					
1		107.1	50	68.48	85.63	82.27	75.89
		107.1	60	70.17	83.74	81.14	75.59
		107.1	70	71.76	81.40	79.60	75.09
		107.1	80	72.53	79.74	78.42	75.31
		107.1	90	72.95	78.50	77.49	74.73
		107.1	100	73.23	77.59	76.81	74.88
		107.1	110	73.41	76.89	76.27	74.64
		107.1	120	73.68	76.50	76.00	74.60
		107.1	130	75.33	77.70	77.28	75.78
		107.2	135	75.21	76.87	76.58	75.51
		107.2	145	75.01	76.50	76.24	75.49
		107.2	155	74.86	76.10	75.88	75.22
		107.2	165	74.87	75.89	75.71	75.28
		107.2	175	74.88	75.72	75.57	75.12
		107.2	185	74.89	75.58	75.46	75.16
	Upstream edge of U/S floor sec A1(X=50m)	107.2	195	74.90	75.47	75.37	75.06
		107.2	205	74.91	75.38	75.29	75.09
		107.2	215	74.91	75.30	75.23	75.00
		107.2	225	74.92	75.24	75.18	75.04
		107.2	235	74.92	75.19	75.14	75.03
		107.2	245	74.93	75.15	75.11	75.01
		107.2	255	74.93	75.11	75.08	74.96
		107.2	265	74.93	75.08	75.05	74.99
		107.2	275	74.93	75.05	75.03	74.98
		107.2	285	74.93	75.03	75.01	74.97
		107.2	295	74.92	75.01	75.00	74.93
		107.2	305	74.92	74.99	74.98	74.95
		107.2	315	74.91	74.98	74.97	74.94
		107.2	325	74.91	74.97	74.96	74.93
		107.2	335	74.92	74.97	74.96	75.06
		107.2	345	75.05	75.10	75.09	74.94
		107.2	355	75.23	75.28	75.27	75.24
		107.2	360	75.23	75.28	75.27	75.24

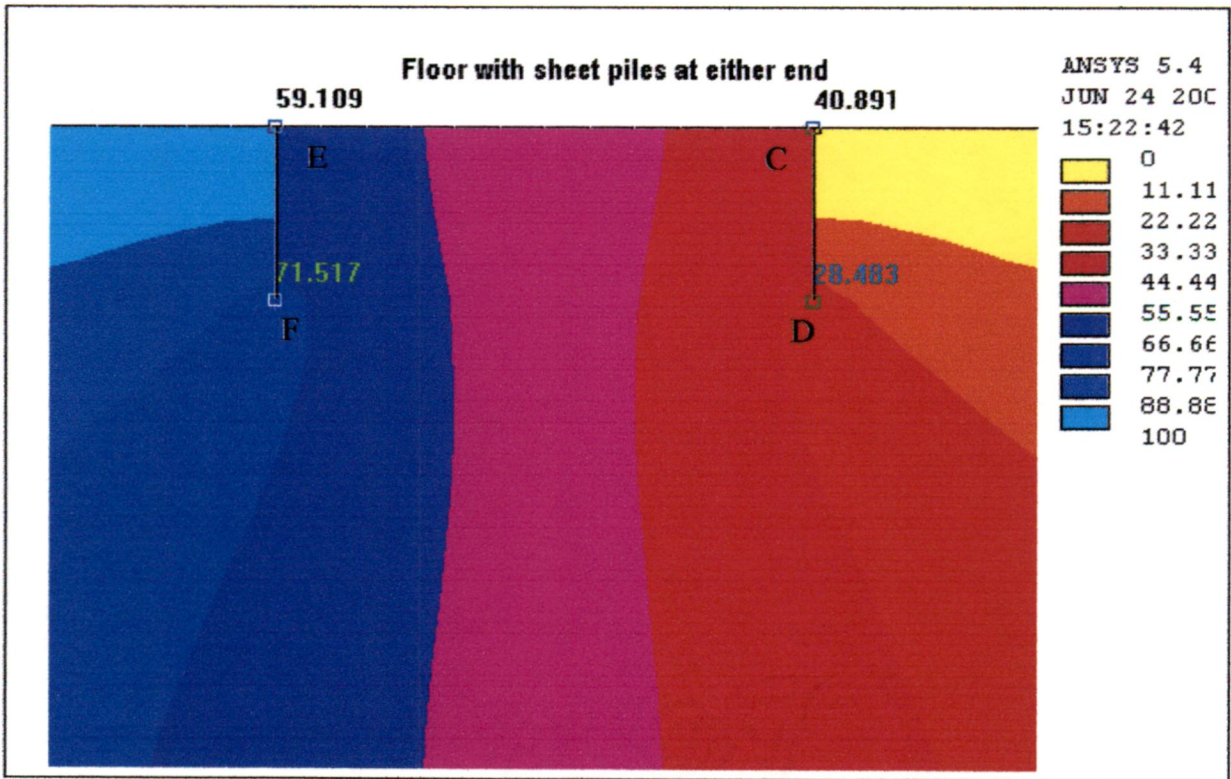|				Uplift pressure in %			

Table 5.5

Comparison of uplift pressures for different Test condition A2 (X=62m)

S.No.	Location	Level Y in m	Distance along floor width in m.	Test condition 1	Test condition 2	Test condition 3	Test condition 4
1		106.10	50.00	61.71	82.07	78.05	69.29
		106.10	60.00	62.82	78.92	75.83	68.69
		106.10	70.00	64.01	75.59	73.44	68.09
		106.10	80.00	64.66	73.38	71.78	67.67
		106.10	90.00	65.04	71.75	70.53	67.33
		106.10	100.00	65.28	70.55	69.60	67.07
		106.10	110.00	65.49	69.69	68.94	66.91
		106.10	120.00	65.78	69.19	68.58	66.93
		106.10	130.00	66.04	69.05	68.51	67.05
		106.60	135.00	66.19	68.24	67.87	66.88
		106.60	145.00	66.14	67.98	67.65	66.76
		106.60	155.00	66.07	67.60	67.33	66.58
		106.60	165.00	66.06	67.32	67.10	66.49
		106.60	175.00	66.07	67.11	66.93	66.42
		106.60	185.00	66.09	66.94	66.79	66.37
		106.60	195.00	66.10	66.80	66.68	66.33
		106.60	205.00	66.11	66.69	66.59	66.30
		106.60	215.00	66.12	66.60	66.51	66.28
	End of U/S floor sec A2(X=62m)	106.60	225.00	66.12	66.52	66.45	66.26
		106.60	235.00	66.13	66.46	66.40	66.24
		106.60	245.00	66.13	66.40	66.35	66.22
		106.60	255.00	66.13	66.36	66.32	66.21
		106.60	265.00	66.13	66.32	66.29	66.20
		106.60	275.00	66.13	66.29	66.26	66.18
		106.60	285.00	66.13	66.26	66.24	66.17
		106.60	295.00	66.12	66.23	66.21	66.16
		106.60	305.00	66.11	66.21	66.19	66.14
		106.60	315.00	66.10	66.18	66.17	66.13
		106.60	325.00	66.09	66.17	66.15	66.12
		106.60	335.00	66.09	66.16	66.15	66.12
		106.60	345.00	66.17	66.23	66.22	66.19
		106.60	355.00	66.25	66.32	66.30	66.27
		106.60	360.00		66.32	66.30	66.27

				Uplift pressure in %			
				Table 5.6			
			Comparison of uplift pressures for different Test condition A3 (X=71m)				
S.No.	Location	Floor Level Y in m	Distance along floor width in m.from abutment	Test condition 1	Test condition 2	Test condition 3	Test condition 4
1	U/S edge of D/S floor section A3(x=71m)	103.25	50	54.05	75.979	71.746	60.94
		103.25	60	54.498	72.146	68.801	60.19
		103.25	80	55.298	65.037	63.253	58.51
		103.25	100	55.627	61.516	60.454	57.58
		103.25	120	55.879	59.701	59.017	57.15
		103.25	130	55.977	59.369	58.763	57.1
		104.25	135	56.032	58.33	58.26	56.79
		104.25	145	55.995	58.06	58	56.68
		104.25	165	55.992	57.4	57.37	56.46
		104.25	245	56.07	56.376	56.37	56.17
		104.25	305	56.043	56.15	56.14	56.07
		104.25	325	55.991	56.07	56.07	56.01
		104.25	345	55.936	56	56	55.96
		104.25	355	55.949	56.01		
		104.25	360	55.949	56.01		

				Uplift pressure in %			
S.No.	Location	Level Y in m	Distance along floor width in m.	Test condition 1	Test condition 2	Test condition 3	Test condition 4
1		103.25	50	42.833	63.987	60.102	48.52
		103.25	60	42.406	59.885	56.675	47.313
		103.25	70	41.837	54.564	52.234	45.625
		103.25	80	41.518	51.046	49.31	44.455
		103.25	90	41.367	48.687	47.36	43.672
		103.25	100	41.299	47.035	46	43.13
		103.25	110	41.267	45.842	45.02	42.741
		103.25	120	41.222	44.951	44.282	42.43
		103.25	130	41.178	44.5	43.906	42.258
		104.25	135	40.998	43.216	42.82	41.723
		104.25	145	41.028	43.031	42.674	41.684
		104.25	155	41.098	42.767	42.47	41.646
		104.25	165	41.143	42.523	42.277	41.597
		104.25	175	41.169	42.306	42.104	41.543
		104.25	185	41.186	42.123	41.957	41.495
	Center of D/S floor sec A4(X=84.5m)	104.25	195	41.198	41.971	41.834	41.453
		104.25	205	41.208	41.845	41.732	41.418
		104.25	215	41.215	41.741	41.647	41.389
		104.25	225	41.22	41.654	41.577	41.364
		104.25	235	41.224	41.583	41.519	41.343
		104.25	245	41.226	41.523	41.471	41.325
		104.25	255	41.227	41.473	41.43	41.309
		104.25	265	41.226	41.431	41.395	41.294
		104.25	275	41.223	41.394	41.364	41.28
		104.25	285	41.217	41.361	41.335	41.265
		104.25	295	41.207	41.329	41.307	41.247
		104.25	305	41.19	41.294	41.275	41.224
		104.25	315	41.155	41.246	41.23	41.185
		104.25	325	41.103	41.183	41.169	41.129
		104.25	335	40.927	41.001	40.988	40.952
		104.25	345	40.665	40.733	40.721	40.687
		104.25	355	40.337	40.403	40.391	40.359

Table 5.7

Comparison of uplift pressures for different Test condition A4 (X=84.5m)

Table 5.8

S.No.	Location	Level Y in m	Distance along floor width in m.	Uplift pressure in %			
				Test condition 1	Test condition 2	Test condition 3	Test condition 4
				Comparison of uplift pressures for different Test condition A5 (X=98m)			
1		103.25	50	34.378	54.241	50.7	39.17
		103.25	60	32.8	48.145	45.38	36.74
		103.25	80	30.87	38.83	37.38	33.19
		103.25	100	30.412	35.18	34.22	31.88
		103.25	120	30.21	33.31	32.75	31.19
	End of D/S floor sec A5(X=98m)	103.25	130	30	32.75	32.26	30.88
		104.25	135	29.04	30.85	30.53	30.14
		104.25	145	29.43	31.08	30.79	29.97
		104.25	165	29.66	30.8	30.6	30.03
		104.25	245	29.73	29.98	29.94	29.82
		104.25	305	29.7	29.78	29.77	29.73
		104.25	325	29.66	29.73	29.72	29.69
		104.25	345	30.65	30.71	30.7	30.67

Figure 5.1 Floor with sheet pile at either end. Potential Φe, Φd, Φc, Φf and equipotential line.

72.709   55.846   31.787

P1   P3   P5   23.539

79.829

	0
	11.111
	22.222
	33.333
	44.444
	55.556
	66.667
	77.778
	88.889
	100
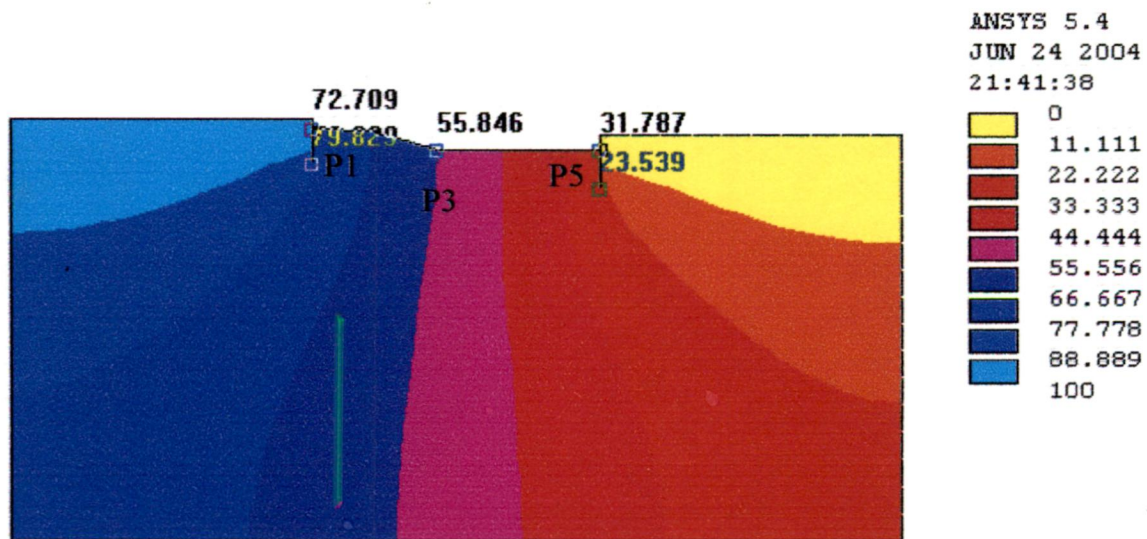
Figure 5.2: Kanpur barrage 2-D uplift distribution

1.775

	.148E-04
	.303756
	.607497
	.911238
	1.215
	1.519
	1.822
	2.126
	2.43
	2.734
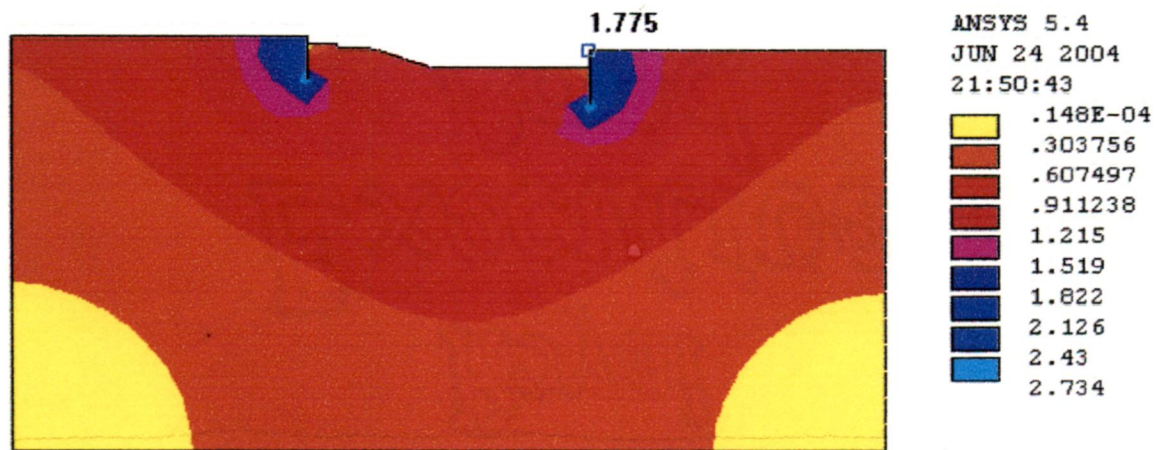
Exit gradient = 1.775*6.9/100=.122

Figure 53: Exit gradient 2D Kanpur barrage

5.2c

Kanpur barrage 3-D uplift pressure distribution
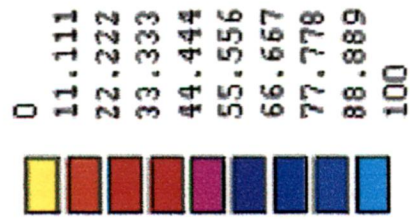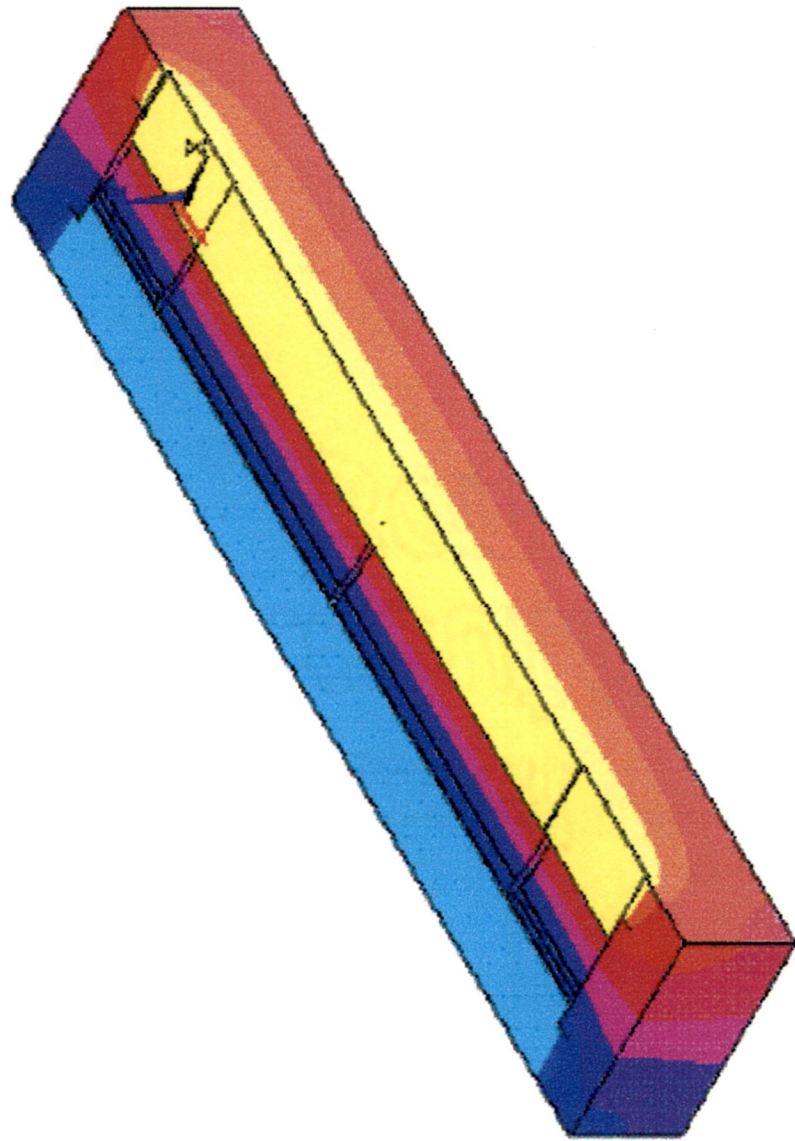
Figure 5.5: 3-D View of Kanpur Barrage pressure distribution test condition 1,u/s 100 % d/s 0 %

kanpur barrage Full model u/s100p/s0 potential (bu100d0)

0		
11.111		
22.222		
33.333		
44.444		
55.556		
66.667		
77.778		
88.889		
100		

5.21

ANSYS 5.4
JUN 27 2004
17:59:58
0
11.111
22.222
33.333
44.444
55.556
66.667
77.778
88.889
100
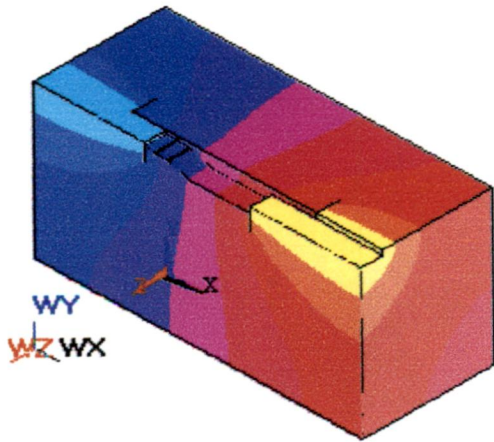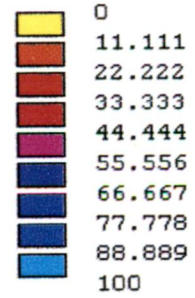
Section at Z=60,uplift pressure contour u/s100d/s0

Figure 5.7, section at Z=60,

ANSYS 5.4
JUN 27 2004
18:10:58
0
11.111
22.222
33.333
44.444
55.556
66.667
77.778
88.889
100
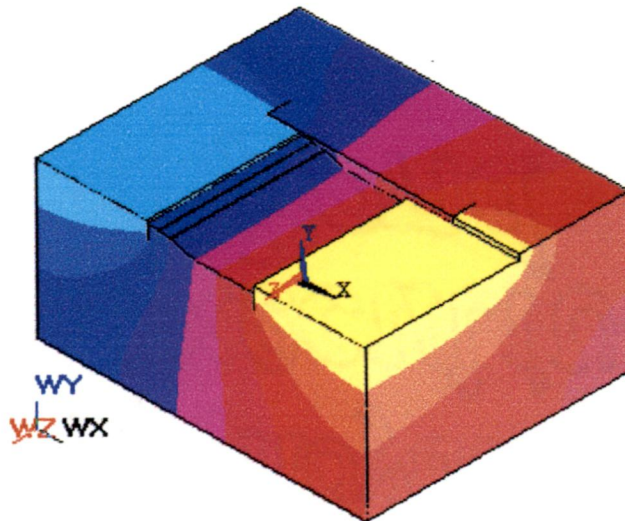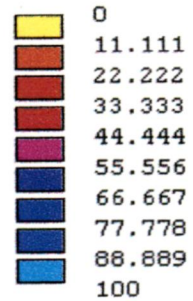
Section at Z=120, 3-D view of pressure distribution u/s100 d/s0

Figure 5.8: Section at Z=120, 3-D uplift pressure distribution

CONTOUR AT SECTION X 120 UNDER SLUICE BAY U/S 100 D/S0
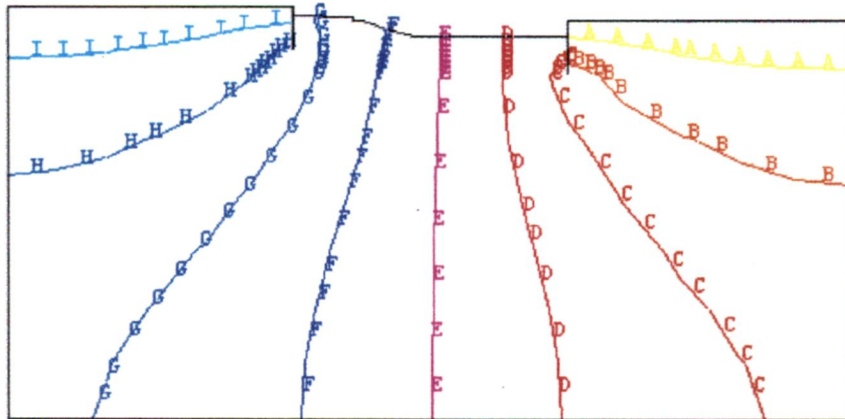
ANSYS 5.4
MAY 9 2004
15:09:27
NODAL SOLUTION
STEP=1
SUB =1
TIME=1
TEMP   (AVG)
RSYS=0
PowerGraphics
EFACET=1
AVRES=Mat
SMX =100
A   =5.556
B   =16.667
C   =27.778
D   =38.889
E   =50
F   =61.111
G   =72.222
H   =83.333
I   =94.444

kanpur barrage Full model U/S100D/S0 potential (bu100d0)

Figure 5.9: Section Z=120 Contours

Figure 5.10: Section Z=145 Contours

Figure 5.11: Section Z=345 Contours

Figure 5.12: The variation of uplift pressure at the center of the D/S floor under test condition 1 U/S potential 100 % D/S potential 0 %.

UNDER SLUICE BAY SEC X 71 U/S 100 D/S US & BB 0
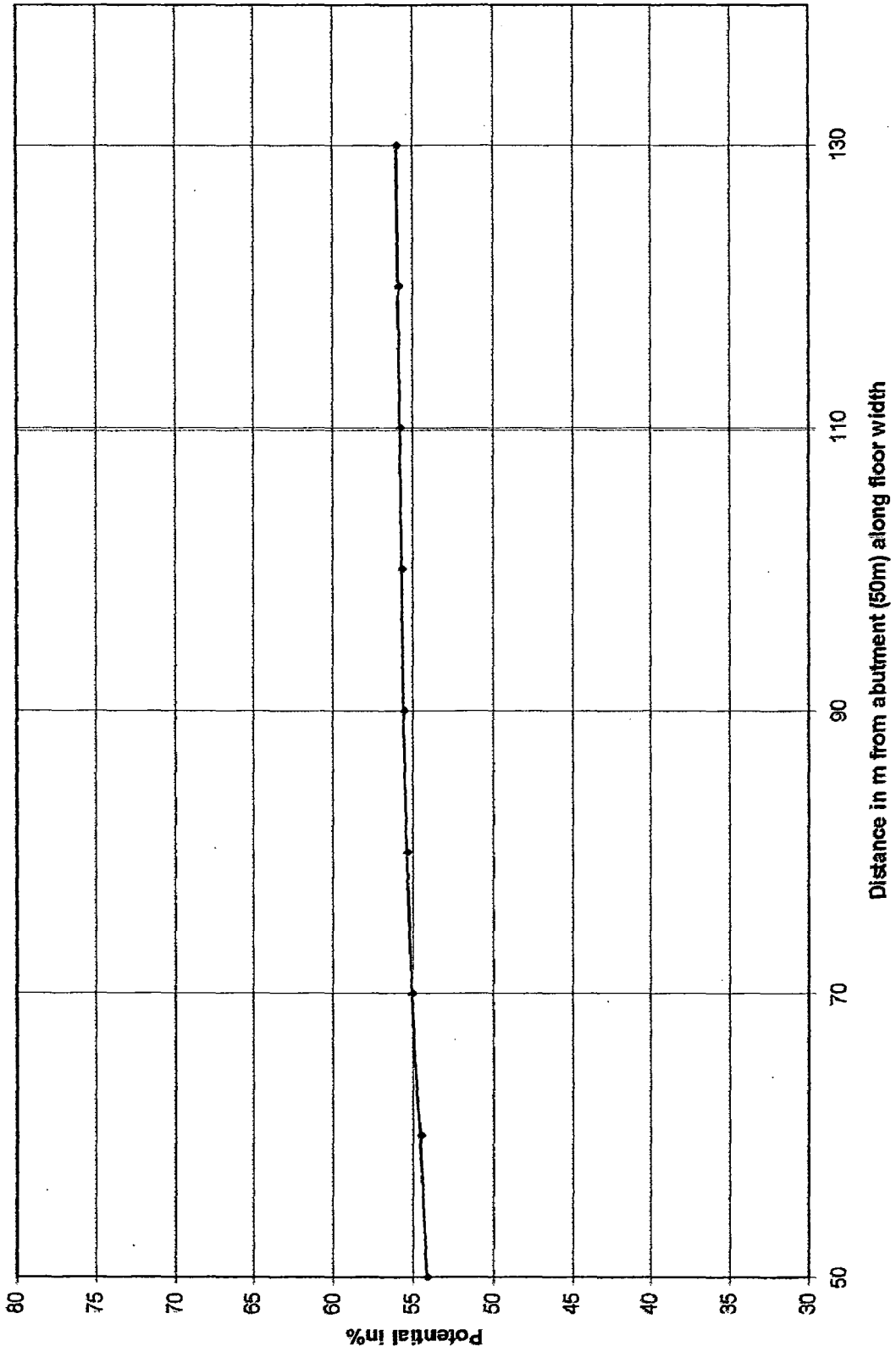
Figure 5.13: The variation of uplift pressure at the P3 (X=71m) of the D/S floor under test condition 1 U/S potential 100 % D/S potential 0 %.along the length of floor.

UNDER SLUICE BAY SEC X 98 U/S 100 D/S US & BB 0
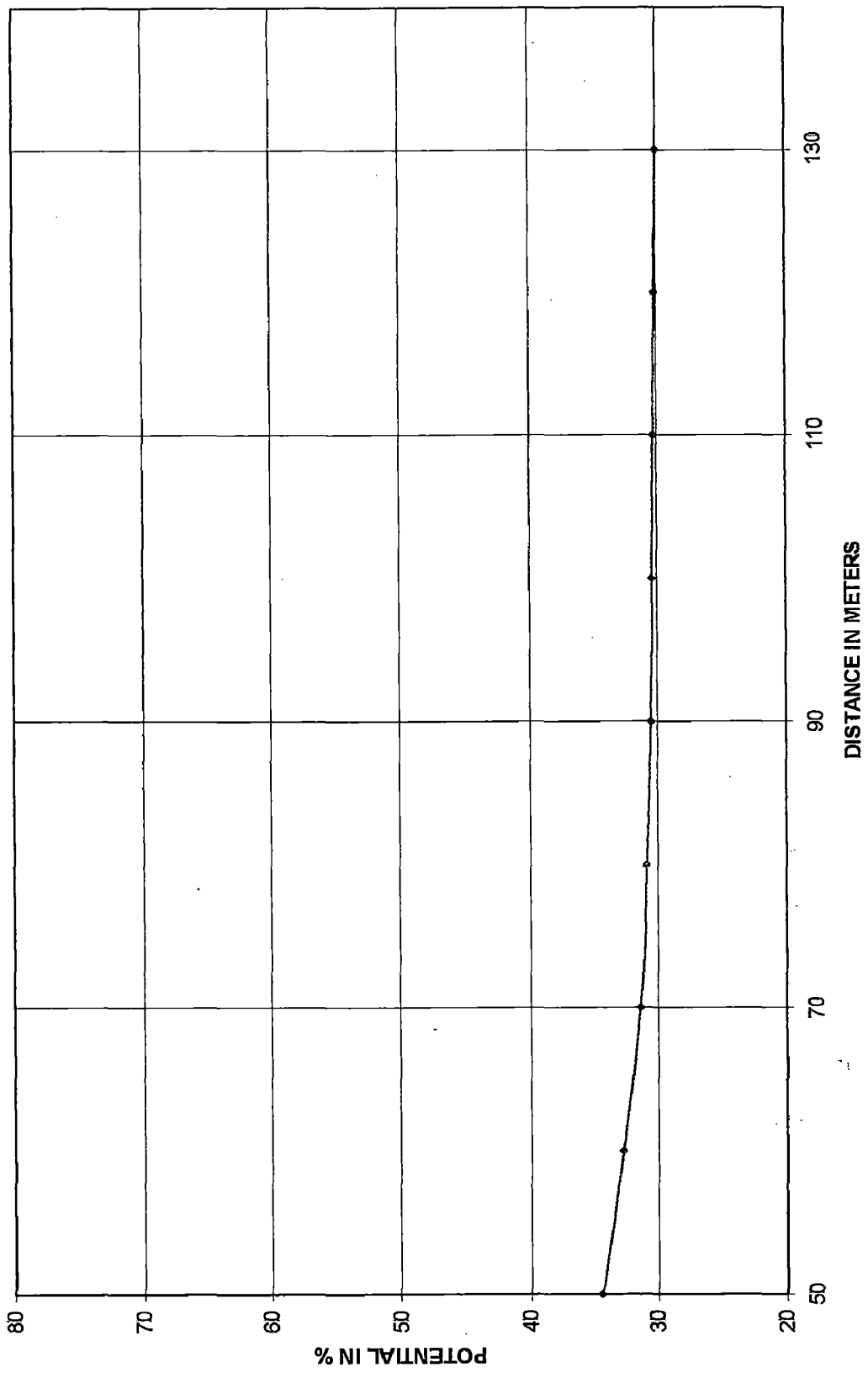
Figure 5.14   The variation of uplift pressure at the P5 (X=98m) of the D/S floor under test condition 1 U/S potential 100 % D/S potential 0 %. Along the length of floor.

D/S SHEET PILE R.L 96.7 U/S 100 D/S US & BB 0
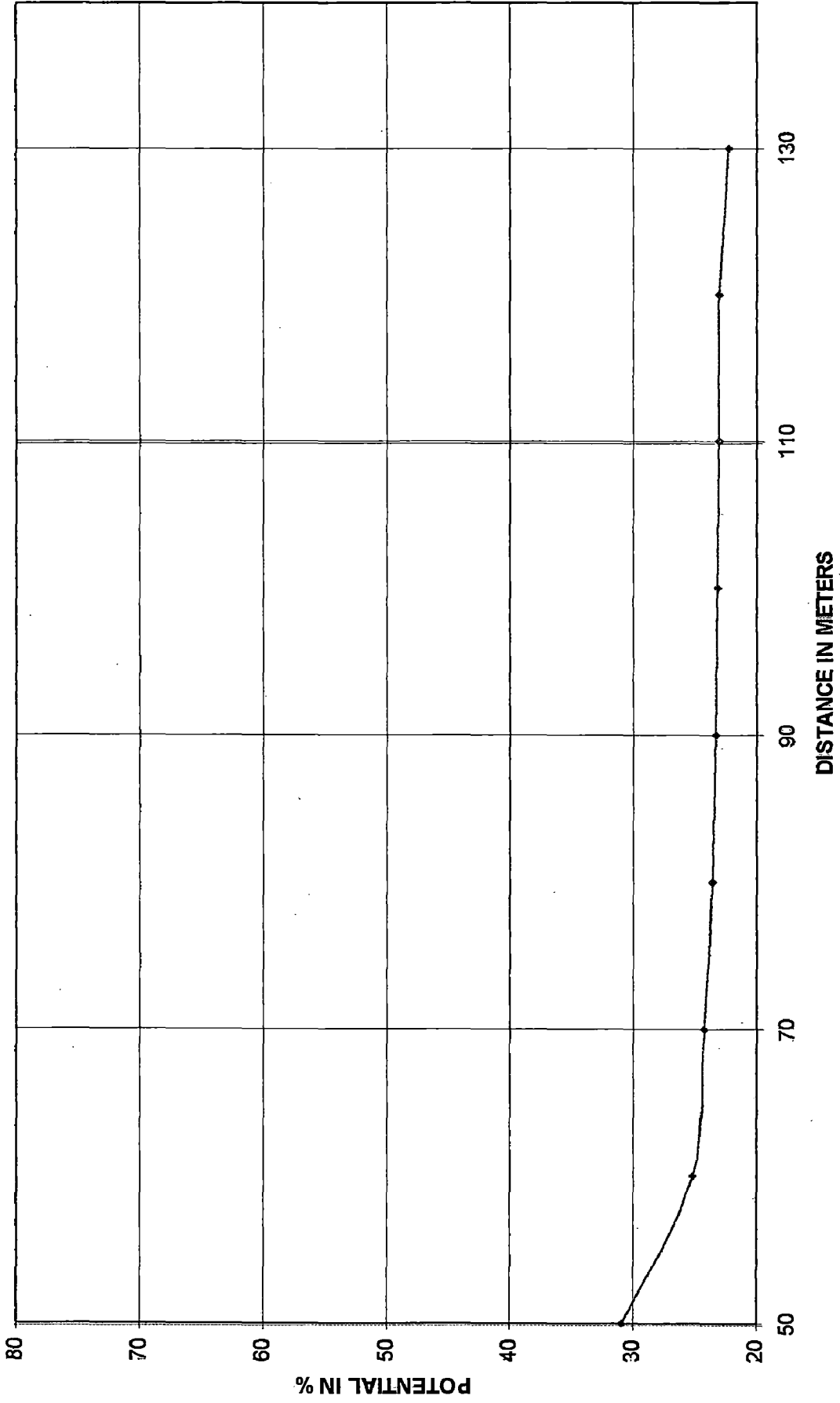
Figure 5.15: The variation of uplift pressure at the (S2) D/S sheet pile under test condition 1 U/S potential 100 % D/S potential 0 %.

UNDER SLUICE BAY SEC X62 U/S 100 D/S US & BB 0
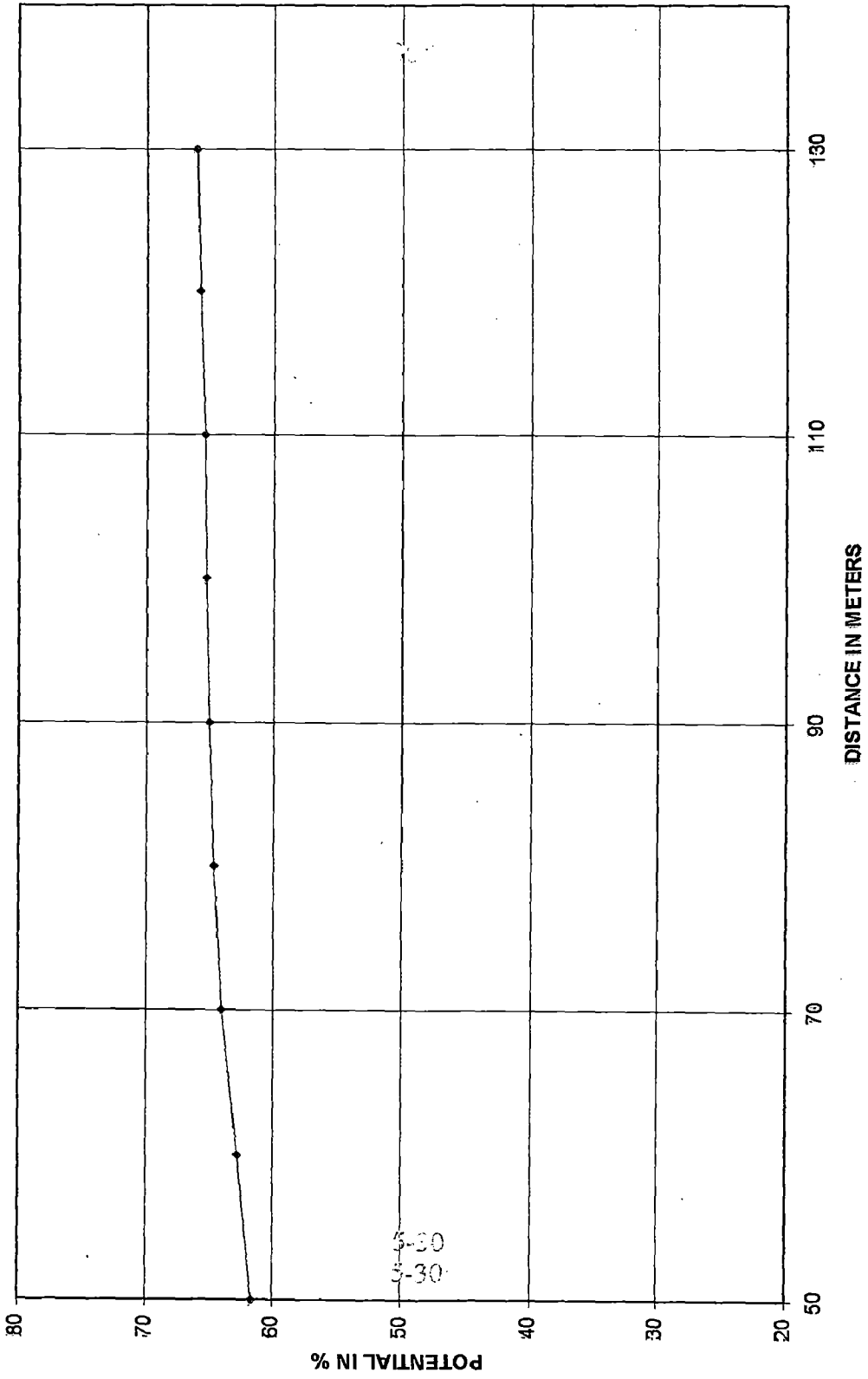
Figure 5.16: The variation of uplift pressure at P2, along the floor width of under
sluice bay under test condition 1 U/S potential 100 % D/S potential 0 %.

BARRAGE BAY SEC X71 R.L. 104.25U/S 100 D/S US&BB 0
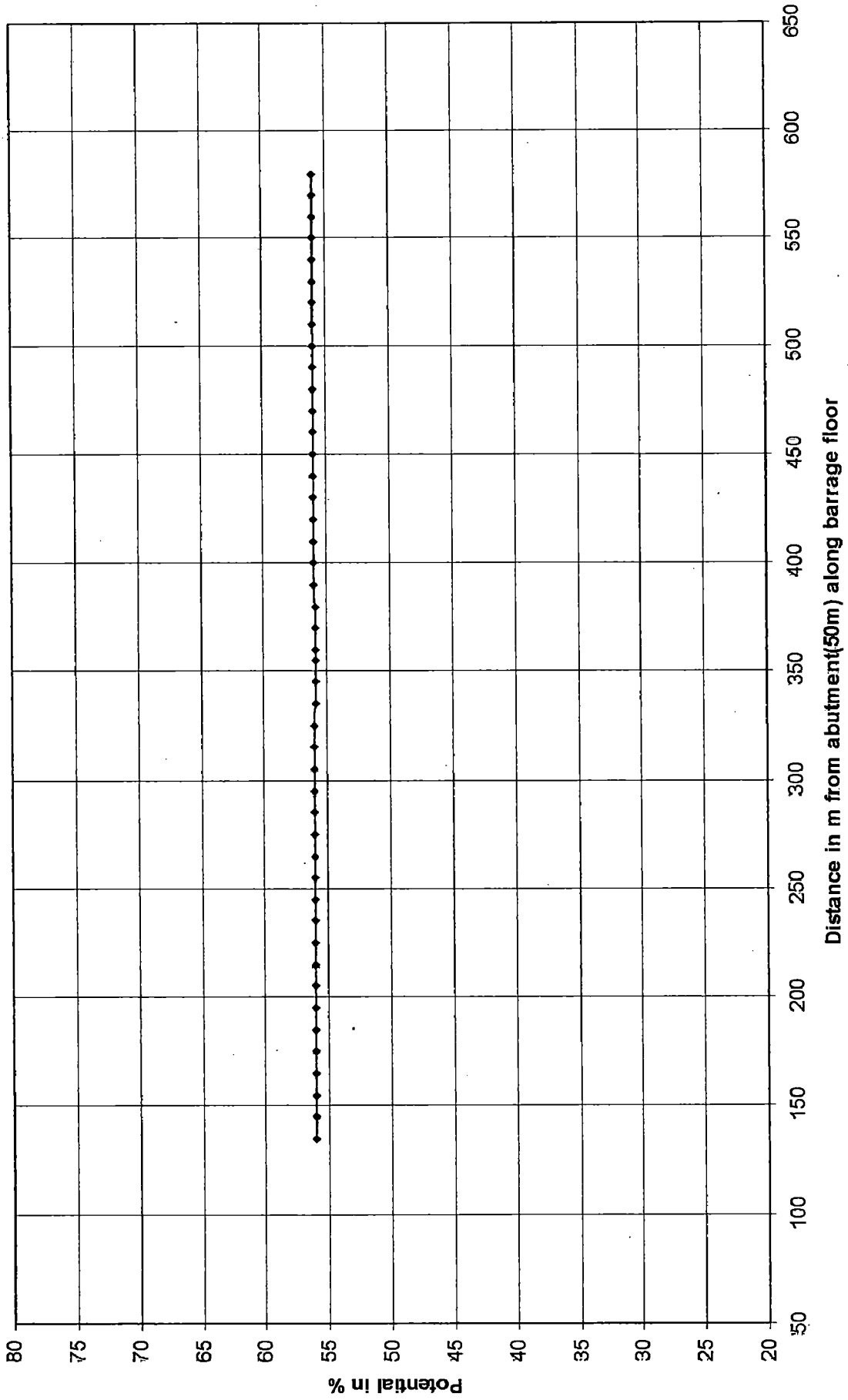
Figure 5.17:   The variation of uplift pressure at the C3   (X=71m) along floor width of the D/S floor barrage bay under test condition 1 U/S potential 100 % D/S potential 0 %.

BARRAGE BAY SEC X 84.5 R.L 104.25U/S 100 D/S US&BB 0
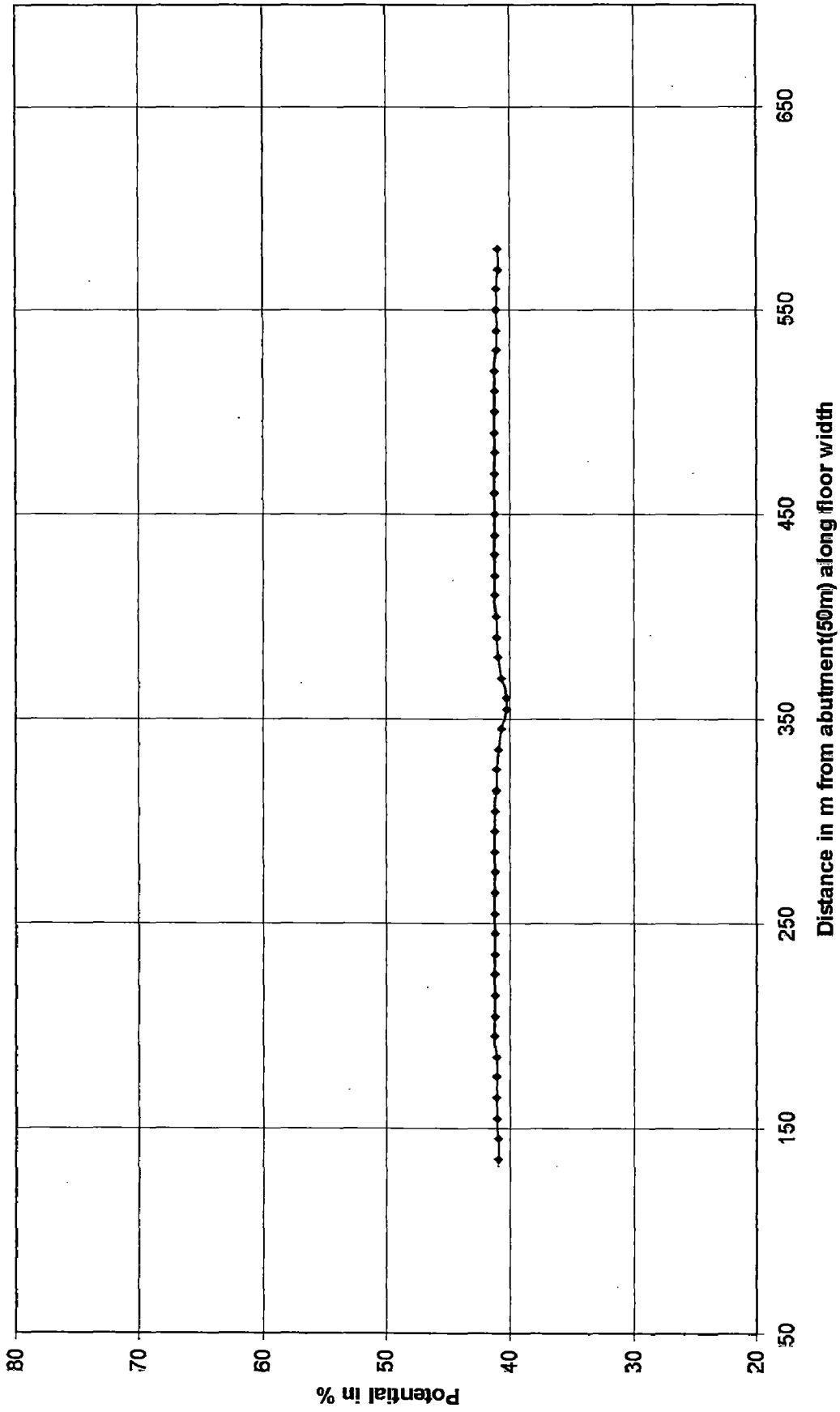
Figure 5.18: The variation of uplift pressure at the C4 (X=84.5m) along floor width of the D/S floor barrage bay under test condition 1 U/S potential 100 % D/S potential 0 %.

UNDER SLUICE BAY EXIT GRADIENT U/S 100 D/S US&BB 0
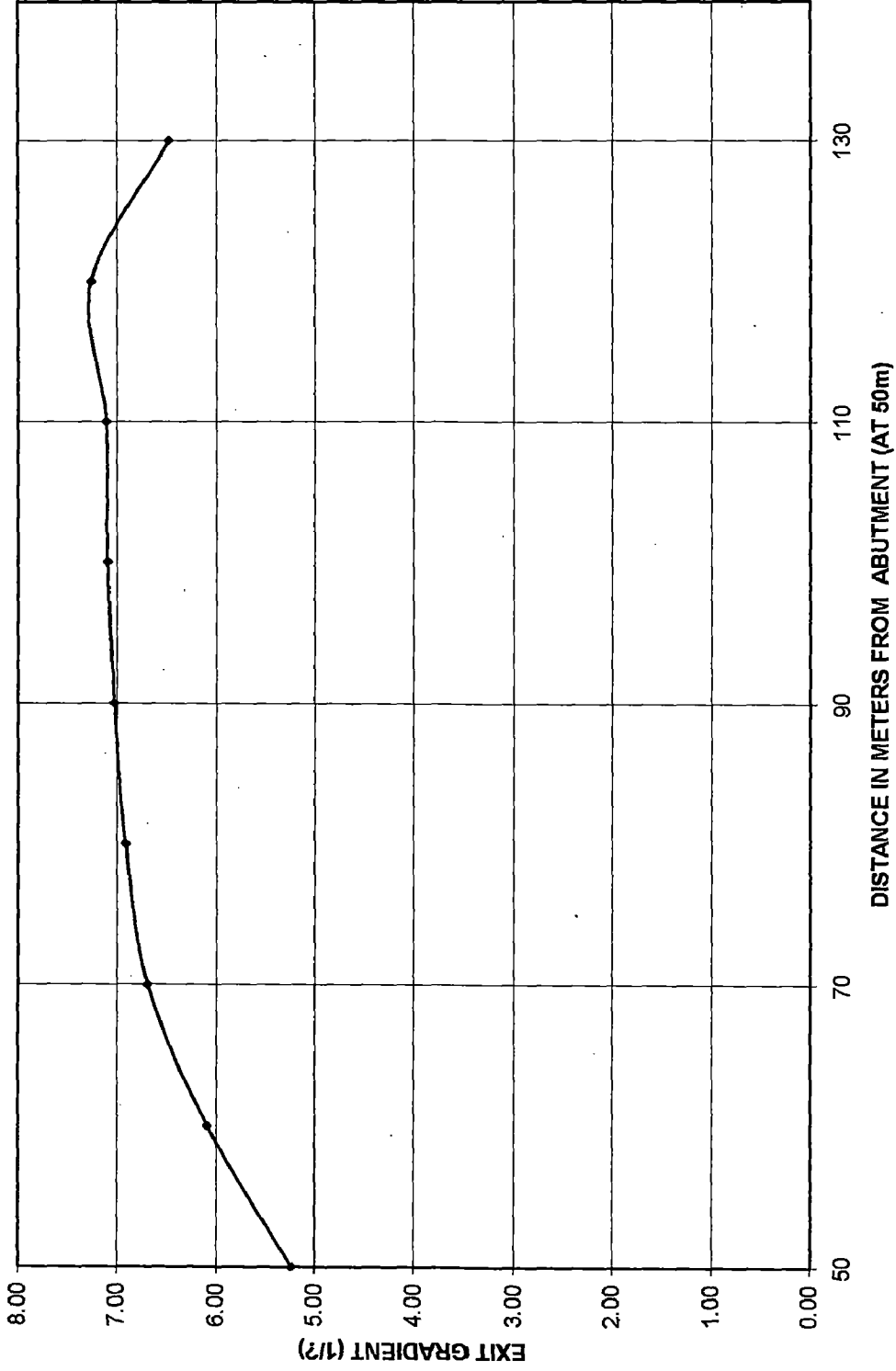
Figure 5.19: The variation of exit gradient D/S sheet pile in under sluice bay ,from bay No.1 to 4, under
test condition 1

BARRAGE BAY EXIT GRADIENT U/S 100 D/S US&BB 0
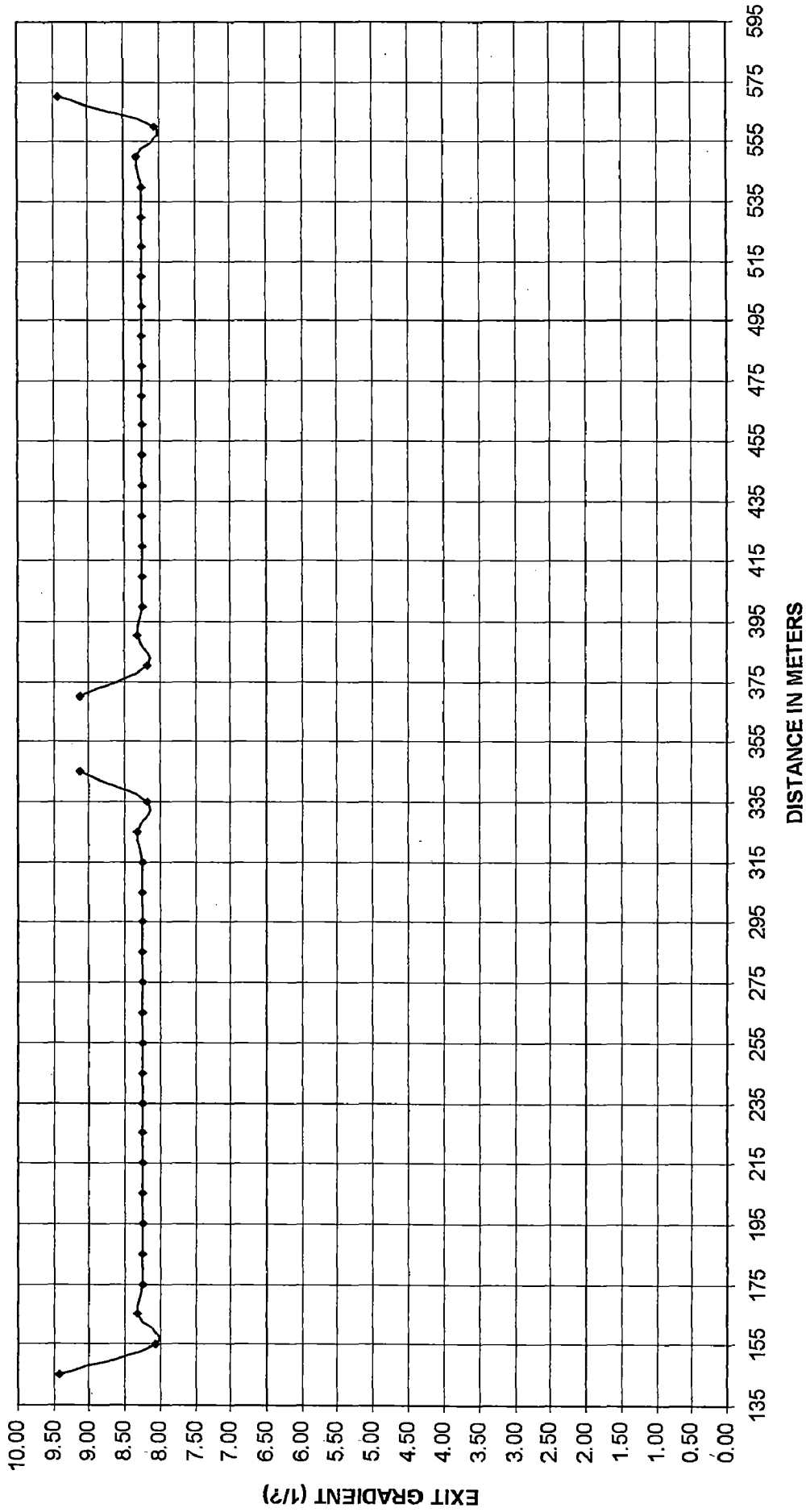
Figure 5.20: The variation of exit gradient at G4 in barrage bay, from bay No.1 to 22, under test condition 1 U/S potential 100 % D/S potential 0 %.

UNDER SLUICE BAY SEC Z 60 U/S100 D/S US%BB0
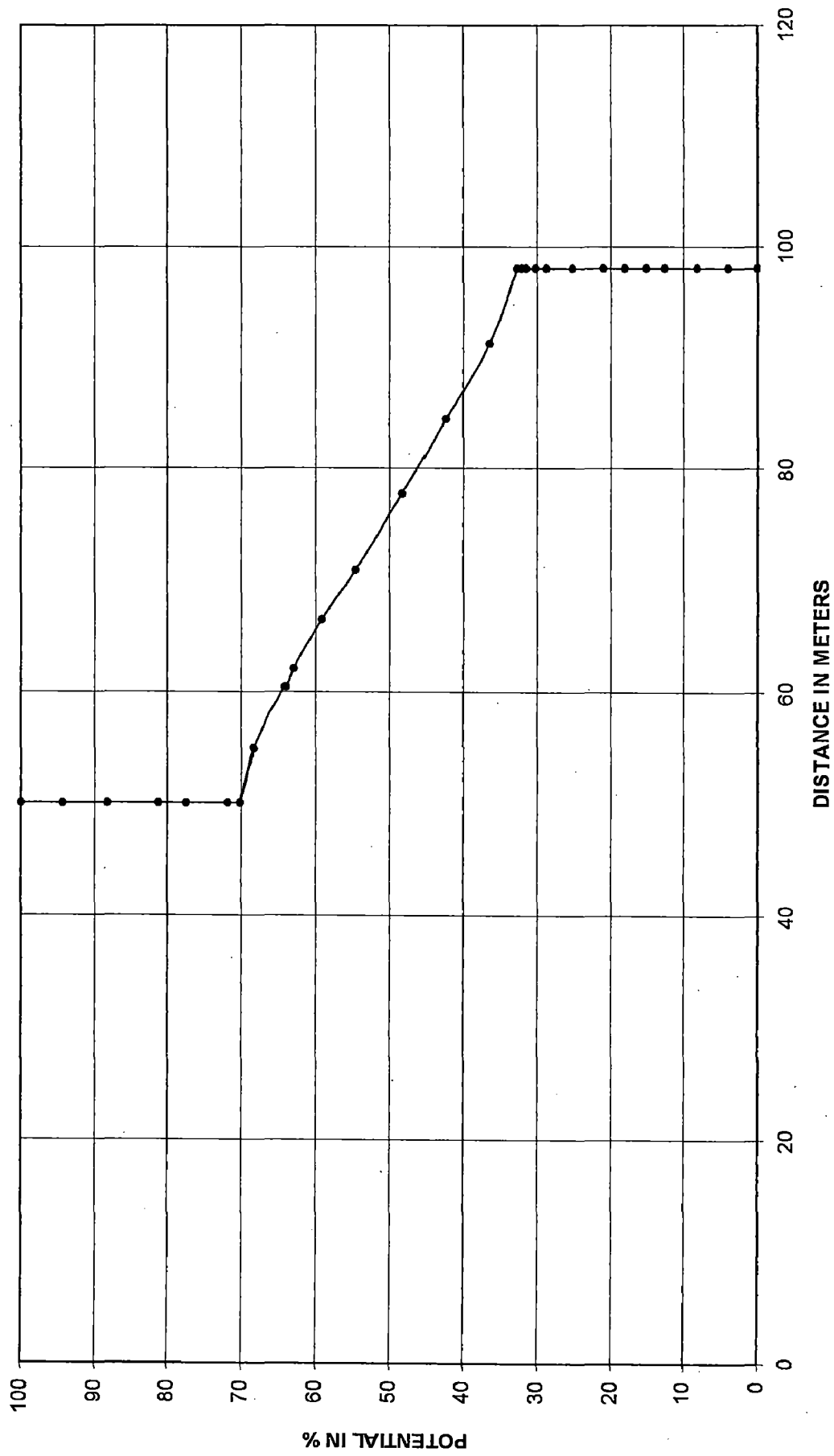
Figure 5.20a: The variation of uplift pressure along flow direction U1(Z=60m) test condition1
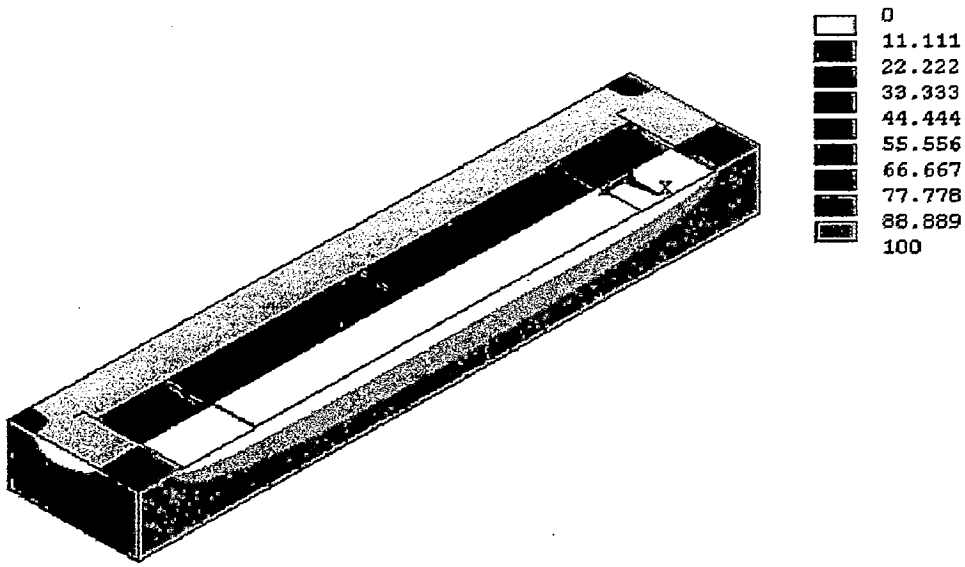
kanpur barrage Full model us100ds0abutment100 (u100d0ab100)

Figure 5.21:   3D View of uplift pressure distribution test condition 2
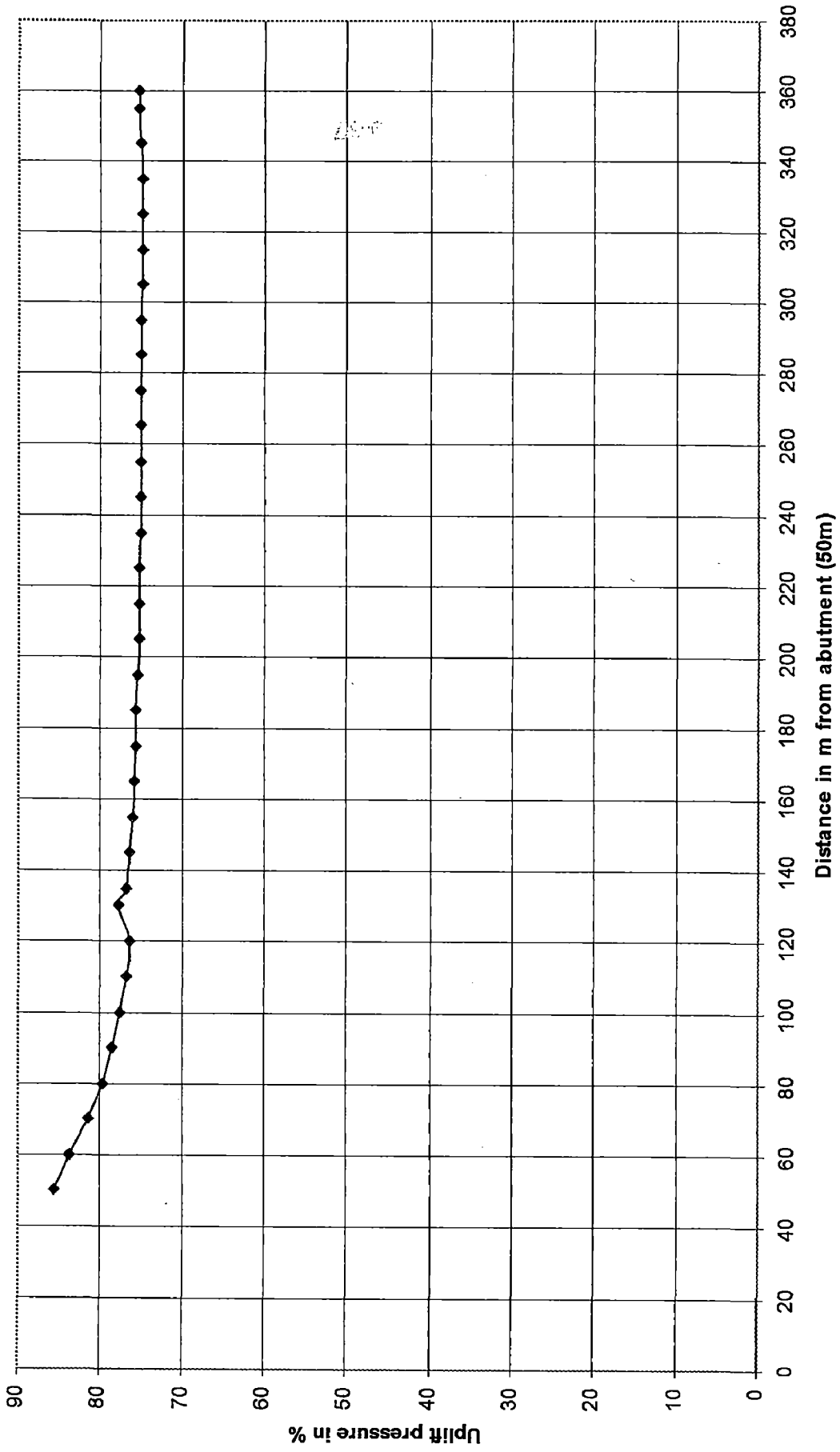
Figure 5.22: The variation of uplift pressure along floor width at A1(X=50m) test condition2

The Variation of Uplift Pressure for load condition 2 Sec A2 (X=62m)

Uplift pressure in %

Distance in m from abutment (50m)
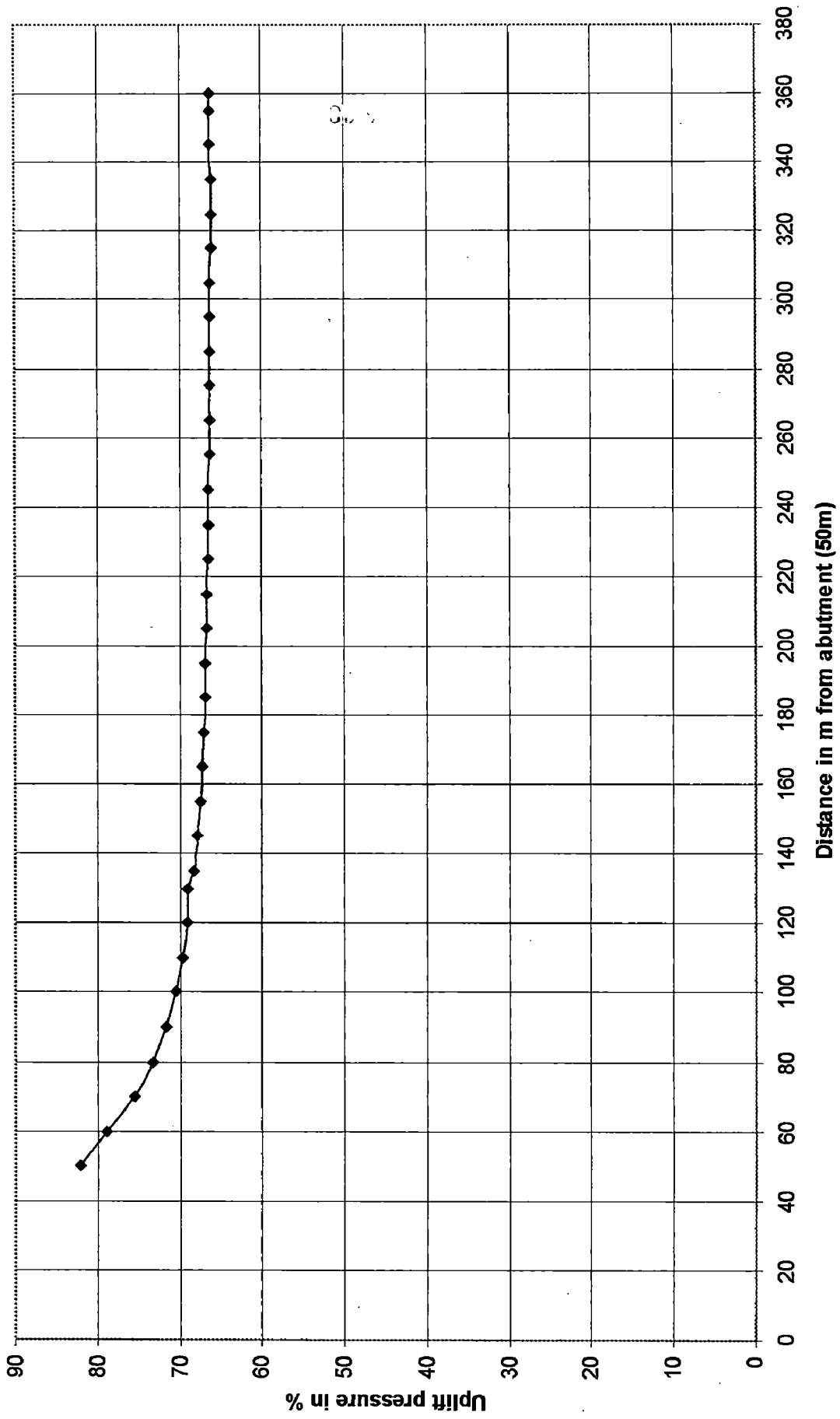
Figure 5.23: The variation of uplift pressure along floor width at A2(X=62m) test condition2

The Variation of Uplift Pressure for load condition 2 Sec A3 (X=71m)
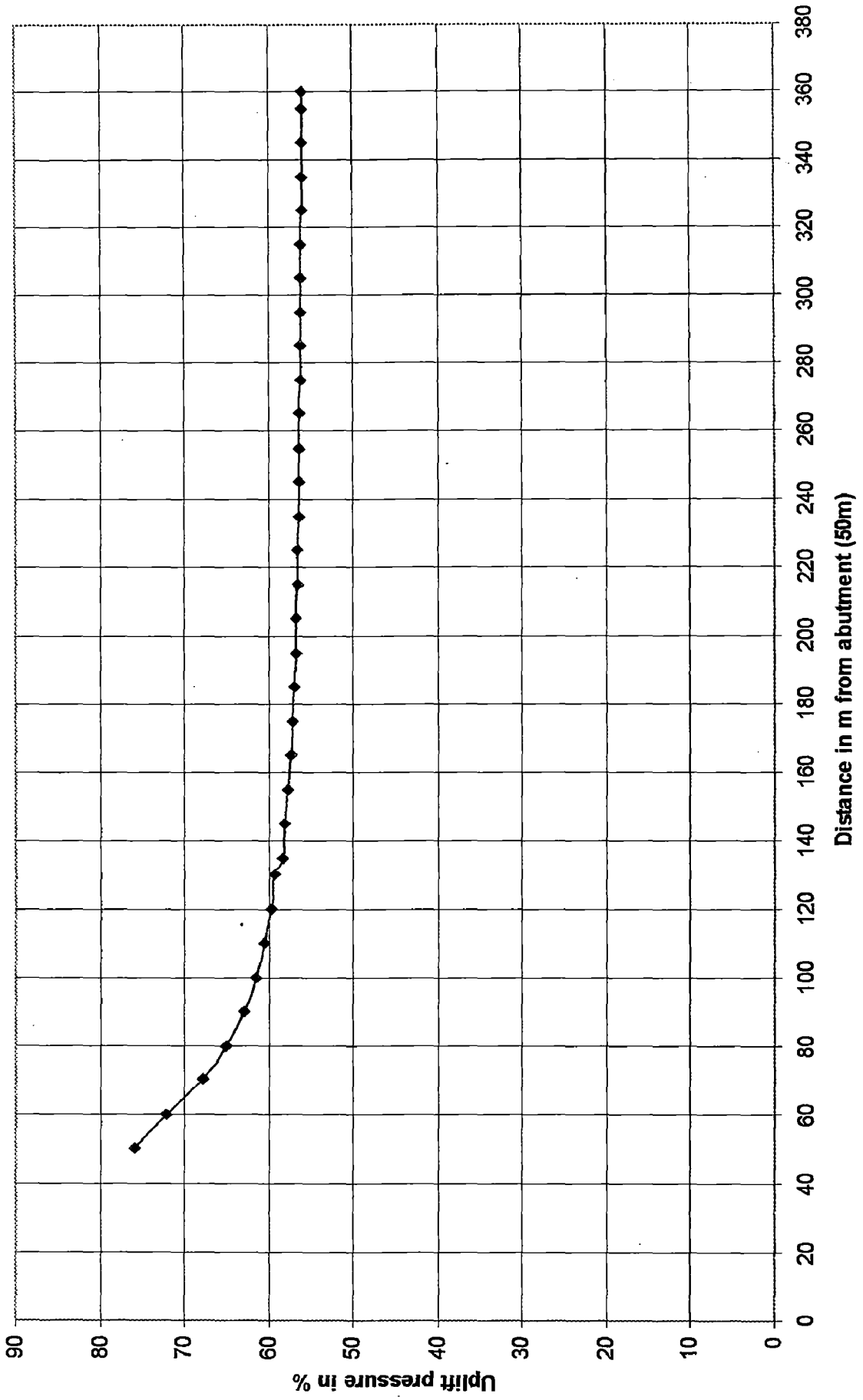
Figure 5.24: The variation of uplift pressure along floor width at A3(X=71m) test condition2

The Variation of Uplift Pressure for load condition 2 Sec A4 (X=84.5m)
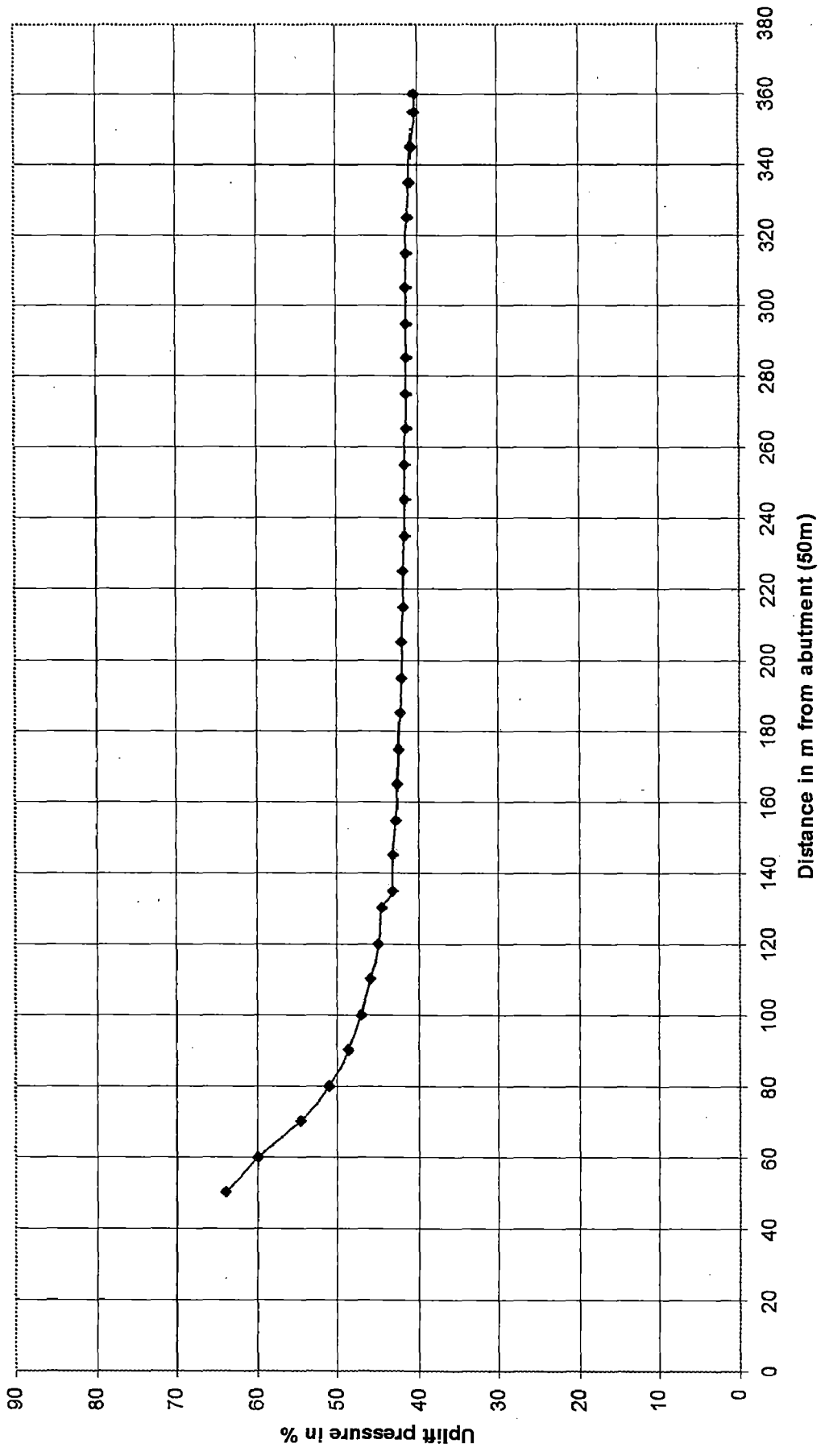
Figure 5.25: The variation of uplift pressure along floor width at A4(X=84.5m) test condition2

5-39

The Variation of Uplift Pressure for load condition 2 Sec A5 (X=98m)
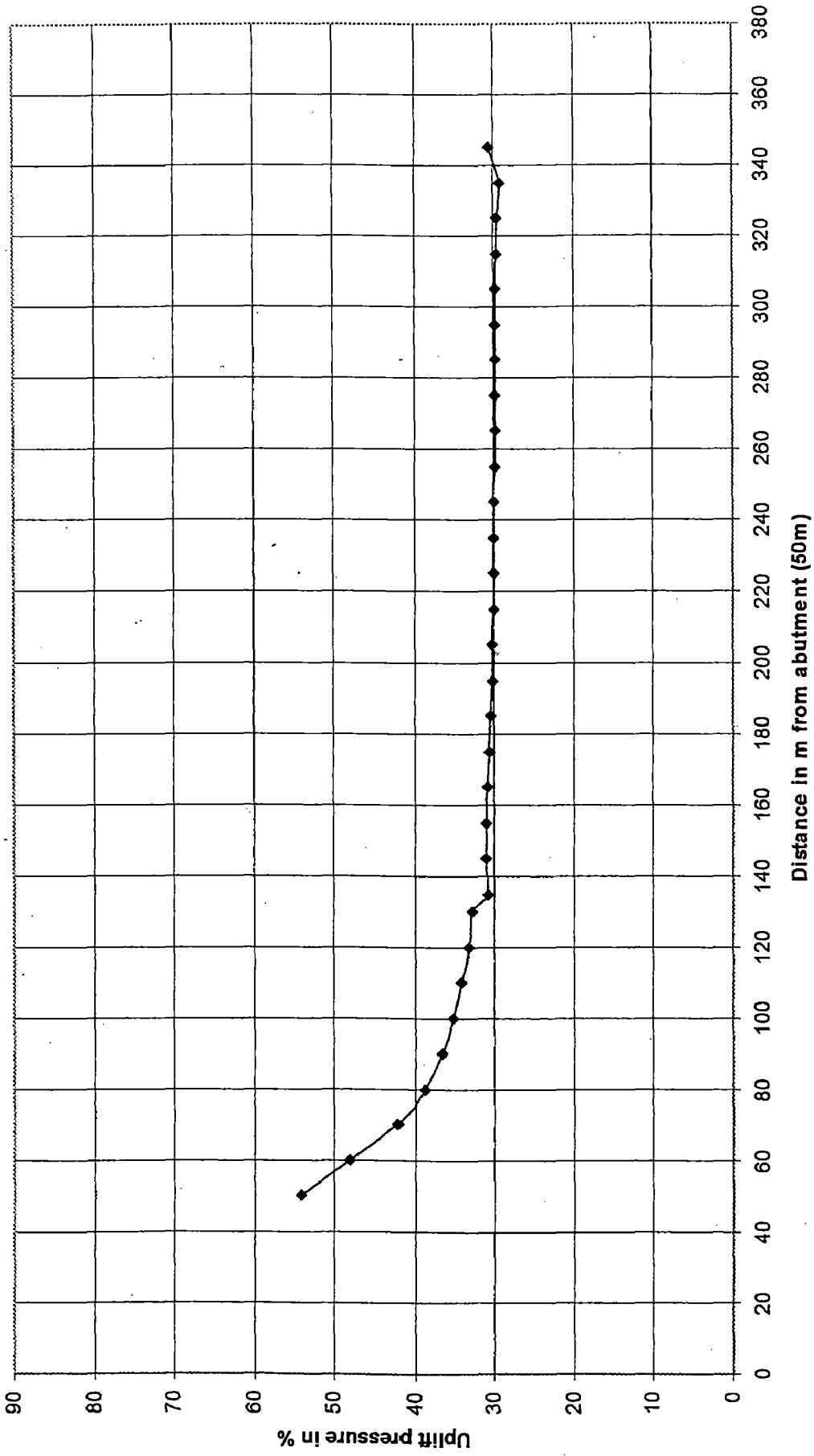
Figure 5.26: The variation of uplift pressure along floor width at A5(X=98m) test condition2
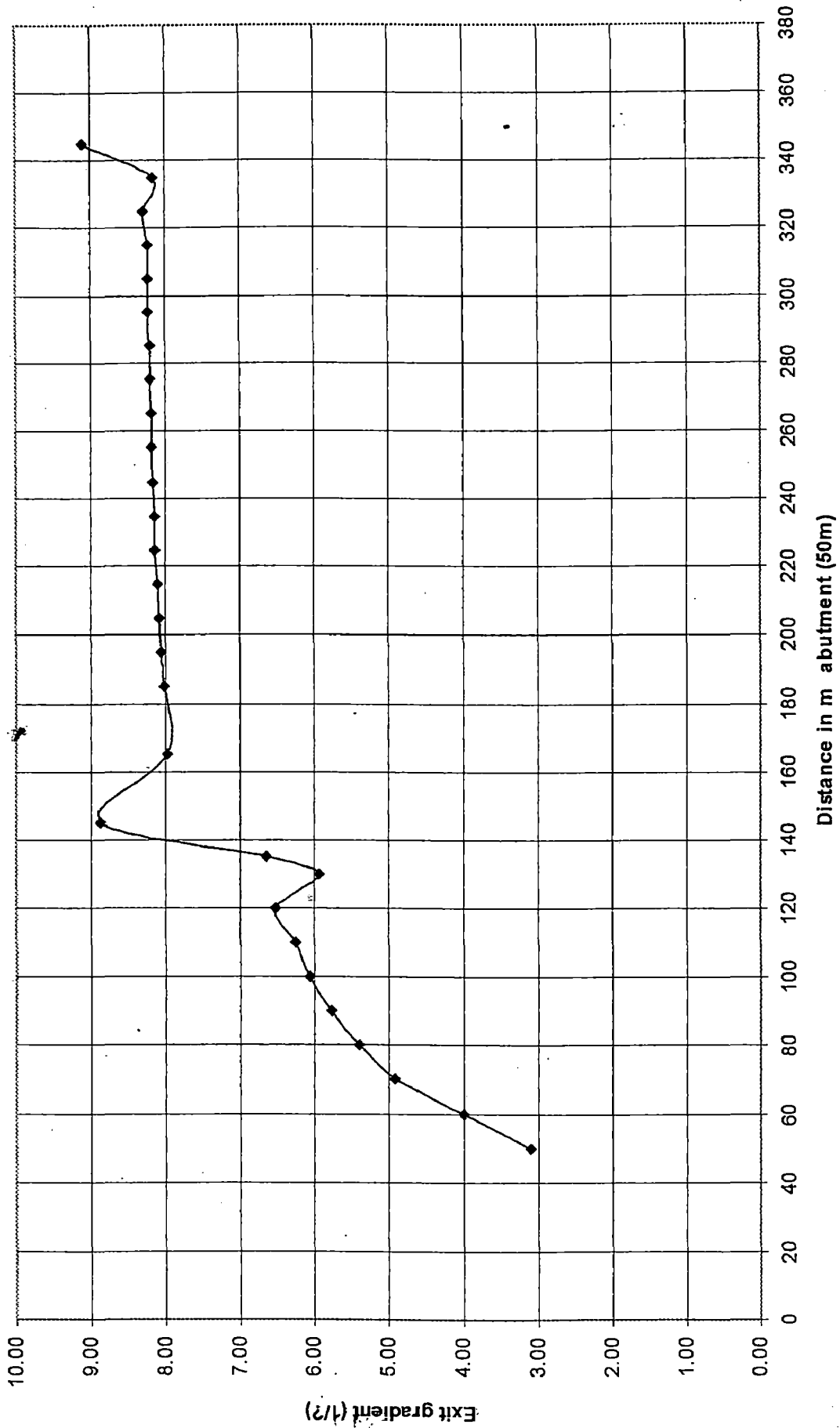
Figure 5.27: The variation of exit gradient for test condition 2 along floor width at D/S Sheet pile

Figure 5.28: 3D View of uplift pressure distribution test condition 3
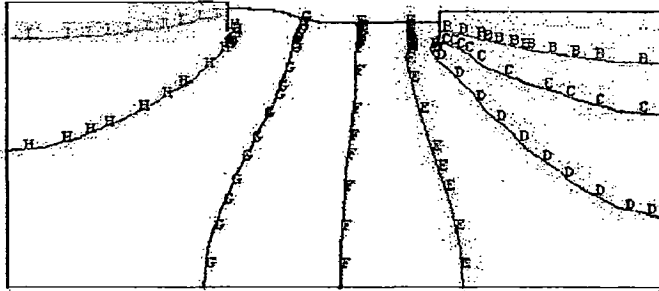
Figure 5.28a: Contour at Section U1 for test condition 3

Figure 5.28b: Contour at Section U3 for test condition 3
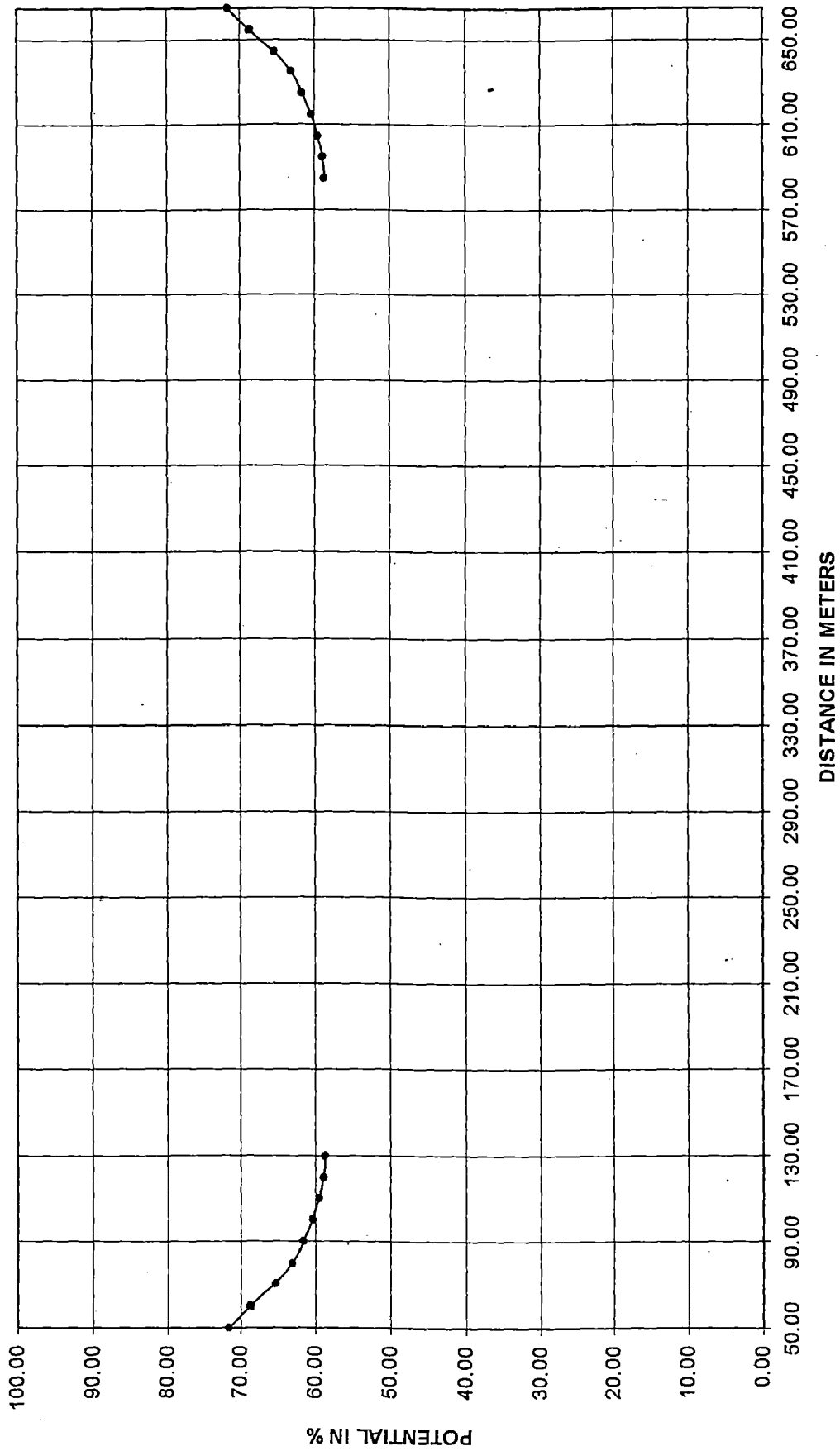
UNDER SLUICE BAY SEC X 71 U/S 100 D/S US&BB 0 ABUTMENT TOP90

Figure 5.29: The variation of uplift pressure at P3 (A3) along the floor width of under sluice bay under test condition 3
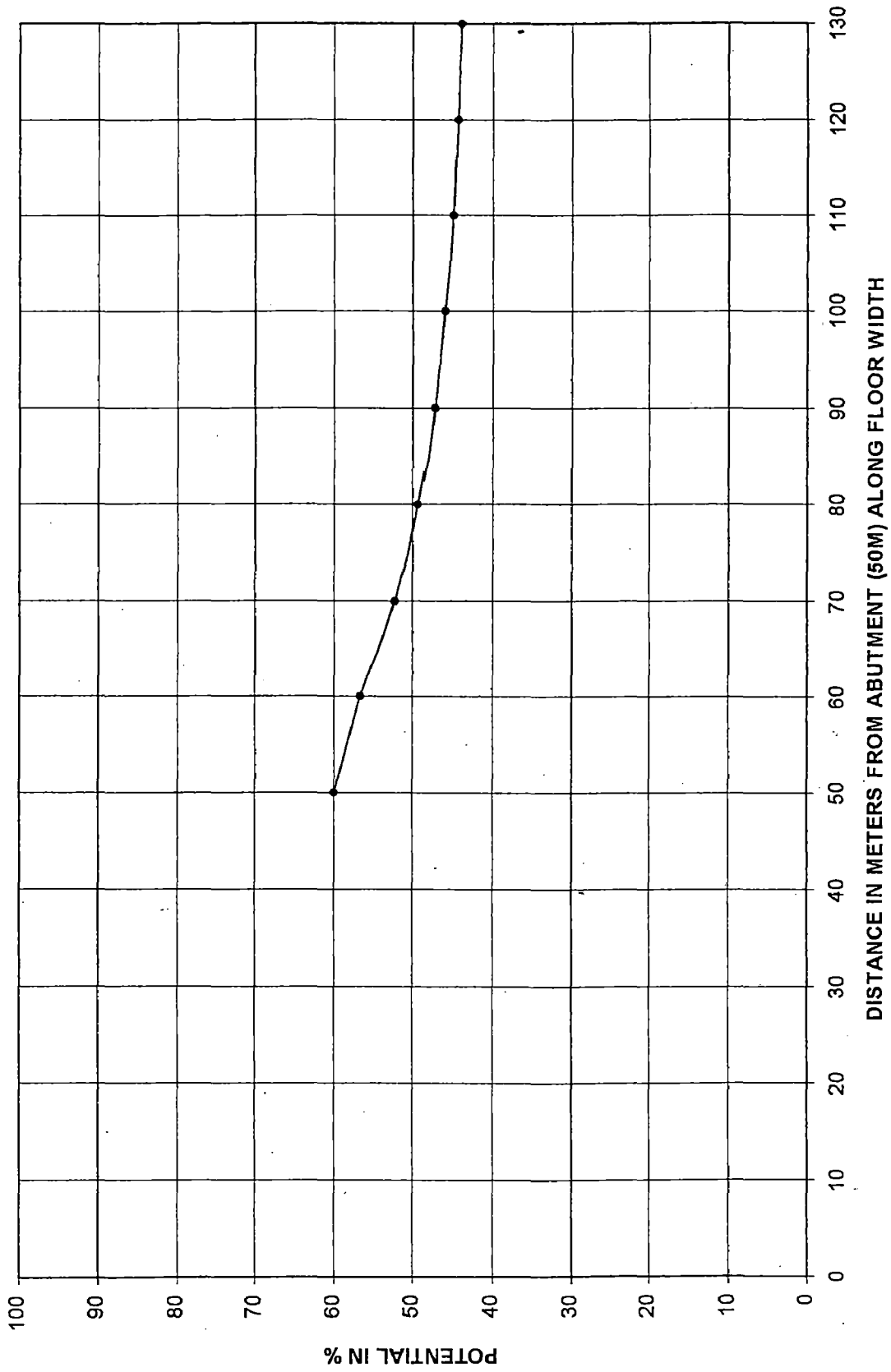
Figure 5.30 The variation of uplift pressure at P4 (A4) along the floor width of under sluice bay under test condition 3

UPLIFT PRESSURE VARIATION BARRAGE BAY(SECX71US100DS0ABUT90)
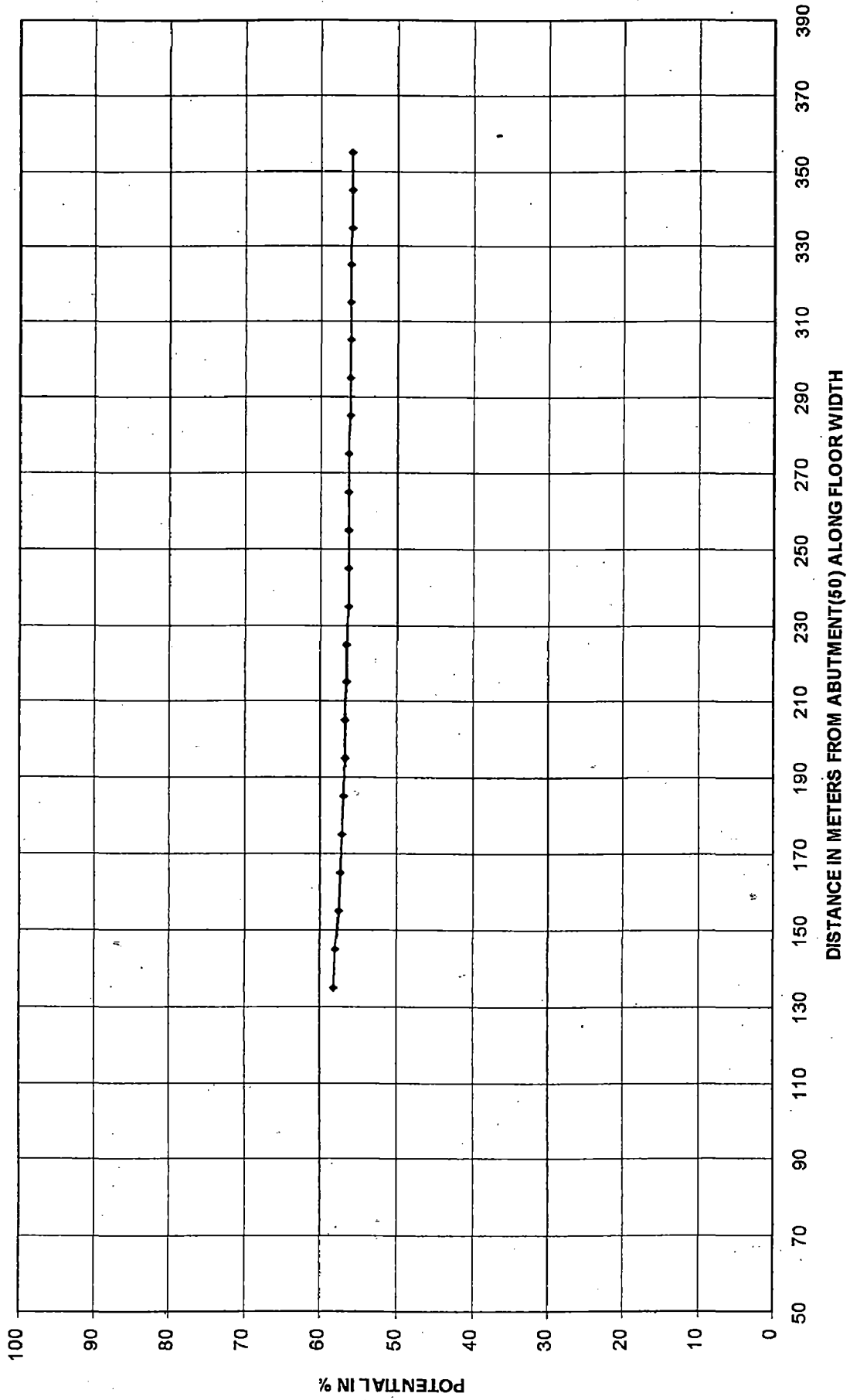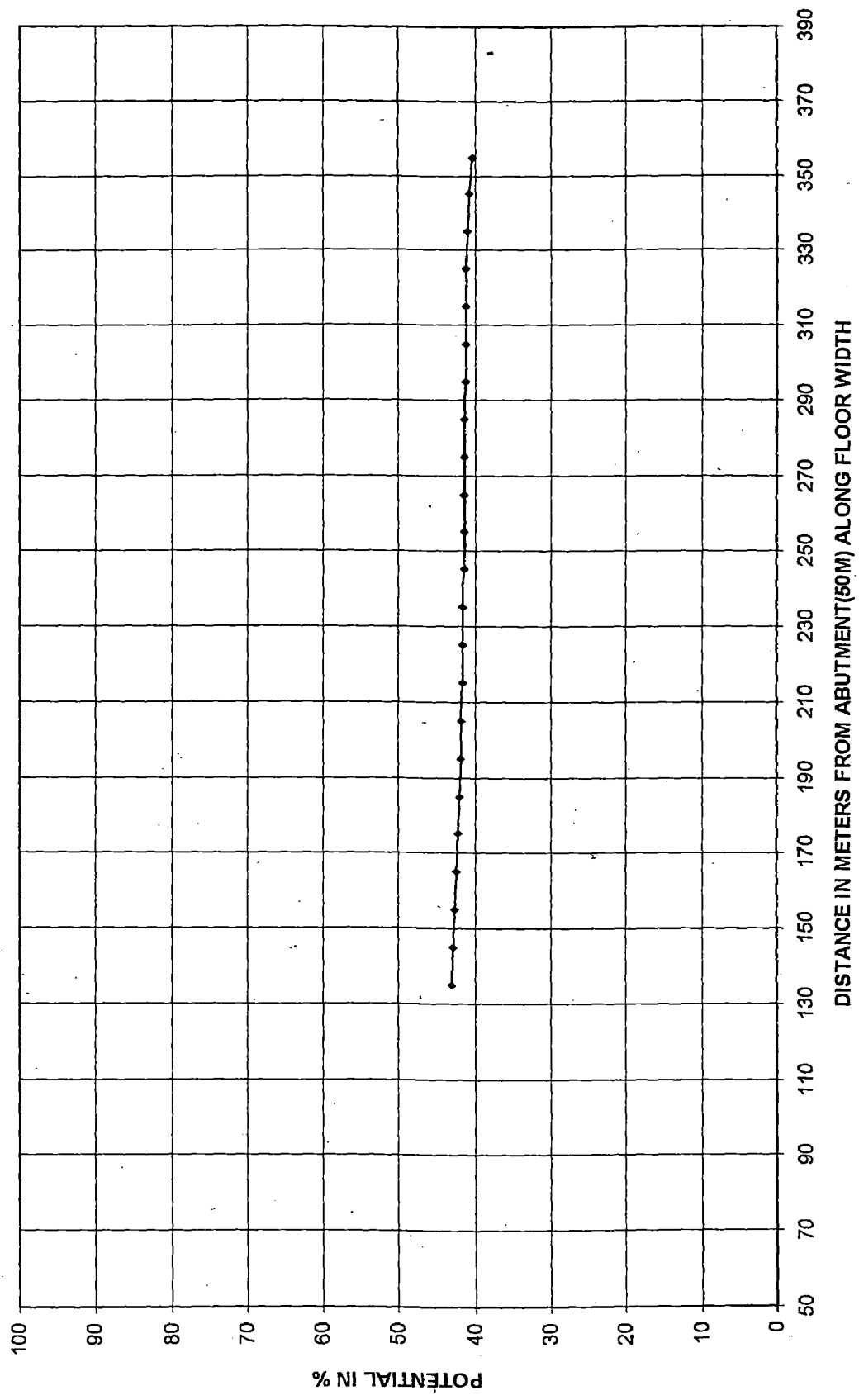

Figure 5.32: The variation of uplift pressure at C3 (A3) along the floor width of barrage bay under test condition 3

UPLIFT PRESSURE VARIATION BARRAGE BAY FLOOR(SECX84.5US100DS0ABU90)

DISTANCE IN METERS FROM ABUTMENT(50M) ALONG FLOOR WIDTH

POTENTIAL IN %

Figure 5.33: The variation of uplift pressure at C4 (A4) along the floor width of barrage bay under test condition 3

BARRAGE BAY SEC X 98 U/S 100 D/S US&BB 0 ABUTMENT TOP 90
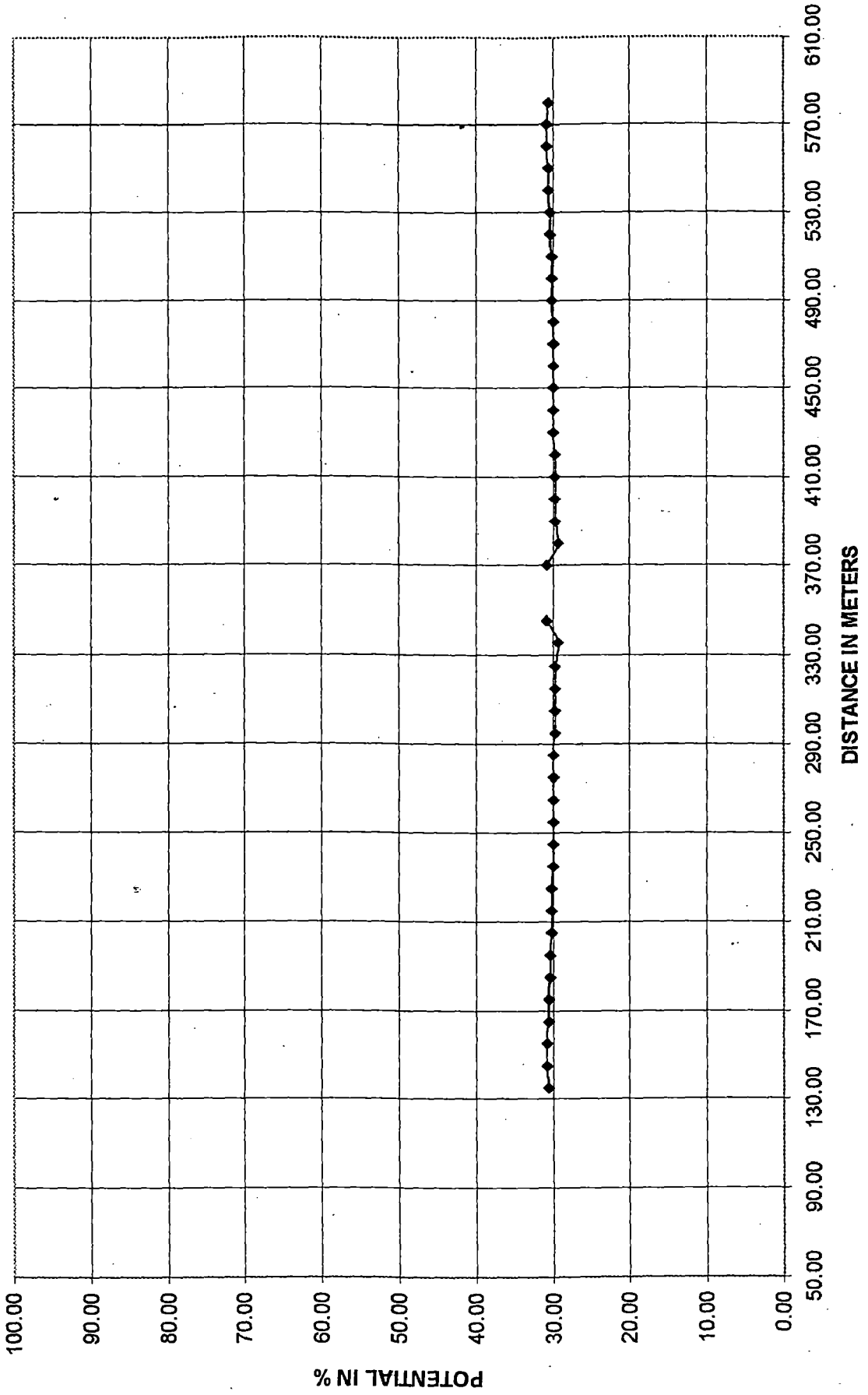
Figure 5.34: The variation of uplift pressure at C5 (A5) along the floor width of barrage bay under test condition 3

EXIT GRADIENT UNDERSLUICE BAY U/S 100 D/S US&BB 0 ABUTMENT TOP 90

DISTANCE IN METERS FROM ABUTMENT(50 M)
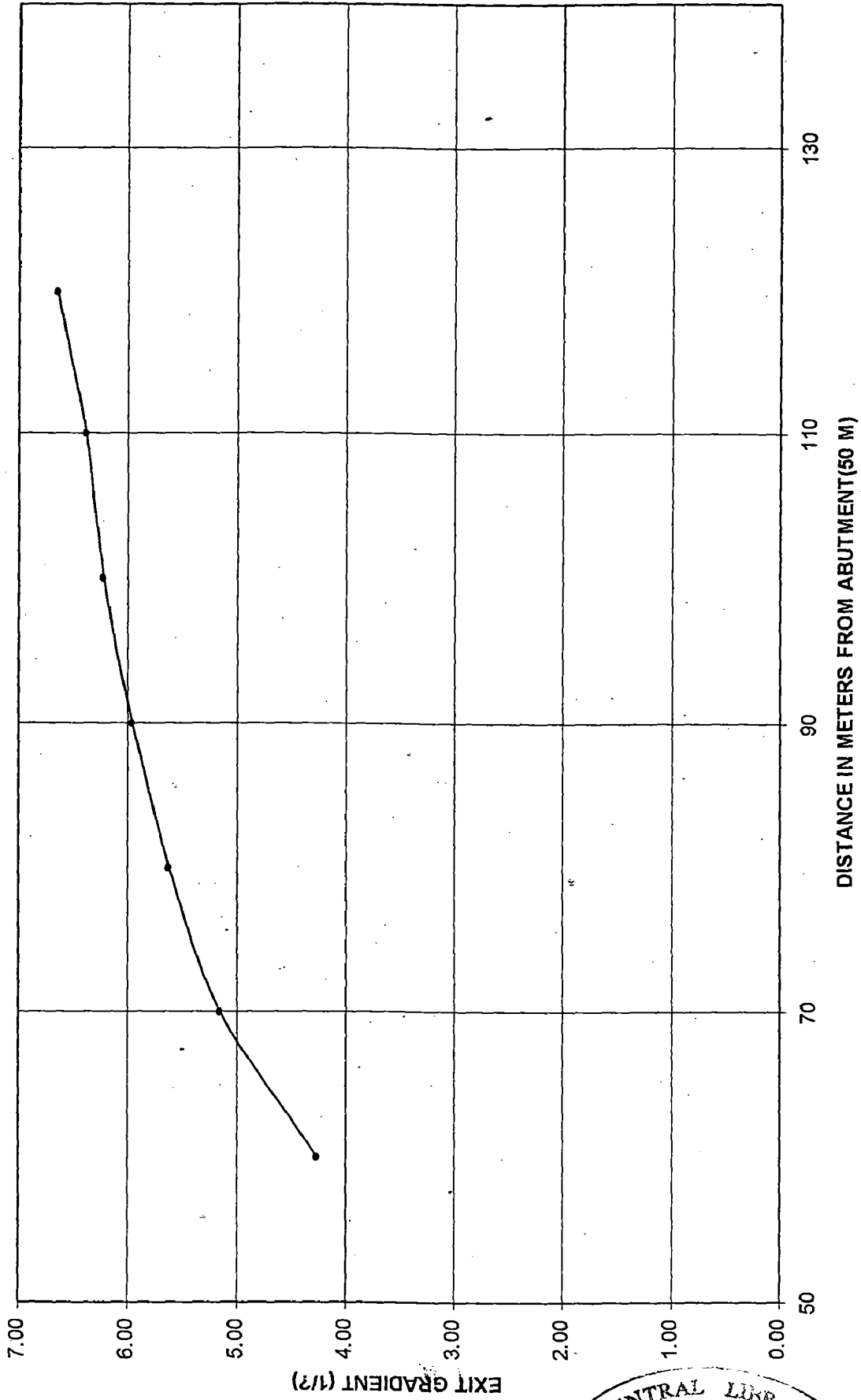
Figure 5.35: The variation of exit gradient, along the floor width of under sluice bay at D/S Sheet pile under test condition 3
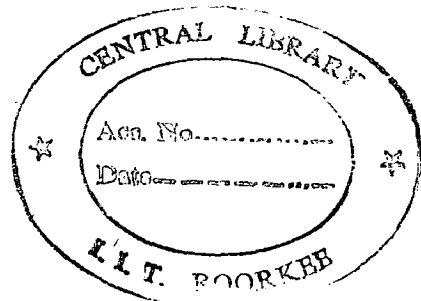
EXIT GRADIENT BARRAGE BAY U/S 100 D/S US&BB 0 ABUTMENT TOP 90
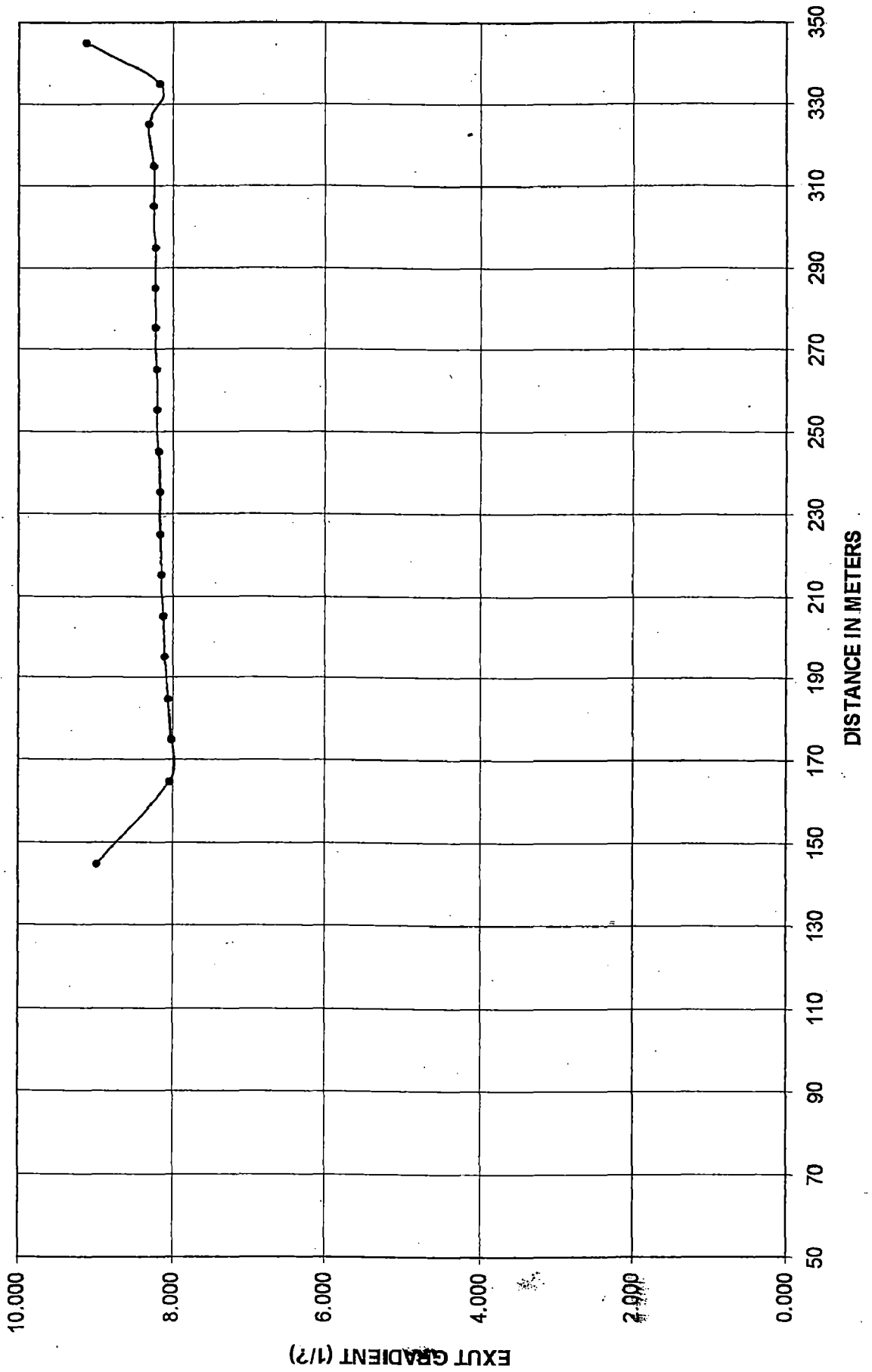
Figure 5.36: The variation of exit gradient, along the floor width of barrage bay at D/S Sheet pile under test condition 3

3-D uplift pressure variation load condition 4 U/S 100% D/S 0% abutment (90%-50%)


```
        0
11.111
22.222
33.333
44.444
55.556
66.667
77.778
88.889
       100
```
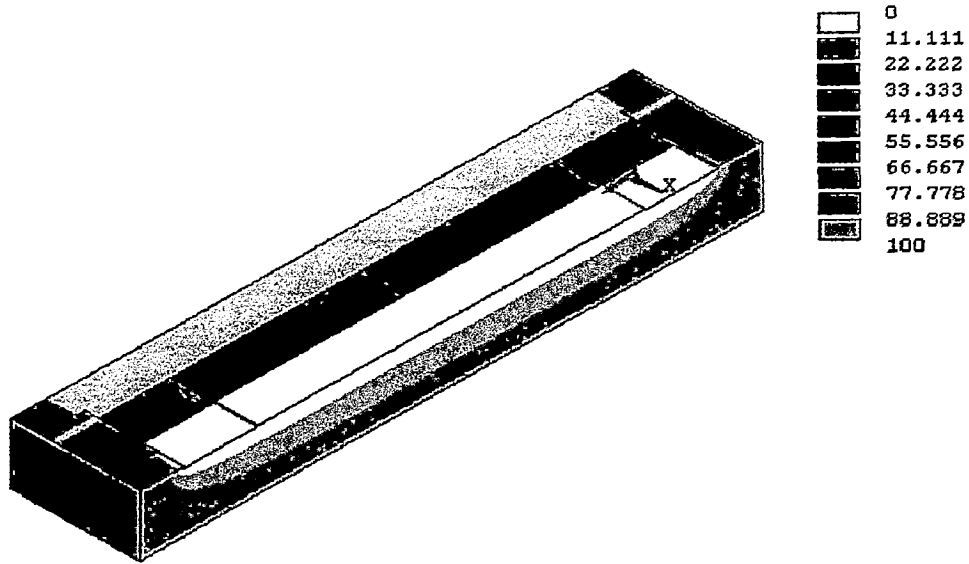
kanpur barrage u/s100d/susbb0abutment90_50 (u100d0a90_50)

Figure 5.37: 3-D View of uplift pressure distribution test condition 4

Uplift pressure variation along floor width of under sluice bay (X=84.5m) Load condition No.4

X=84.5 m,
Y=103.25 m

Bay No. 4

Bay No. 1

Distance in m from abutment (50m) along floor width

Potential in %

Figure 5.38: The variation of uplift pressure at the P4 (A4) along the floor width of under sluice bay under test condition 4 potential(90% - 50%)

5-5⅔

UNDER SLUICE BAY SEC X 98 U/S100 D/SUSBB0AB90_50

DISTANCE IN METERS

% IN POTENTIAL

Figure 5.39: The variation of uplift pressure at the P5 (A5) along the floor width of under sluice bay under test condition 4

The variation of uplift pressure at(X=71m)load condition 4

X=71m
Y=103.25m

Potential in %

Distance in m from abutment(50m)along floor width
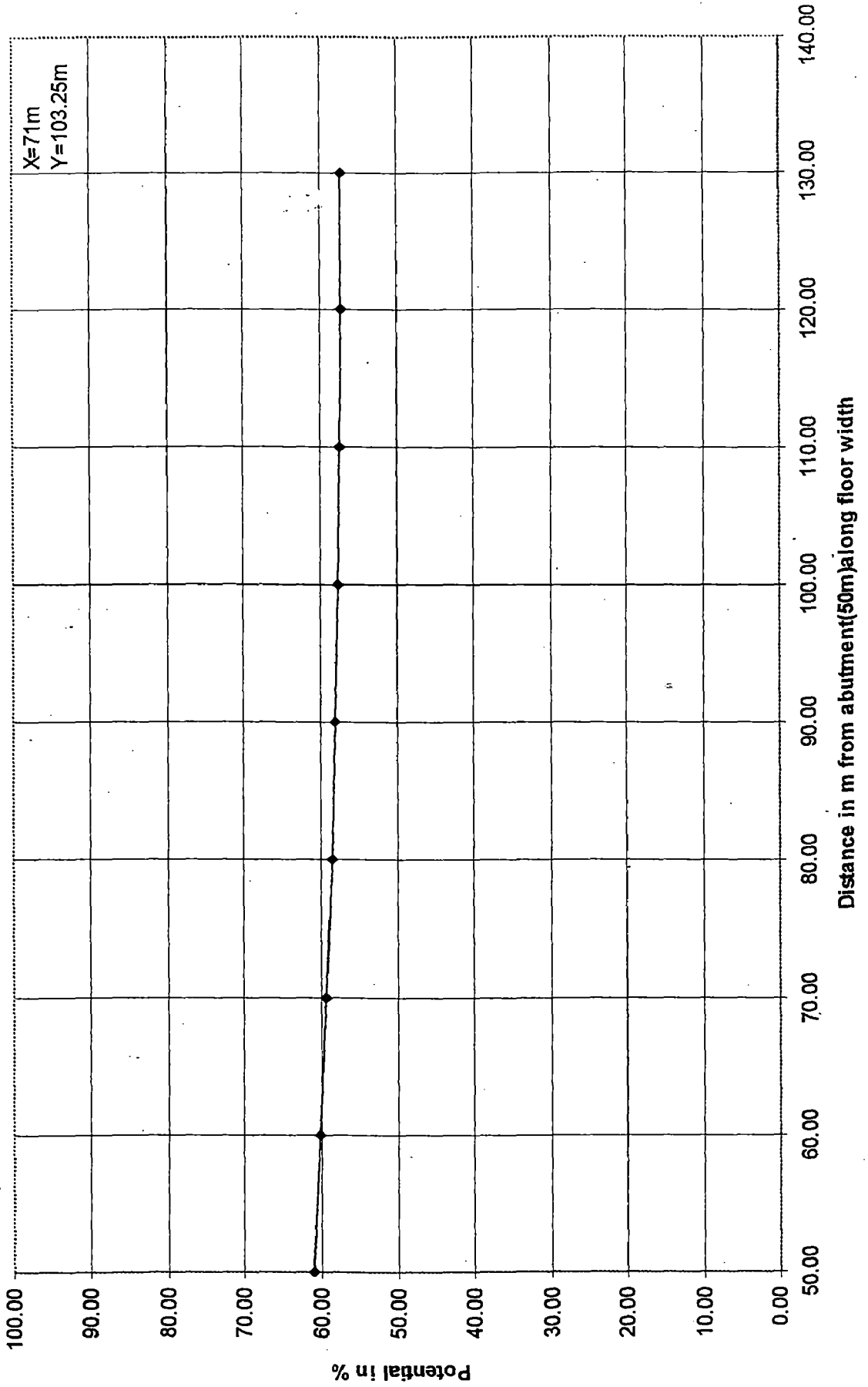
Figure 5.40: The variation of uplift pressure at P3 (A3) along the floor width of under sluice bay under test condition 4

BARRAGE BAY SEC X 84.5 U/S 100 D/S US&BB 0 ABUTMENT 90_50
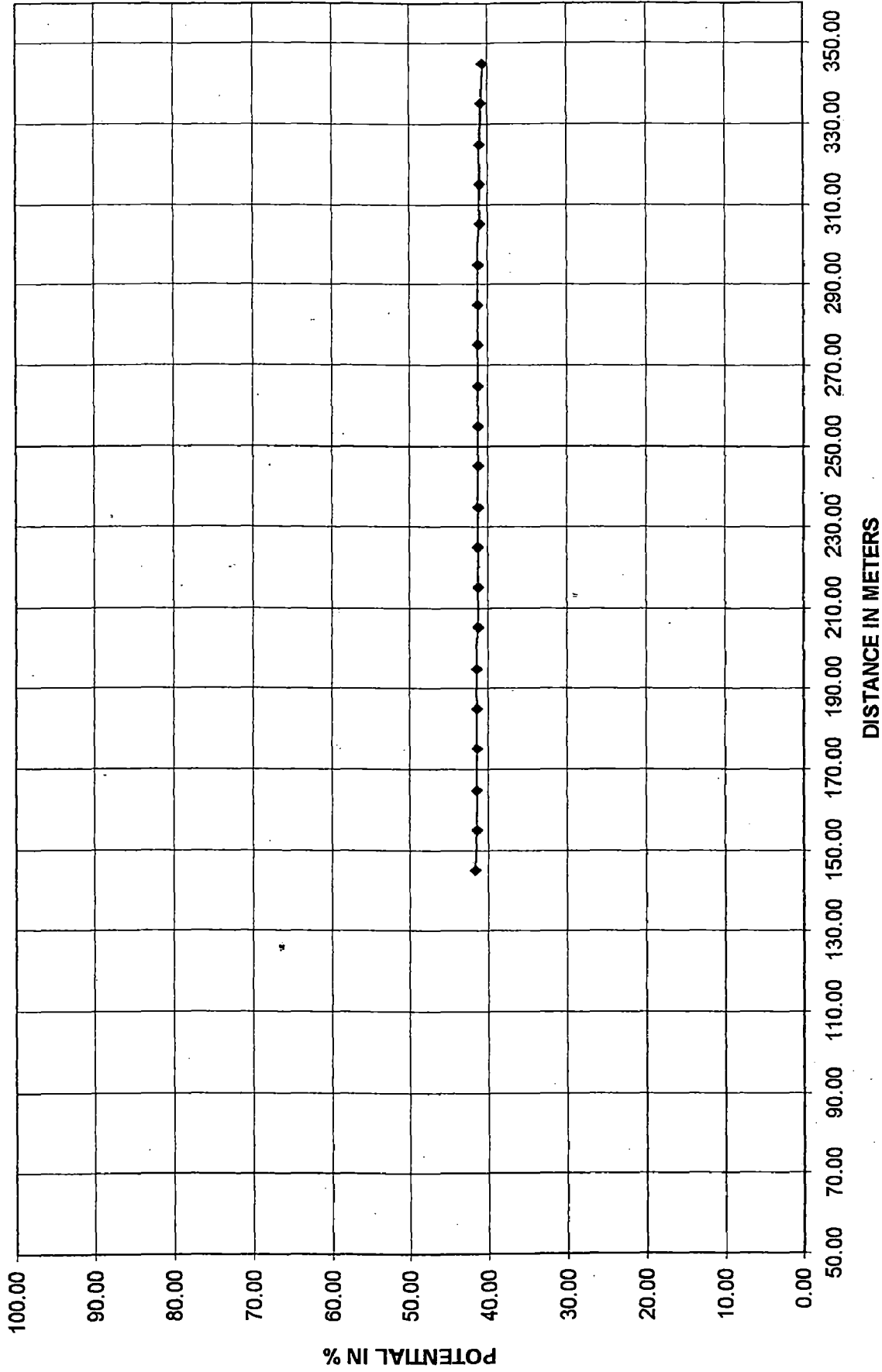
Figure 5.41: The variation of uplift pressure at C4 (A4) along the floor width of under sluice bay under test condition 4

DISTANCE IN METERS
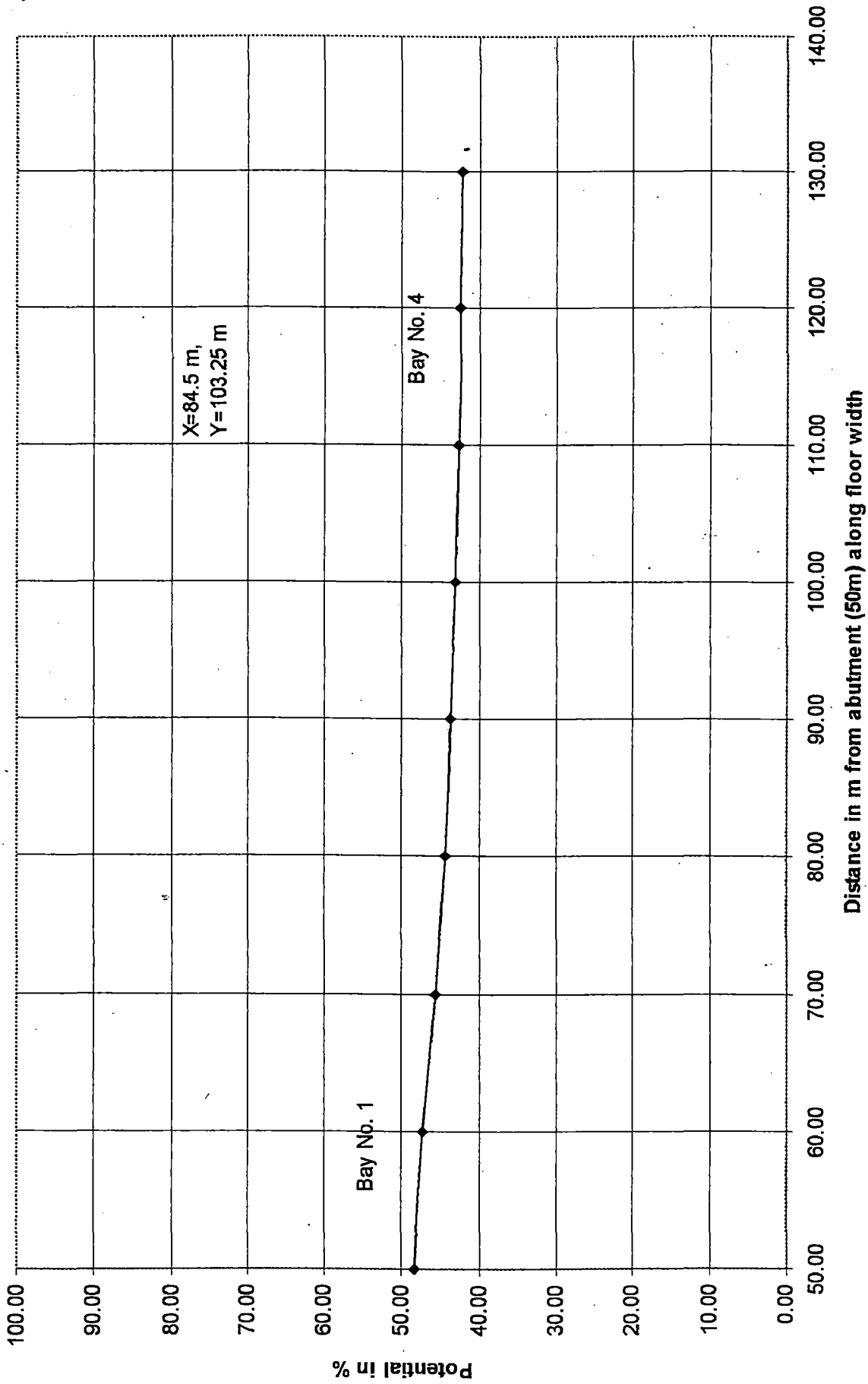
POTENTIAL IN %

Uplift pressure variation at(X=98) end point load condition 4
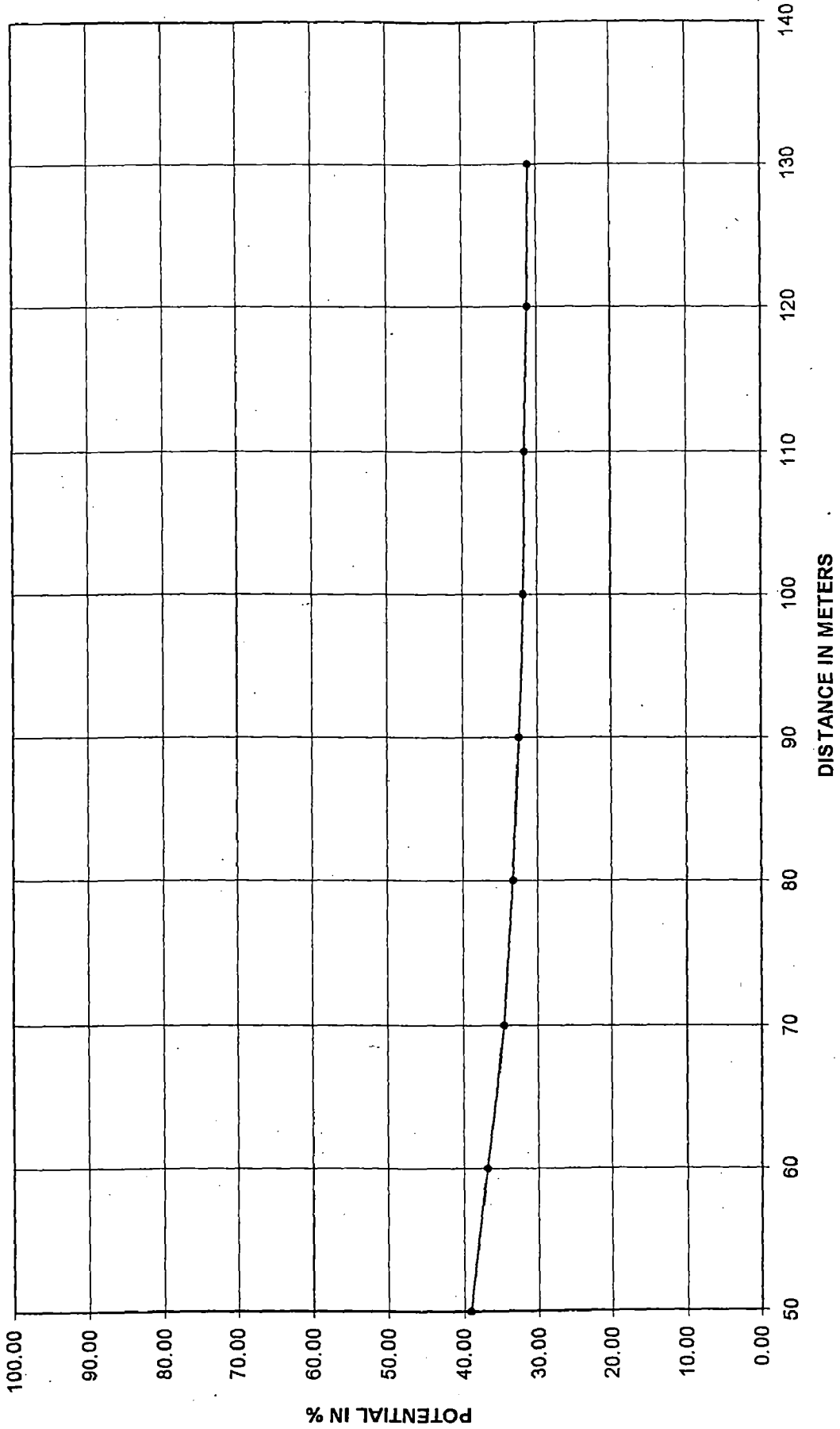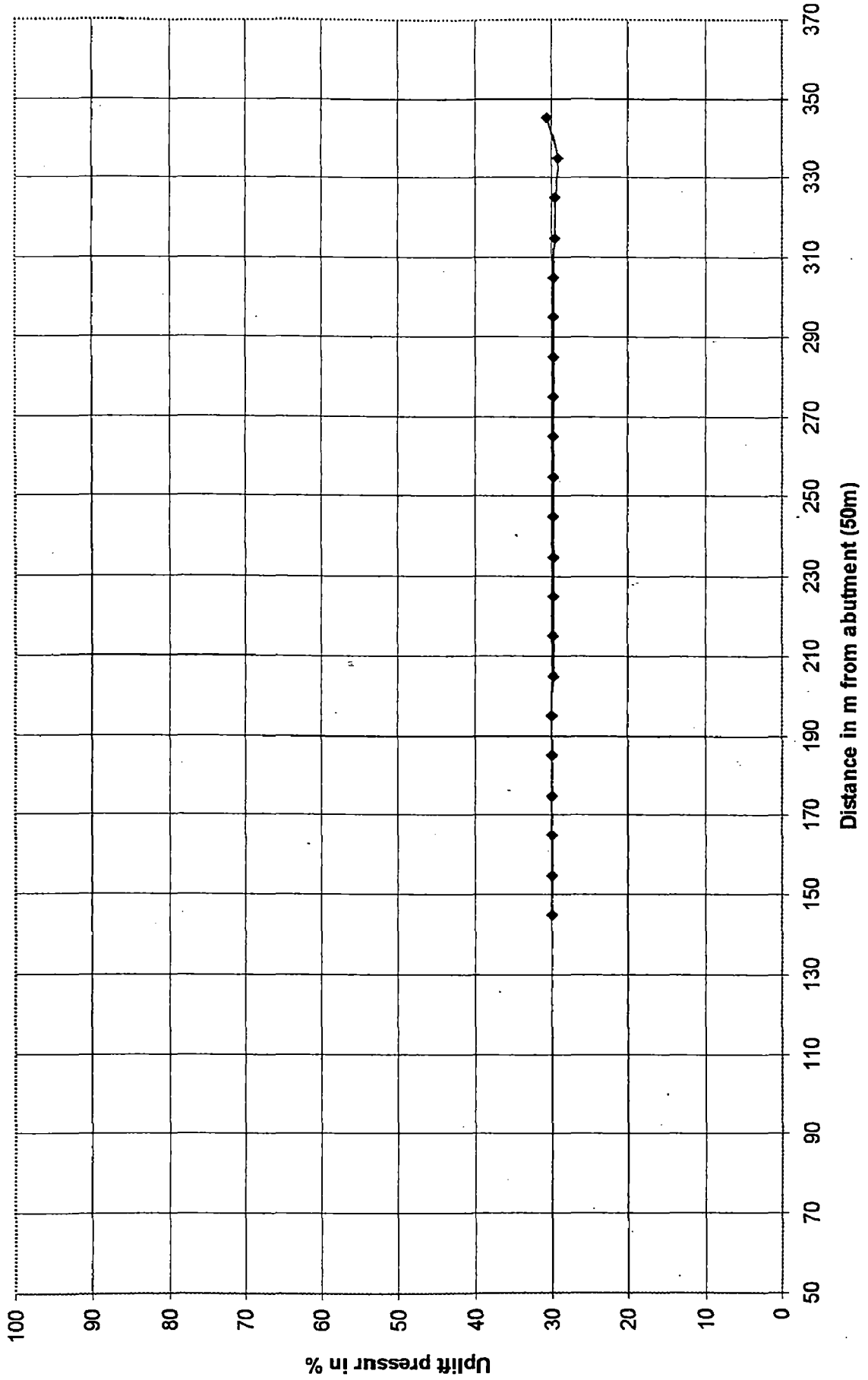

Figure 5.42: The variation of uplift pressure at C5 (A5) along the floor width of under sluice bay under test condition 4

Under sluice bay variation of exit gradient U/S 100D/SUS &BB 0 ABUTMENT 90-50,

EXIT GRADIENT (1/?

DISTANCE IN METERS
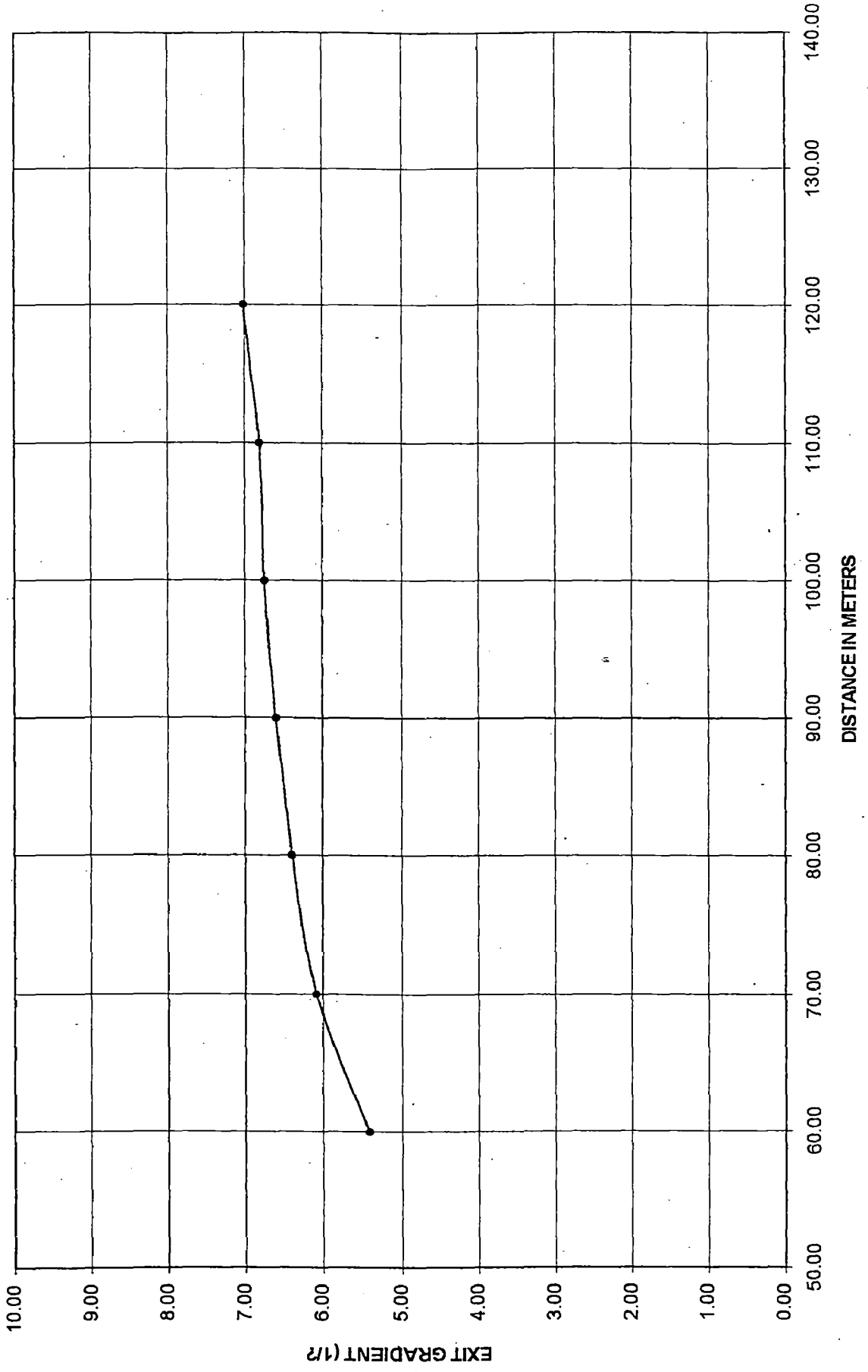
Figure 5.43: The variation of exit gradient at the exit point , along the floor width of under sluice bay under test condition 4

The variation of exit gradient in barrage bay under load codition no.4
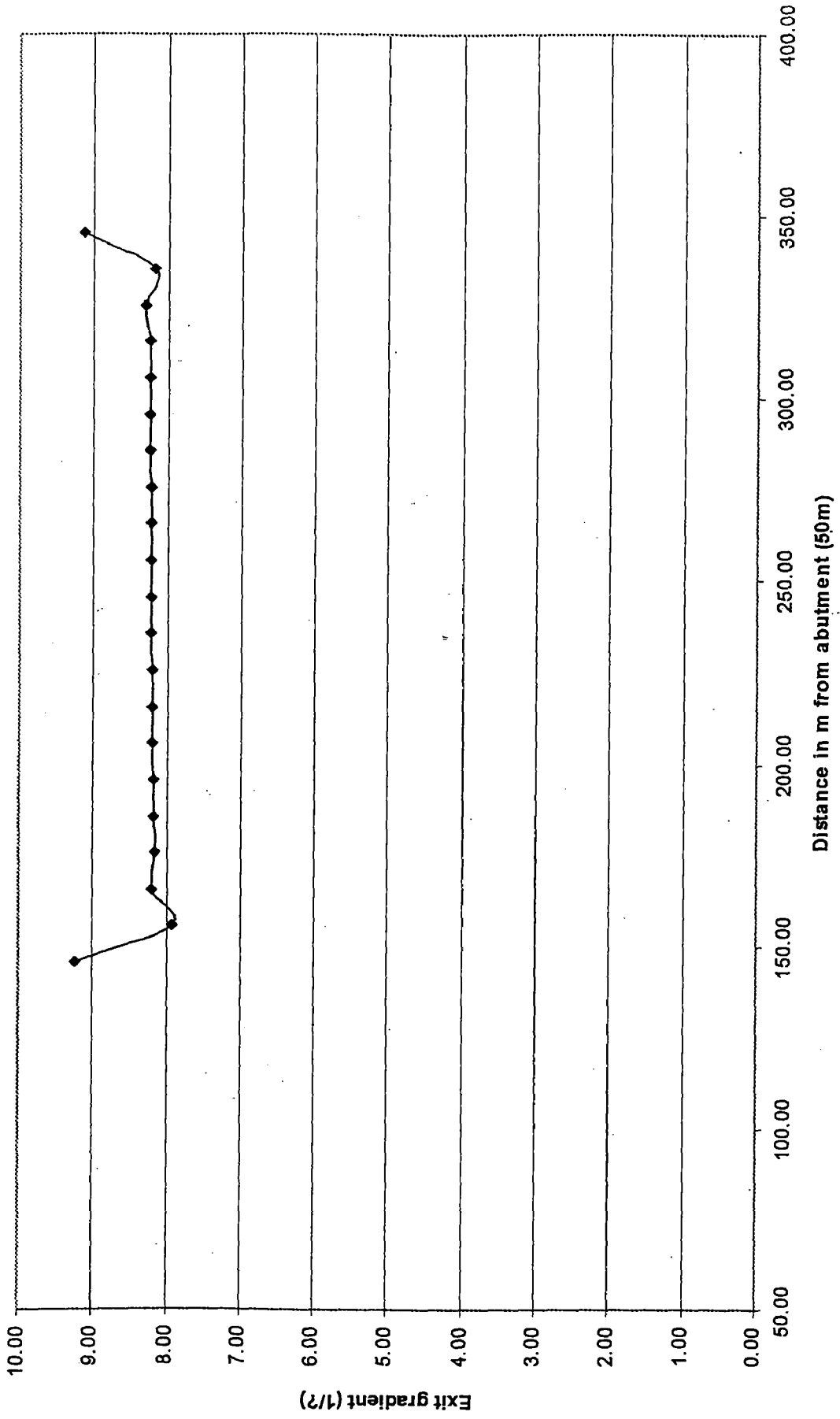
Figure 5.44: The variation of exit gradient at the exit point, along the floor width of barrage bay under test condition 4

Comparision of uplift pressures for different load conditions Sec A1 (X=50m)
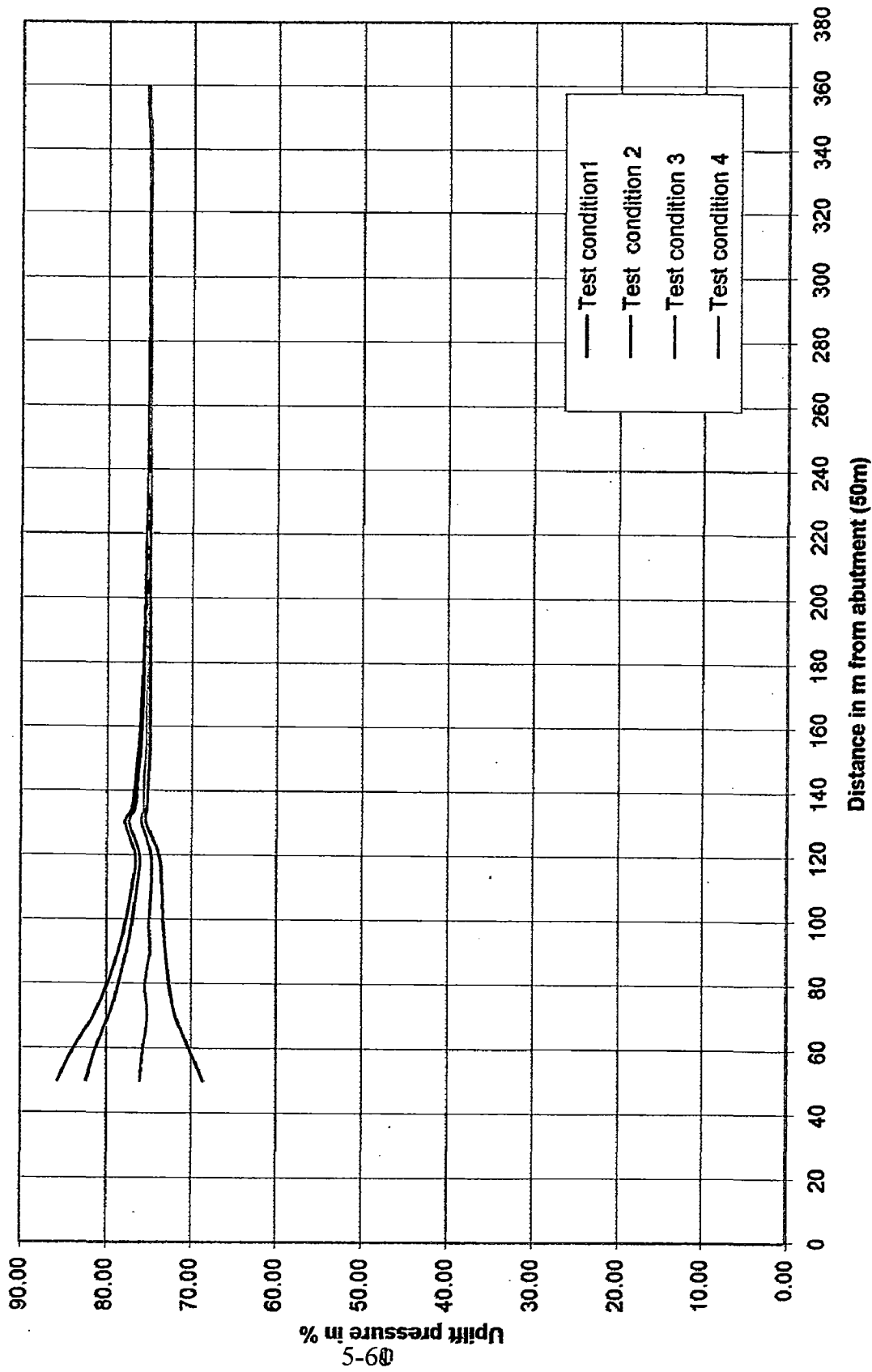
Figure 5.45 : Comparison of uplift pressure at sec. A1 (X=50m,) for different test conditions

Comparision of uplift pressure for different load conditions Sec A2(X=62m)
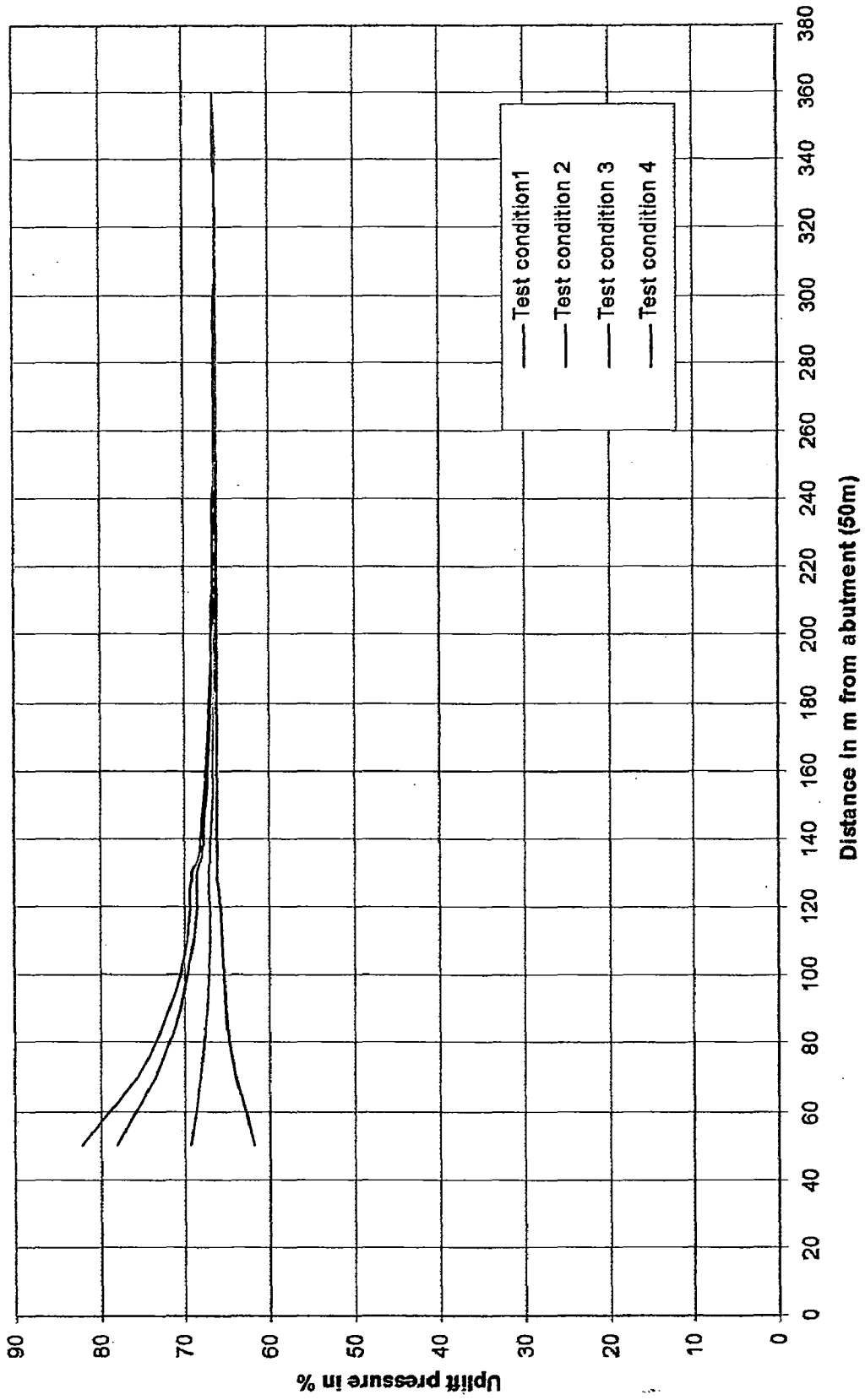
Figure 5.46 : Comparison of uplift pressure at sec. A2 (X=62m,) for different test conditions

Comparision of uplift pressure for different load conditions Sec A3 (X=71m)
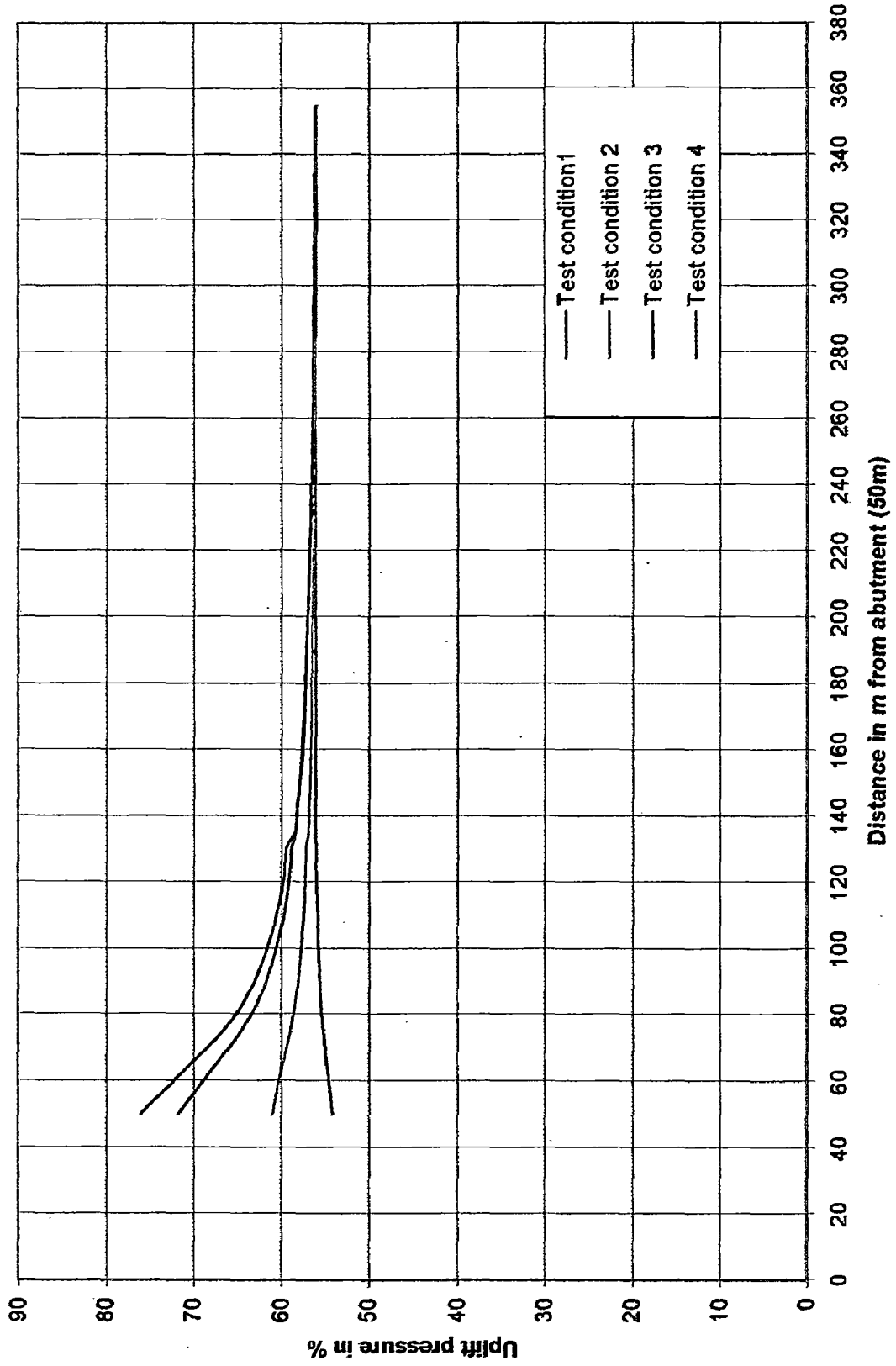
Figure 5.47 :Comparison of uplift pressure at the sec. A3 (X=71m,) for different test conditions
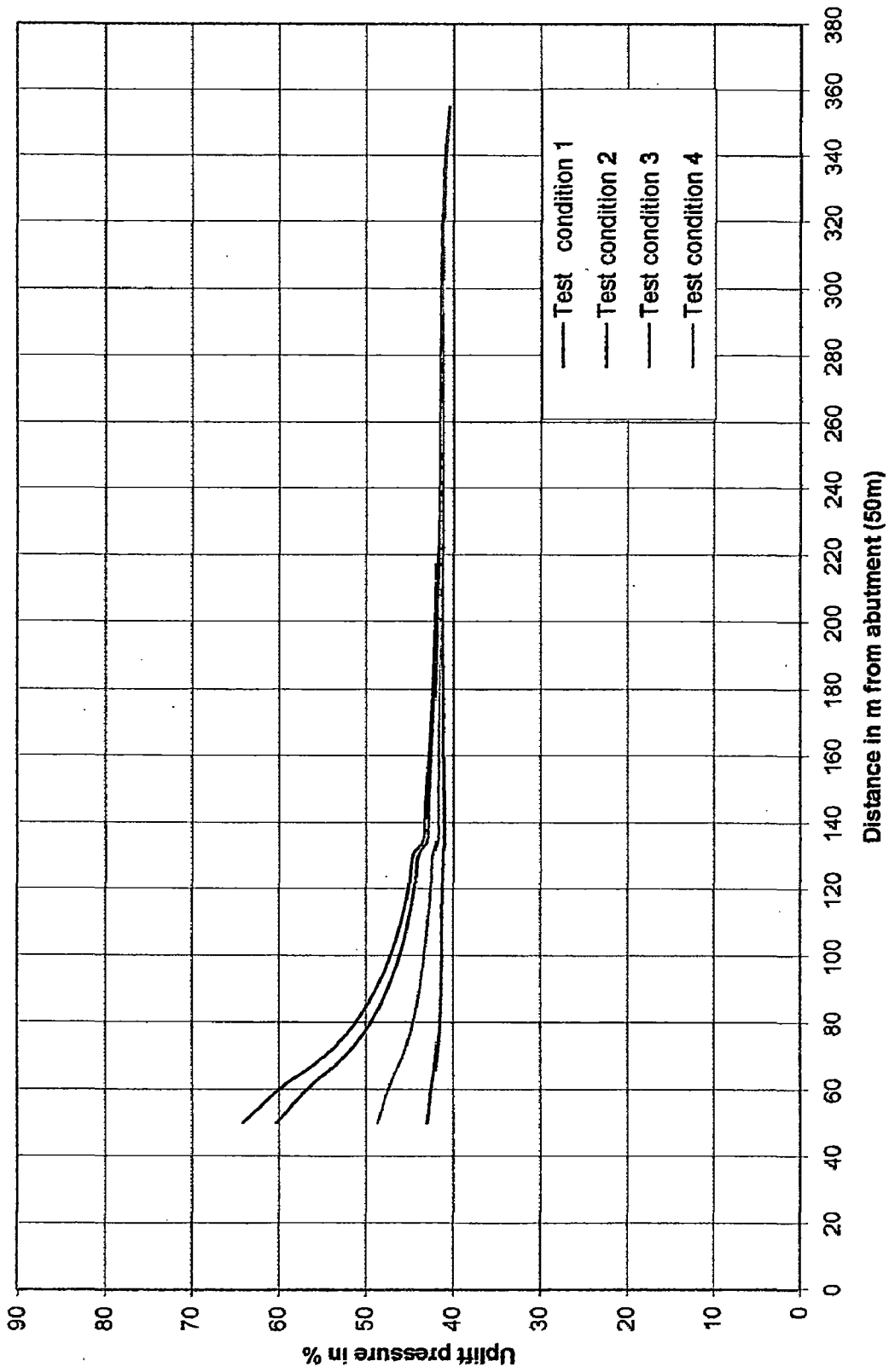
Figure 5.48 : Comparison of uplift pressure at sec. A4 (X=84.5m,) for different test conditions
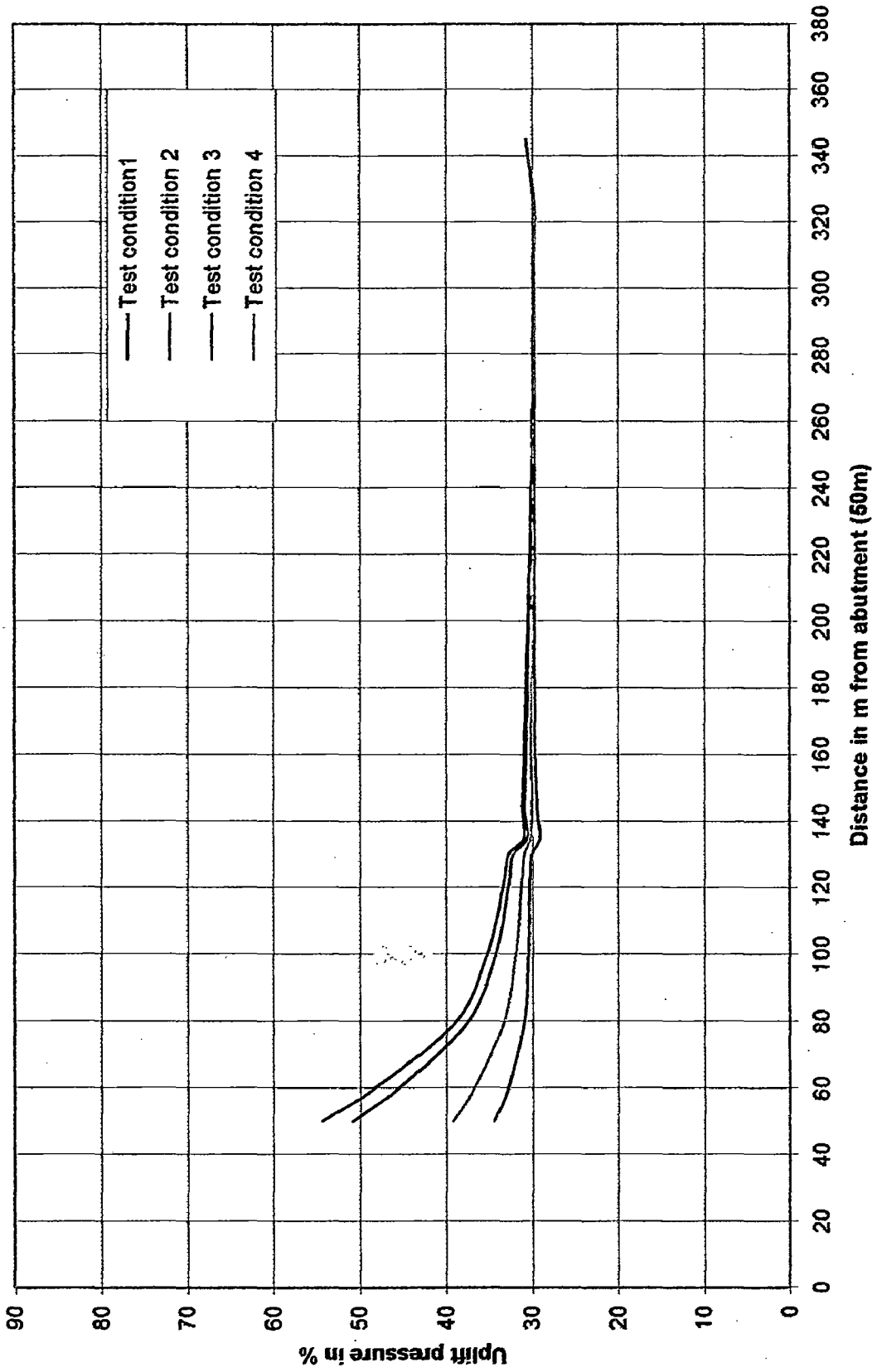
Figure 5.49 : Comparison of uplift pressure at sec. A5 (X=98m,) for different test conditions

CONCLUSIONS AND RECOMMENDATIONS

6.1 CONCLUSION

From the results of FEM analysis described in chapter 5 for the 2D and 3D analysis of a barrage resting over a homogeneous, isotropic and porous medium of infinite depth, the following conclusions are made.

1. In case of horizontal weir with equal sheet piles at either ends (standard case [7]), the results obtained using FEM model compared well with the results given in CBI&P Pub. 12 based on theoretical analysis, electrical analogy experiments and Khosla's method. This validated the ANSYS program of FEM analysis.

2. From the comparison of 2-D FEM model with Khosla and electro hydro dynamic analysis it is found the uplift pressures obtained using FEM model are more closer to Khosla's values as compared to the values obtained by EHDA experimental analysis. The experimental method has many limitations described in Chapter -2.

3. From the study on 3-dimensional FEM model under different test conditions, the following conclusions are made from the analysis.

   (a) If no potential is applied near the abutment and 100% and 0% potential on upstream and downstream river bed, respectively, then the seepage flow can be treated as 2D flow in the entire structure except near the abutments where the uplift pressures are found slightly higher.

(b)   If 100% potential is applied behind the abutment and 100% and 0% potential on upstream and downstream river bed, respectively, then the affect of head behind abutment on uplift pressures and exit gradient becomes quiet significant near the abutment. The maximum increase in uplift pressure goes as high as 50% at the under sluice bay at the downstream floor near the abutment with respect to 2D analysis.

(c)   The uplift pressure and exit gradient at downstream sheet pile for the bay near abutment increases as the water level behind abutment increases.

(d)   The plane seepage flow (2D seepage condition) is obtained at a distance of 0.37L, 0.28L and 0.26L corresponding to 100%, 90% and varying from 90% to 50% along the length of abutment, for the applied potential behind the abutment, respectively.

6.2   RECOMMENDATIONS

Finite element method is the method which can give quick results for uplift pressures and exit gradient with fair degree of accuracy for 3-dimensional studies as compared to EHDA results.

6.3   FUTURE STUDIES

3-D seepage analysis below barrage by FEM model may be conducted for different potential heads and different length – width ratio of the floor of the structure to develop design charts for the use in design of hydraulic structures.

REFERENCES

1.   Aravin V.L.& Numerov S.N. "Theory of fluid flow in undeformable porous media", Israel programme for Scientific Translations, Jerusalem 1965.

2.   BIS,1989, "IS:6966(part I)-1989, Hydraulic Design of barrages and weirs – Guidelines", New Delhi.

3.   Desai C. S. & Abel, J.F., "Introduction to the Finite Element Method A numerical method for Engineering analysis", Affiliated East West Pvt. Ltd New Delhi, Madras.

4.   Harr, M.E., "Ground Water and Seepage", McGraw Hill, 1962.

5.   Jagdhessan..A,1971,"Study of Effect of boxing on 3-dimensional seepage pressure below floor of hydraulic structures", M.E. Thesis .

6.   Khosla, A.N.,1936, Bose, N.K., Taylor Mckensie, "Design of Weirs on Permeable Foundations", C.B.I.P. No. 12, 1936.

7.   Khosla A.N., 1954, "Design of weirs on permeable foundations", Central Board of Irrigation Publication No.12(Reprint), New Delhi June 1954.

8.   Mohammad Mohy Mo Hammed,2002, "Seepage Analysis through permeable foundation on finite depth under a weir using F.E.M." , M.E. Thesis.

9.   Twelker, N.H., 1957, "Analysis of seepage in pervious abutment of dams", Proceedings Fourth International Conference on Soil Mechanics and Foundation Engineering, Vol. II, 1957.

10. U.P. Irrigation Research Institute, Technical Memorandum No. 27 R.R. (G-2), 1957, "Hydraulic Structures on Permeable Foundations-Necessity of 3-Diemsnional Approach in Design".

11. U.P. Irrigation Research Institute Technical memorandum No,67 RR(GA-3), 1996, "Uplift pressure & exit gradient below under sluice by of Kanpur Barrage (Ganga barrage) for different elevation under Lane Clay layer by 2 dimensional analogue method".

12. U.P.Irrigatioin Research Institute Technical memorandum No, 67 RR(GA-4),1996,"3-D E.H.D.A. studies for determination of uplift pressure & exit gradient below the foundation of Ganga Barrage at Kanpur".

Steps in Ansys solving 2-D problem are:

Step 1

(i)   Enter in the Ansys programme →Interactive →Product selection → (i) Ansys /Multiphysics/ unlimited

Choose working directory

(ii) Initial job name.

(iii) Set memory requested (megabytes) for total work space >256, for data base>128>Run.

Step 2. Give Analysis a title, (i) Utility menu → File > change title

Step 3. Set Measurement units > Preprocessor>material propos >material library> select units> SI (mks)

Step 4. Define element type: Main Manu > Preprocessor>Element type> Add/Edit/Delete. Plane 55/ plane 77> element No.1 for soil

Element No. 2 for floor & sheet pile.

Step 5. Define material properties>Preprocessor>Material props>Constant > Isotropic > Thermal conductivity

Material No. 1 k_{xx} 0.864

Material No. 2 k_{xx} i.e. .864e-5

Step 6. Create model

    i)   Preprocessor > Modeling > create> key points > in active C.S,

    ii)   Preprocessor > modeling > create > lines > straight lines.

Annex-I-1

iii)   Preprocessor > Modeling > create> areas > Arbitrary > Through KP'S,

iv)   Processor > Modeling > operate > Glue > Area

Step 7. Define attributes: (i) Preprocessor> Attribute defines picked lines

(ii) Programme > Attributes defined > Picked areas.

Step 8. Meshing the model:

(i) Preprocessor> meshing >mesher option > mapped

(ii) Set meshing density

Preprocessor > Meshing > Size controls > Manual Size> Global > Size.

(iii)   Meshing the model

        Preprocess > Meshing > mesh > Areas > Mapped

Check there is no bed element, other wise revise the model.

Step 9: Define Solution type & options

Main Manu > Solution> Analysis Type > New Analysis > Steady state.

Step 10: Apply potentials loads (Temperature)

Main Menu > Solution > Apply > Thermal > Temperature > on key points

Step 11: Solve the model.

        Main menu > Solution > Solve > current LS.

Step 12: Review the Nodal Temperature results

    (i)   Main Manu > General post proce. > Plot results > Contour plots> Nodal solu.

            DOF solution → Temp.

    (ii)   Main Manu > General Post proc. > Contour plot > Vector plot > Predefined

            → Flux & Gradient> thermal Gradient TG sum.

Save the model Exit.

StepsIn 3d-Analysis (Ansys Software)

Step 1

i).   Enter in the Ansys programme → Interactive →Product selection → Ansys

/Multiphysics / (Unlimited)

Choose working Directory: 'C'

ii).   Initial Job name - Kanpur

iii).   Set memory requested (megabytes)

   a) For total work space – 256

   b) For data Base → 128. > Run > O.K.

Step 2.   Give Analysis a title → Utility menu > File > Change Title.

Step 3.   Set measurement Units> Preprocessor > Material Props > Material Library

> Select Units > SI (MKS)

Step 4.   Define Element type: Main Menu > Preprocessor > Element Type >

Add/Edit/Delete.> Solid 70/ Brick 20 Node solid 90.

Step 5. Define Material Properties > Preprocessor> Material props. > Constant> Isotropic

> Thermal Conductivity.

   Material No.1: K_{xx} = 0.864

   Material No.2: K_{xx}= 1e–9.

Step 6. Create Model

   i)   Preprocessor > Modeling >create> Key points> In Active C.S.

   ii)   Preprocessor > Modeling > Create> Line > Straight lines> Through kp's

iii) Preprocessor > Modeling >Create > Areas > Arbitrary > Through kp's

iv) Preprocessor > Modeling > operate > Extrude /Sweep > Areas > By XYZ offset.

Give the offset as per requirement of detail sectional results.

v) Preprocessor > Modeling > Operate> Glue > volumes > Areas > line: As per requirement.

Create half model, as barrage is symmetrical.

v) Preprocessor > Modeling > Reflect > Volumes.

Step 7. -- Define Attributes:

i) Preprocessor > Attributes. Defines > All volumes /picked volumes> All area /Picked Areas> all lines/ Picked lines.

Step 8. Concatenate Areas and lines

Main Menu > Preprocessor> Meshing > Mesh > Volumes > Mapped > Concatenate> Areas / lines

Step 9.. Meshing the Model: i) Meshing options > Preprocessor > Meshing > Mesher options > Mapped

ii) Set Meshing Density

Preprocessor >Meshing >Size controls> Manual Size Decide Element edge length as per requirements of results and as per experience.

iii) Meshing the model

Preprocessor > Meshing > Mesh > Areas > Mapped.

Check there are no bad elements, otherwise revise the model.

Step 10. Define solution types and options.

Main Menu> Solution > Analysis Type> New Analysis > Steady state.

Step 11. Apply loads: (Temperature)

Main Menu> Solution> Apply > Thermal > Temperature > on Key points> Extends to nodes.

Step 12: Solve the model

Main Menu > solution > Solve > Current L.S.

Step 13. Review the nodal temperature Results.

i)   Main Menu> General Post processor> Plot Results > Contour plots > Nodal Soln. > D.O.F. Soln. > Temperature.

ii)   Main Menu > General Post process > Plot results > Vector plots > Predefined > Flux and Gradient > Thermal Flux /Thermal Gradient.

Step 14.   Save the mode.   Exit.

The 3-D views of model at different stages are given in figures 4.7 to 4.8 and meshed model Fig. 4.9.

Table 5.2: KANPUR BARRAGE 2-D, UPLIFT PRESSURE

NODE		X	Y	POTENTIAL IN %
	1	50	108.5	100
	48	50	106.625	96.364
	47	50	104.75	92.498
	46	50	102.875	87.088
	26	**50**	**101**	**79.829**
	1558	50	102.275	76.214
	1557	50	103.55	73.864
	1556	50	104.825	73.098
	510	50	106.1	72.765
P₁	**503**	**50**	**107.1**	**72.709**
	504	52.5	107.1	72.103
	502	**55**	**107.1**	**71.003**
	509	55	106.85	70.963
	507	**55**	**106.6**	**70.897**
	518	56.375	106.6	69.652
	517	57.75	106.6	68.563
	516	59.125	106.6	67.466
	515	**60.5**	**106.6**	**66.708**
	523	60.5	106.35	66.629
	519	**60.5**	**106.1**	**66.5**
	660	61.25	106.1	65.782
P₂	**659**	**62**	**106.1**	**65.174**
	794	64.25	105.3875	63.231
	793	66.5	104.675	61.014
	792	68.75	103.9625	58.597
P₃	**788**	**71**	**103.25**	**55.846**
	811	73.25	103.25	53.167
	810	75.5	103.25	50.75
	809	77.75	103.25	48.447
	808	80	103.25	46.195
	807	82.25	103.25	43.961
P₄	**806**	**84.5**	**103.25**	**41.754**
	805	86.75	103.25	39.576
	804	89	103.25	37.467
	803	91.25	103.25	35.451
	802	93.5	103.25	33.632
	801	95.75	103.25	32.424
P₅	**800**	**98**	**103.25**	**31.787**
	826	98	101.6125	31.707
	825	98	99.975	30.964
	824	98	98.3375	28.293
	812	**98**	**96.7**	**23.539**
	1495	98	99.05	14.777
	1494	98	101.4	8.6669
	1493	98	103.75	4.1972
	1492	98	106.1	0

Annex-III-1